University of Naples "Federico II"

Ph.D in Chemical Sciences

XXX Cycle

Thesis in Physical chemistry

"Effect of polyunsaturated fatty acids on the structure and dynamics of lipid bilayers and on the interaction with peptides"

Candidate

Augusta De Santis

Tutors

Prof. Luigi Paduano

Prof. Gerardino D'Errico

Advisor

Prof.ssa Angelina Lombardi

2014-2017

Tables of contents

Introduction

DocosaHexaenoic Acid (DHA) is the longest and most unsaturated fatty acid in cell membranes, associated to numerous health benefits in physiological conditions, by exerting a strong neuroprotective effect as well as pathological ones, including cardiovascular disease, Alzheimer's disease and other neurodegenerative processes. From a molecular viewpoint these pathologies have been associated to intrinsic disordered proteins, which can adopt a high number of conformations. The partially folded/unfolded states of a protein are vulnerable to *misfolding* and to aggregation into amyloid structures. Soluble oligomeric intermediates, rather than fully formed fibrils, are currently recognized as the predominant toxic species, capable of initiating pathogenic events. Many experimental evidences indicate that the interactions with neuronal membranes play an important role in the amyloid aggregation processes. However, the correlation between the role of membranes, amyloid aggregates and the pathogenesis of neurodegenerative diseases, such as Alzheimer, Parkinson or Huntington diseases, is still unclear. The elucidation of the role played by omega-3 fatty acids, to which DHA belongs, and the way they can explicate their beneficial effects is an intriguing challenge. Among the other hypotheses, mainly based on their radical-scavenging and anti-inflammatory action, it has been proposed that, once converted to lipids, they could alter the structure of biological membranes, whose involvement in the amyloid aggregation processes is assessed. Indeed, lipid diversity regulates a wealth of bio-membranes processes, because these molecules can tune the physicochemical characteristics of the lipid bilayer, that is characterized by a lamellar phase, such as elasticity, curvature, surface charge, hydration and the formation of domains, depending on their chemical structure. It has been shown that certain lipids, defined non-bilayer lipids, are able to promote non-lamellar phase formation, such as inverted hexagonal and cubic phases, as well as favour the insertion of proteins into the membrane. Moreover, both theoretical and experimental data provide clear indications that, at least

transiently, non-lamellar structural intermediates must exist *in vivo*. With the aim to understand the functional role of DHA, we characterized lipid membranes with different phospholipid containing this fatty acid, the 1-stearoyl-2-docosahexanoyl-glycerophosphocholine, SDPC, and the 1,2-docosahexanoyl-glycerophosphocholine, DDPC, (**Figure 1**) embedded, at different scale levels, from micro-structure to overall morphology. We used lipid membranes composed by pure 1-palmitoyl-2-oleoyl-phosphatidylcholine (POPC) and in combination with Cholesterol (Chol) (**Figure 1**), because they are characterized by different liquid crystalline meso-structures (e.g., ordered, L_o, vs. disordered, L_d).

POPC   **Chol**

SDPC   **DDPC**
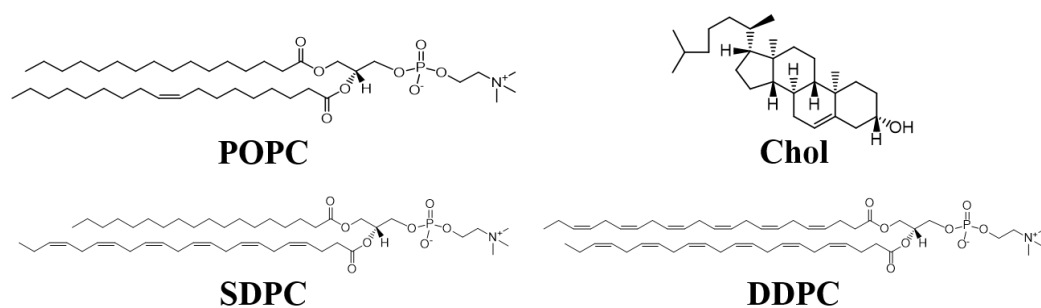
Figure 1: structures of the phospholipids under investigation.

A combination of two physico-chemical techniques, Electron Spin Resonance (ESR) spectroscopy with the spin-labelling approach and Neutron Reflectivity (NR), was used to achieve our aims.

Moving from the characterization of the lipid systems, we attempt to rationalize the DHA-phospholipids effect the DDPC, on peptide/lipid interaction, focusing on the role played in amyloidogenic processes. Through a combined ESR and Circular Dichroism (CD) approach, the interaction of model membranes, containing DDPC, with different amyloidogenic peptides have been investigated. Two novel short amyloidogenic peptides derived from nucleophosmin-1 (NPM-1), a nucleolar protein with a likely involvement in Huntington Disease and Amyloid Leukaemia, corresponding to helix H2 and the N-terminal extended H2,

Nterm, regions of NPM1 have been chosen. Then, the work has been scaled up to more biomimetic lipid membrane containing DDPC, to study the interaction with peptide hallmark of Alzheimer's disease: Aβ 1–42 aggregation process. Nevertheless, also the role of free fatty acid, DHA, should be considered; indeed, it has been found vesicles cycling, which is an important biological event, involves the interplay between membrane lipids and proteins, among which the enzyme phospholipase A2 (PLA2) plays a critical role. In nervous cells, PLA2 was also shown to control the metabolic transformation of phospholipid (PL) molecules that contain polyunsaturated fatty acids. In addition, it has been found, using raftlike lipid mixtures, that line tension and elastic properties govern budding formation after the addition of phospholipase A2 (PLA2), which explains why docosahexaenoic acid (DHA)-containing phosphatidylcholine (PC), but not Oleic Acid (OA)-containing PC, are able to exhibit liquid-ordered (L_o) domain budding. In this context, very little is known about the interaction of omega-3 free fatty acids with model membranes, thus their effect, i.e. DHA and OA as control on DPPC membranes were investigated during a period of five months spent abroad at Biofisika Institute of UPV/EHU and the main results reported in the appendix.

Chapter 1:

Biomembranes

1.1. The fluid mosaic model

In 1972, Singer and Nicolson conceived a model, which is known as the fluid mosaic model, to describe the structure of plasma membranes[1].

Biological membranes can be considered as a pseudo-two-dimensional liquid in which both lipids and membrane-associated protein molecules move laterally or sideways throughout the membrane to allow for function. The plasma membrane was postulated to be composed of different kinds of lipid and protein and the overall random appearance of the composite made the membrane looks like a mosaic (**Figure 1.1**).
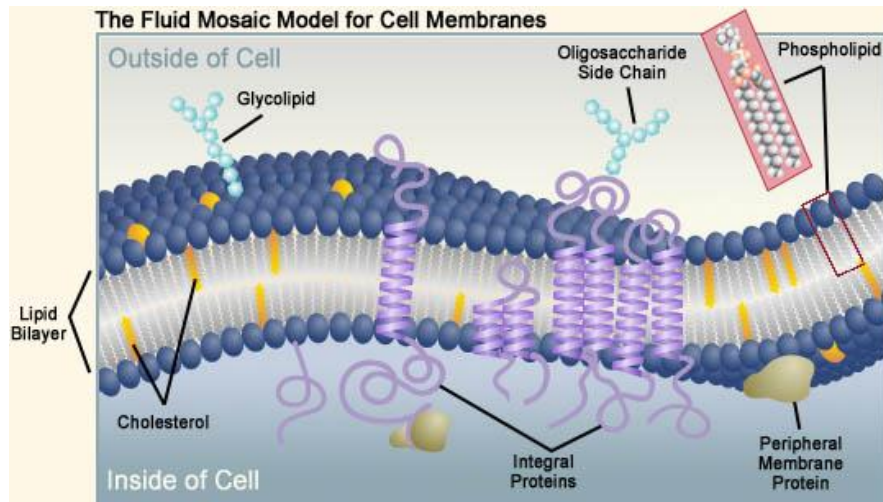
Figure 1.1: The Fluid Mosaic Model for cell membrane.

Natural lipids are amphipathic biomolecules usually insoluble in water, but soluble in organic solvents. Due to this amphipathic character, when diluted in aqueous solutions they generally tend to self-aggregate into bilayer structures, becoming essential constituents of cell membranes[2]. Lipids comprise a large number of different molecules each of them possesses different properties that play an important role in biological functions.

Glycerophospholipids, sphingolipids and sterols are crucial structural components of cell membranes and depending on their chemical structure can

modulate the physical properties of plasma membranes. In this scenario, the understanding of the physiological significance of lipid diversity in biological membranes is a key issue in membrane research.

Glycerophospholipids

The general structure of a glycerophospholipid is reported in **Figure 1.2**; they typically consist on a hydrophilic head characterized by a glycerol esterified in the 3rd position by a negatively charged phosphate group, which can be esterified by an alcohol derived molecule (R) and in the 1st and 2nd positions by hydrophobic tails (R_1, R_2).
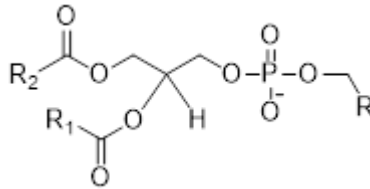
Figure 1.2: Structures of a general phospholipid R_1 and R_2 represent the different possibilities of fatty acid chains, while R represents the different possibilities for the polar head group.

The R group attached to the phosphate characterizes the hydrophilic headgroup, and according to it, glycerophospholipids are classified:

- Phosphatidylcholine (PC);
- Phosphatidylethanolamine (PE);
- Phosphatidylglycerol (PG);
- Phosphatidylserine (PS);
- Phosphatidylinositol (PI).

Regarding the hydrophobic part (R_1 and R_2), glycerophospholipids can incorporate fatty acids (FA) of various lengths and unsaturation degree, which define the membrane fluidity.

It is clear that all the possible combinations between different headgroup and different chains give rise to an infinite variety of phospholipids that play a

decisive role for many cell functions; indeed, their relative abundance depends on both the type of living organisms and tissues indicating its biological significance.

Sphingolipids

Johann L.W. Thudichum first isolated a brain-derived compound with mysterious properties that he called sphingolipid with regard to the likewise enigmatic sphinx[3]. Nowadays, structurally well-characterised sphingolipids represent a crucial lipid group for many central biological mechanisms. Sphingolipids are structurally based on sphingosine, (2S, 3R, 4E) -2-amino-4-octadecene-1,3-diol (**Figure 1.3**) and have been considered for decades as inert structural components of cell plasma membranes.
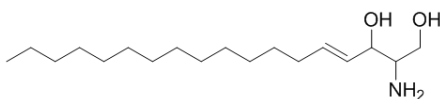
Figure 1.3: Sphingosine structure.

Recently, the unravelling of basic lipid metabolism and the discovery of the sphingolipid signalling pathway[4,5], made sphingolipids the object of great interest for many scientists[6]. Nowadays, several sphingolipids are considered as bioactive molecules and are assumed to act as secondary messengers in many signalling pathways. These principal bioactive sphingolipids are: sphingosine, ceramide and their related phosphate analogues sphingosine-1-phosphate and ceramide-1-phosphate[7]. Binding of more complex structures based on one or more sugar residues produces largest sphingolipids, namely the glycosphingolipids, which can be classified into two groups, cerebrosides and gangliosides, depending on the number of sugar residues and the presence of sialic acids. A further important discovery was the sphingolipid involvement in the generation of lateral structures or membrane domains, among which the most relevant was the proposal of sphingolipid and cholesterol-based membrane rafts[8]. The simple formation and/or

functional role of these rafts has originated a huge amount of experimental work, but with important controversy to their real existence and possible roles.

Deep studies of lipid raft generation have resulted in research of other sphingolipids with similar behaviour on the generation of such structures, as is the case of ceramide.

Sterols

An additional major group of lipid constituents of cell membranes are sterols; they are found in animals, plants and eukaryotic microorganisms, constituting as well as high percentage of total membrane lipids.

The cholestane structure characterizes this group of lipids and consists on a hydrocarbon tail linked to a on four-ring structure in which a single hydroxyl group exists, giving the molecule its amphipathic character (**Figure 1.4**).
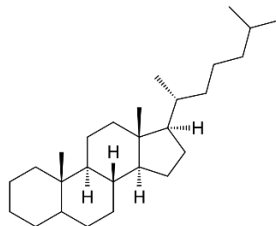
Figure 1.4: Structures of cholestane group.

The most abundant sterol in animal tissues is cholesterol and it is principally found in plasma membranes where it can reach up to 30 mol % of total lipid. In red blood cells and ocular lens membranes its amount is significantly increased, accounting for 50 and 80 mol % of total lipid respectively[9]. Several studies have shown that cholesterol has been implicated in the modulation of the activities of some integral membrane proteins[10,11,12] and in the regulation of cellular proteins through the oxysterol-binding protein[13]; in addition, it is involved in cellular processes, particular cell signaling in, through specific interactions with the components of major signaling pathways[14]. The main hypothesis on the

mechanism of action is the regulation of physical properties of the membrane, most notably the formation of cholesterol-rich lipid rafts, deriving from the association with sphingolipids and saturated phospholipids[15].

1.2. Lipids polymorphism and its significance

Cell membrane lipids are basically organised in unidimensional lamellar structure due to the same amphipathic property, which allow them to constitute and modulate the bilayer structure, which is the platform of fluid mosaic model. However, some crucial biological processes are characterised by the formation of more complex non-lamellar structures, such as the inverted hexagonal or cubic phases. From macromolecule transversal motion across the membrane to cell division, numerous processes require the generation of these unstable structures. Membrane fusion and fission processes[16,17], that include virus infection, vesicular transport from the ER to the Golgi or endocytic and exocytic transport, are good examples of energetically unfavourable events that require the formation of non-lamellar structures. However, lipid polymorphism is not only associated to two-dimensional structural changes. For instance, the formation of laterally segregated structures within a membrane, where protein complexes can adopt a more stable conformation[18] is dependent on unidimensional alterations of lipid order or rigidity.

Owing to their low water solubility, when dispersed in an aqueous solution lipids self-aggregate into different structures, basically depending on the solution ionic strength, pH, temperature, pressure, hydration level and on the lipid nature and morphological geometry. In this extent, lipids exist in a particular phase. Phases are thermodynamic idealisations defined under equilibrium conditions and characterised by particular physical properties.

Lipids phases are classified according to three general criteria:

i)   kind of lattice;

ii)   lipid acyl chain order (ordered or disordered);

iii)   overall structure curvature (normal or inverted).

An accepted nomenclature to distinguish the various lipid phases is that proposed back in 1968 by Vittorio Luzzati based on x-ray studies[19]: 1D micellar (**M**), 1D lamellar (**L**), 2D hexagonal (**H**), 2D oblique (**P**), 3D cubic (**Q**) and 3D crystalline (**C**). Finally, the lipid phases are classified owing to the overall structure curvature, being of type I or type II, and represented as well by the subscript **I** or **II** respectively. Type I conformation denotes an overall positive curvature with the hydrophobic acyl chains towards the centre and away from the aqueous environment, while type II, or inverted, reflects and overall negative curvature with the polar lipid headgroups towards the centre and the acyl chains in close contact with the aqueous environment.
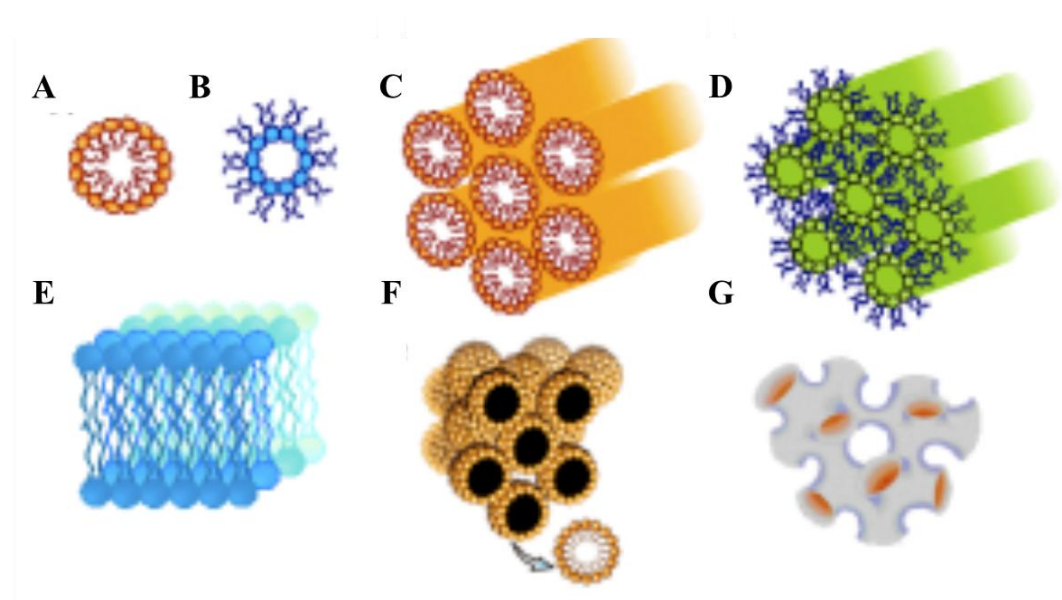
Figure 1.5: Overview of the different structures. A) micelle; B) inverted micelle; C) hexagonal; D) inverted hexagonal; E) lamellar; F) cubic; G) inverted cubic.

The most biologically relevant phases are: lamellar (L), hexagonal (H), micellar (M) and cubic (Q). Permutations between phases are called *phase transitions* and occur when the specific physical parameters that define a certain phase are changed. Phase transitions can be induced upon changes in system temperature

(thermotropic transitions), pressure (barotropic transitions) or solvent proportions (lyotropic transitions). Of great importance for many biological processes is the characterisation of the thermotropic transitions in pure or lipid mixtures, principally in those exhibiting thermotropic transitions in temperature ranges close to that of physiological relevance (37 ºC). These transitions are strongly dependent on the lipid acyl chain length and unsaturation level. For example, lipids with unsaturated acyl chains hardly display lamellar gel-fluid thermotropic phase transitions at temperatures higher than 0 ºC, reflecting a complete fluidity under physiological conditions.

Micellar phase (M)

This one-dimensional phase is inherent to lipids with inverted-cone-shaped structures (see lipid molecular geometry at the end of this section) as is the case for Lyso-phospholipids (phospholipids that lack one of the acyl chains). This kind of lipids self-aggregate in aqueous environments into micelles with the acyl chains located away from the aqueous medium and towards the centre of the micelle. These lipids display properties opposite to those of lipids with high propensity for hexagonal phases, but both kinds may be crucial for the above-mentioned biological mechanisms to be undertaken. For instance, in a membrane fission event, when the final neck is generated, the high curvature inherent to the neck will require lipids with opposite shapes to be in the two opposite layers of the membrane for proper fission. A typical parameter to refer to a micelle-forming lipid is the critical micellar concentration (CMC), which reflects the concentration at which a lipid monomer-micelle transition occurs. The generation or introduction of high amounts of a lipid with these characteristics into a specific region within a membrane can cause an overall destabilisation of the bilayer structure, inducing the formation of positive curvature in the external monolayer and possible membrane solubilisation and subsequent micelle. This behaviour is inherent to molecules with detergent-like properties[20].

Lamellar phases (L$_α$)

The lamellar phases are classified according to acyl chain order as: disordered or fluid (**L$_d$**), ordered and perpendicular to the plane of the membrane (gel) (**L$_β$**), ordered and tilted with respect to the plane of the membrane (**P$_β$´**). Later, a new lamellar phase was introduced with intermediate properties between fluid and gel, namely, liquid-ordered phase (**L$_o$**). These subscripts are used to classify the different phases only in a unidimensional lamellar lattice, as the only phase that can be organised with their acyl chains in an ordered or disordered configuration. Biological membranes under equilibrium conditions are composed of a lipid bilayer in a lamellar configuration, where the most significant phases are: fluid, liquid-disordered, or liquid-crystalline (L$_α$). In a Lα phase, lipids are free to diffuse laterally or rotationally, and display their acyl chains in a complete disordered state with high flexibility. In this phase, the acyl chains present low proportions of *trans* carbon- carbon (C-C) bound conformers, and at least one of the acyl chains is normally unsaturated. Certain lipids can be present in a lamellar gel L$_β$ phase. In this phase, the acyl chains are highly ordered and display high proportions of *trans* C-C conformers, being almost immobile and not allowing lateral or rotational motion[21]. The L$_β$ to L$_α$ phase transition is usually known as the main phase transition. Lipids with high gel-fluid thermotropic phase transitions are usually composed of saturated acyl chains, and present these acyl chains in a perpendicular disposition to the plane of the membrane. The third phase is called liquid-ordered (L$_o$), and reflects a phase with intermediate properties between the gel and the fluid phases. It was recently named to denote lipid mixtures of sphingolipids or glycerolipids with sterols, and it is a phase in which lateral diffusion is allowed but there is a low level of *gauche* conformers. This is the phase in which "membrane rafts" are supposed to exist[22].

Hexagonal phases (H)

The formation of non-lamellar structures is apparently contradictory to the normal function of a natural cell membrane. However, lipids with the ability to form such

phases have been related to several important mechanisms such as fusion or fission processes. Among non-lamellar structures, the hexagonal phase appears as one of the most relevant conformations. Hexagonal phases are fluid 2-D structures that can be of type I (H_I) or type II (H_{II}). In both cases, large parallel cylinders with a hexagonal packing are formed. In the normal or H_I type, lipids arrange with the acyl chains disposed to the centre of the cylinder. H_{II} is called inverted hexagonal phase and presents the polar headgroups to the centre of the cylinder and the acyl chains towards the external environment and in close contact with hydrophobic tails from other cylinders.

The biological relevance of these structures becomes significant in processes as membrane lipid- and protein-mediated pore and/or channel formation, which appear to recruit non-lamellar forming lipids for proper structure stability, and membrane fusion and fission events, in which lipids with a high propensity for hexagonal phases are required both for the contact sites between membranes in fusion mechanisms and for the final neck generation prior to fission events.

Cubic phases (Q)

The last, but not least, kind of biologically relevant phase refers to the periodic three dimensional cubic phases[19]. Seven classes of cubic phases are known, among which the most important two are the micellar and the bicontinuous type I and II. The bicontinuous type II cubic phase (Q_{II}) represents a highly convoluted lipid bilayer, which subdivides 3-D space into two unconnected polar labyrinths divided by an apolar septum. In the case of the bicontinuous type I cubic phase (Q_I) the septum and the two labyrinths are filled by the polar and the apolar medium, respectively.

1.3. Lipid molecular geometry

The formation of the various structures is strongly influenced by the lipid molecular geometry. Jacob Israelachvili described how differences in the cross-sectional area between the polar headgroup and the hydrophobic tail of the

different lipids could determine the overall structure of the lipid aggregates[23]. On this basis, lipids can be classified into three groups by having: cone, cylindrical or inverted-cone shapes. This fact is summarised by the morphological parameter N_s defined in **Equation 1.1:**

$$N_S = \frac{V_C}{a_C \cdot L_C} \quad \textbf{Eq. 1.1}$$

where "V" is the volume of the lipid molecule, "a_o" is the area of the molecule in the lipid-water interface and "L_c" the length of the extended acyl chain.

Considering these parameters and the lipid cross-sectional area in the hydrophobic tail "a_H", which would reflect a volume of $V = a_H L_c$ for a lipid displaying cylindrical shape, we can review the different morphological geometries as:

- $a_0 = a_H$ ($N_s = 1$), the molecule presents a cylindrical shape;
- $a_0 < a_H$ ($N_s > 1$), the molecule presents a cone shape;
- $a_0 > a_H$ ($N_s < 1$), the molecule presents an inverted cone shape.

As described in **Figure 1.5**, pure lipids in aqueous solutions will self-aggregate into different structures depending on their molecular geometry. Cylindrical shapes displaying lipids as PC or SM will become organised in the form of lamellar bilayers. Cone shaped lipids as PE or sterols will tend to form hexagonal arrangements, while inverted-cone shaped lipids as is the case of lyso-phospholipids will aggregate into micelles. Thus, it could be summarised that lipid polymorphism reflects the lipid behaviour under specific physical conditions in which long-range ordered structures are generated with the lipids in a given phase.

1.4. Polyunsaturated fatty acids

Polyunsaturated fatty acids (PUFA) contain more than one double bond in one acyl chain. PUFA includes many important compounds such as essential fatty acids (EFA). Essential fatty acids are indispensable for the health of mammalian

animals. It can only be ingested from food and cannot be synthesized in human body. Only two EFAs are known for humans: alpha-linolenic acid (an omega-3 fatty acid) and linoleic acid (an omega-6 fatty acid). Docosahexaenoic acid (DHA) with 22-carbons and six double bonds is the most polyunsaturated fatty acid commonly found in biological systems and it can be synthesized from alpha-linolenic acid or obtained directly from fish oil[24]. In the inner leaflet of some animal cell plasma membranes PUFAs comprise up to ~50% of *sn*-2 fatty acyl chains[25]. In retinal rod outer segment disk membranes DHA comprises ~50% of the total acyl chains, with this high percentage required for optimal rhodopsin function[26]. DHA is also found at high concentrations in certain other membranes, including synaptosomes[27] and sperm[28]. The importance of DHA and PUFAs for human health has been well-studied[29]: spectroscopic, computational, and other biophysical methods[30] have established significant PUFA effects on membrane properties. It has been shown that phospholipid containing DHA with a phosphoethanolamine headgroup, or a di-polyunsaturated phospholipid in particular condition, can give a non-lamellar phase[31]. In addition, PUFAs seem to have a weaker interaction with cholesterol compared with saturated or monounsaturated acyl chains. A relatively low solubility of cholesterol in PUFA-containing membranes was measured using both X-ray diffraction and solid-state 2H NMR[32]. By the investigation of model membranes with increasing number of components, it has been proposed that DHA could be directly involved in inducing lateral phase separations into DHA-rich/cholesterol-poor and DHA-poor/cholesterol-rich lipid domains[33]. It becomes clear that despite the abundance and importance of DHA-containing lipids such as SDPC, SDPE (1-stearoyl-2-docosahexaenoyl-*sn*-glycero-3-phosphatidylethanolamine), PDPC (1-palmitoyl-2-docosahexaenoyl-*sn*-glycero-3-phosphocholine), and PDPE (1-palmitoyl-2-docosahexaenoyl-*sn*-glycero-3-phosphatidylethanolamine), DDPC and DDPE very few different PUFA containing lipid compositions have been examined, especially if it is taken into consideration that the lipid geometry affects

supramolecular organization. The vast majority of studies conducted on DHA-containing lipids have focused on only a few sample compositions, most commonly 1/1/1 = DHA-containing lipid/SM/Chol[34,35,36]. Feigenson et al.[37] presented the first mixing behaviour overall possible compositions of these three-component mixtures, including the key regions of immiscibility, can be described by use of a triangular phase diagram. The phase diagram is a Type II mixture, that is, having three macroscopic phase separation regions $L_d + L_o$; $L_d + L_o + L_\beta$; and $L_d + L_\beta$, showing the same immiscibility regions observed for the lipid mixtures contained POPC instead of SDPC. In this context the aim of the present work is to asses if a different behaviour exists depending on the phospholipids containing the DHA: different lipid mixtures in the presence of different amount of mono-esterified and di-esterified phospholipids containing DHA were analysed.

1.5. References

1 Singer, S. J. & Nicolson, G. L. The fluid mosaic model of the structure of cell membranes. *Science* **175**, 720-731 (1972).

2 Alberts, B. *Molecular biology of the cell*. 4th edn, (Garland Science, 2002).

3 Chun, J. & Hartung, H. P. Mechanism of action of oral fingolimod (FTY720) in multiple sclerosis. *Clinical neuropharmacology* **33**, 91-101, doi:10.1097/WNF.0b013e3181cbf825 (2010).

4 Kolesnick, R. N. & Paley, A. E. 1,2-Diacylglycerols and phorbol esters stimulate phosphatidylcholine metabolism in GH3 pituitary cells. Evidence for separate mechanisms of action. *The Journal of biological chemistry* **262**, 9204-9210 (1987).

5 Okazaki, T., Bell, R. M. & Hannun, Y. A. Sphingomyelin turnover induced by vitamin D3 in HL-60 cells. Role in cell differentiation. *The Journal of biological chemistry* **264**, 19076-19080 (1989).

6 Maggio, B. The surface behavior of glycosphingolipids in biomembranes: a new frontier of molecular ecology. *Progress in biophysics and molecular biology* **62**, 55-117 (1994).

7 Goni, F. M. & Alonso, A. Biophysics of sphingolipids I. Membrane properties of sphingosine, ceramides and other simple sphingolipids. *Biochimica et biophysica acta* **1758**, 1902-1921, doi:10.1016/j.bbamem.2006.09.011 (2006).

8 Simons, K. & Ikonen, E. Functional rafts in cell membranes. *Nature* **387**, 569-572, doi:10.1038/42408 (1997).

9 Li, L. K., So, L. & Spector, A. Membrane cholesterol and phospholipid in consecutive concentric sections of human lenses. *Journal of lipid research* **26**, 600-609 (1985).

10 Barrantes, F. J. Cholesterol effects on nicotinic acetylcholine receptor: cellular aspects. *Sub-cellular biochemistry* **51**, 467-487, doi:10.1007/978-90-481-8622-8_17 (2010).

11 Levitan, I., Fang, Y., Rosenhouse-Dantsker, A. & Romanenko, V. Cholesterol and ion channels. *Sub-cellular biochemistry* **51**, 509-549, doi:10.1007/978-90-481-8622-8_19 (2010).

12 Paila, Y. D. & Chattopadhyay, A. Membrane cholesterol in the function and organization of G-protein coupled receptors. *Sub-cellular biochemistry* **51**, 439-466, doi:10.1007/978-90-481-8622-8_16 (2010).

13 Wang, P. Y., Weng, F. & Anderson, R. G. W. OSBP is a cholesterol-regrulated scaffolding protein in control of ERK1/2 activation. *Science* **307**, 1472-1476, doi:10.1126/science.1107710 (2005).

14 Sheng, R. *et al.* Cholesterol modulates cell signaling and protein networking by specifically interacting with PDZ domain-containing scaffold proteins. *Nature communications* **3**, 1249, doi:10.1038/ncomms2221 (2012).

15 Lingwood, D. & Simons, K. Lipid Rafts As a Membrane-Organizing Principle. *Science* **327**, 46-50, doi:10.1126/science.1174621 (2010).

16 Burger, K. N. Greasing membrane fusion and fission machineries. *Traffic* **1**, 605-613 (2000).

17 Chernomordik, L. V., Zimmerberg, J. & Kozlov, M. M. Membranes of the world unite! *The Journal of cell biology* **175**, 201-207, doi:10.1083/jcb.200607083 (2006).

18 Cullis, P. R. & de Kruijff, B. Lipid polymorphism and the functional roles of lipids in biological membranes. *Biochimica et biophysica acta* **559**, 399-420 (1979).

19 Luzzati, V. Biological significance of lipid polymorphism: the cubic phases. *Current opinion in structural biology* **7**, 661-668 (1997).

20 Sot, J., Goni, F. M. & Alonso, A. Molecular associations and surface-active properties of short- and long-N-acyl chain ceramides. *Biochimica et biophysica acta* **1711**, 12-19, doi:10.1016/j.bbamem.2005.02.014 (2005).

21 Marsh, D. Molecular motion in phospholipid bilayers in the gel phase: long axis rotation. *Biochemistry* **19**, 1632-1637 (1980).

22 Brown, R. E. Sphingolipid organization in biomembranes: what physical studies of model membranes reveal. *Journal of cell science* **111 (Pt 1)**, 1-9 (1998).

23 Israelachvili, J. N., Marcelja, S. & Horn, R. G. Physical principles of membrane organization. *Quarterly reviews of biophysics* **13**, 121-200 (1980).

24 Simopoulos, A. P. Human requirement for N-3 polyunsaturated fatty acids. *Poultry science* **79**, 961-970 (2000).

25 Wassall, S. R. & Stillwell, W. Polyunsaturated fatty acid-cholesterol interactions: domain formation in membranes. *Biochimica et biophysica acta* **1788**, 24-32, doi:10.1016/j.bbamem.2008.10.011 (2009).

26 Lin, D. S., Anderson, G. J., Connor, W. E. & Neuringer, M. Effect of Dietary N-3 Fatty-Acids Upon the Phospholipid Molecular-Species of the Monkey Retina. *Investigative ophthalmology & visual science* **35**, 794-803 (1994).

27 Anderson, R. E., Feldman, L. S. & Feldman, G. L. Lipids of ocular tissues. II. The phospholipids of mature bovine and rabbit whole retina. *Biochimica et biophysica acta* **202**, 367-373 (1970).

28 Stillwell, W., Shaikh, S. R., Zerouga, M., Siddiqui, R. & Wassall, S. R. Docosahexaenoic acid affects cell signaling by altering lipid rafts. *Reproduction, nutrition, development* **45**, 559-579, doi:10.1051/rnd:2005046 (2005).

29 Escriba, P. V. *et al.* Membrane lipid therapy: Modulation of the cell membrane composition and structure as a molecular base for drug discovery and new disease treatment. *Progress in lipid research* **59**, 38-53, doi:10.1016/j.plipres.2015.04.003 (2015).

30 Gawrisch, K., Eldho, N. V. & Holte, L. L. The structure of DHA in phospholipid membranes. *Lipids* **38**, 445-452 (2003).

31 Shaikh, S. R., Brzustowicz, M. R., Stillwell, W. & Wassall, S. R. Formation of inverted hexagonal phase in SDPE as observed by solid-state (31)P NMR. *Biochemical and biophysical research communications* **286**, 758-763, doi:10.1006/bbrc.2001.5454 (2001).

32 Brzustowicz, M. R. *et al.* Controlling membrane cholesterol content. A role for polyunsaturated (docosahexaenoate) phospholipids. *Biochemistry* **41**, 12509-12519 (2002).

33 Shaikh, S. R., Kinnun, J. J., Leng, X., Williams, J. A. & Wassall, S. R. How polyunsaturated fatty acids modify molecular organization in membranes: insight from NMR studies of model systems. *Biochimica et biophysica acta* **1848**, 211-219, doi:10.1016/j.bbamem.2014.04.020 (2015).

34 Shaikh, S. R., Locascio, D. S., Soni, S. P., Wassall, S. R. & Stillwell, W. Oleic- and docosahexaenoic acid-containing phosphatidylethanolamines differentially phase separate from sphingomyelin. *Biochimica et biophysica acta* **1788**, 2421-2426, doi:10.1016/j.bbamem.2009.08.019 (2009).

35 Shaikh, S. R., Brzustowicz, M. R., Gustafson, N., Stillwell, W. & Wassall, S. R. Monounsaturated PE does not phase-separate from the lipid raft molecules sphingomyelin and cholesterol: role for polyunsaturation? *Biochemistry* **41**, 10593-10602 (2002).

36 Georgieva, R. *et al.* Docosahexaenoic acid promotes micron scale liquid-ordered domains. A comparison study of docosahexaenoic versus oleic acid containing phosphatidylcholine in raft-like mixtures. *Biochimica et biophysica acta* **1848**, 1424-1435, doi:10.1016/j.bbamem.2015.02.027 (2015).

37 Konyakhina, T. M. & Feigenson, G. W. Phase diagram of a polyunsaturated lipid mixture: Brain sphingomyelin/1-stearoyl-2-docosahexaenoyl-*sn*-glycero-3-phosphocholine/cholesterol. *Biochimica et biophysica acta* **1858**, 153-161, doi:10.1016/j.bbamem.2015.10.016 (2016).

Chapter 2:

Amyloidogenic

peptides and proteins

2.1. Definition of amyloid fibril proteins

The chemical diversity of amyloid and amyloidosis has been evident since the mid-1970s[1] and the number of known human amyloid proteins has steadily increased in the last 40 years. Recently, the Nomenclature Committee of the International Society of Amyloidosis (ISA) has reviewed the number of known amyloid fibril proteins and the recommendations for clinical classification of amyloidosis syndromes[2].

Briefly, an amyloid fibril protein is a protein that is deposited as insoluble fibrils, mainly in the extracellular spaces of organs and tissues because of sequential changes in protein folding that result in a condition known as amyloidosis.

From a structural point of view, amyloid fibrils are unbranched, several micrometer long and with a diameter of the order of 10 nm. The existence of differences in amino acid sequences and native structure of the aggregating proteins and peptides arises from the ISA report; thus, three criteria have been identified to define a protein aggregate as an amyloid fibril:

- green birefringence upon staining with Congo Red;

- the fibrillar morphology;

- a universal cross β-sheet quaternary structural organization, in which β-strands are oriented perpendicular to the fibril axis.

In addition, amyloids are very stable, highly resistant to proteolytic degradation and exhibit remarkable mechanical properties with Young's moduli in the range of several GPa[3,4,5].

It has been supposed that the amyloid state could be adopted by many polypeptide sequences and therefore it represents an alternative to the native state of proteins. Thus, it is hypothesized that the cross β-sheet conformation is likely to be the putative cause of the general unique properties of amyloids[6].

Given the high number of diseases associated with amyloid fibrils, the conversion of normally soluble proteins and peptides into amyloid deposits has emerged in recent years as a subject of fundamental importance. In science disciplines,

ranging from physics and chemistry to biology and medicine, with the aim of reaching a thorough understanding of the mechanisms by which protein aggregation occurs and sometimes induces pathogenic behaviour. However, the molecular origin and mechanistic link between amyloid formation and disease aetiology remain unclear.

This lack of comprehension is mainly due to the formidable experimental challenge that is associated with unrevealing amyloid properties and the mechanism of their formation. *In vitro* biophysical studies, mainly based on Thioflavin assay (ThT), infrared spectroscopy and Circular Dichroism[7,8] have been fundamental to shed light into the molecular processes underlying protein aggregation and consequently misfolding diseases.

2.2. Protein misfolding and amyloid formation

The native state of a protein was initially associated with a compact globular conformation possessing a rigid and highly ordered 3D structure. It was demonstrated that the structure of globular proteins is encoded in their amino acids sequences and that these proteins spontaneously fold following a diffusional research of a conformational free energy minimum, which corresponds to the native state[4]. Later on, it was found that only a part of proteins possesses a globular conformation and it has been reported that human proteome can encode proteins with more than 40 consecutive disordered residues. These proteins are termed *intrinsically disordered* proteins (IDPs) and they lack a well-defined 3D structure under physiological conditions. Due to the absence of a precise third structure, IDPs are characterized by a high flexibility that allows them to interact with multiple partners and hence to exert multiple biological functions[9,10].

Globular proteins can also adopt intermediate conformations simply because of thermodynamic fluctuations, which correspond to local minima in their energy landscape[11,12]. It is also supposed that in some cases, partially unfolded states could retain a biological function, such as cellular trafficking and translocations

through mitochondrial and nuclear membranes[13]. The partially folded/unfolded states of a protein, independently of its globular or naturally unfolded conformation, are vulnerable to *misfolding* and to aggregation into amyloid structures[7]. This condition is promoted by conditions that destabilize the native fold of the protein, such as high temperature, high pressure, low pH, organic solvents, natural or post-translational mutations.

The fibrillation process typically takes the form of a nucleation-dependent polymerization reaction[14] and a schematic representation of the aggregation process is reported in **Figure 2.1**[15].
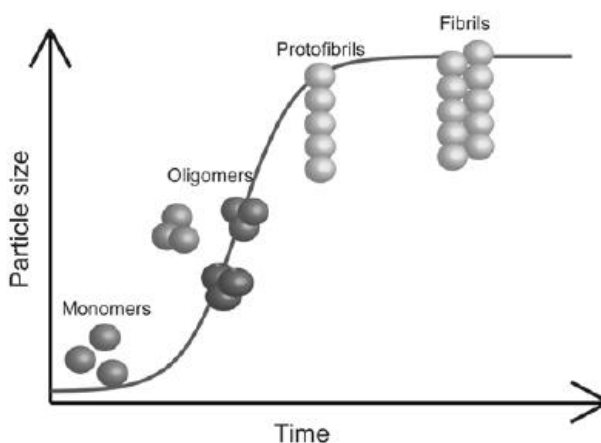
Figure 2.1: Schematic representation of amyloid aggregation process.

This model supposes that the formation of oligomeric structures is necessary to nucleate the first proto-fibrillar structures, ultimately leading to the formation of the mature amyloid fibrils. This process is typically described by a sigmoidal reaction time course, commonly measured by ThT fluorescence and light scattering assays[16,17]. According to the classical nucleation process, a primary nucleation step is necessary for the formation of aggregates, but in the case of amyloid fibrils several secondary steps can also be involved. In these secondary processes, the formation of the nuclei is catalysed either by the fragmentation of the already formed fibrils or through a surface secondary nucleation mechanism,

whereby the existing fibrils act as the nucleation of further nuclei at their surface[18]. Nevertheless, the conventional "first-misfolding-then-aggregation" paradigm is the generally accepted process of amyloid formation, but several observations have shown that the misfolding process could take place after a first step in which native monomers aggregate, i.e. "first-aggregation-then-misfolding". These native oligomers undergo a structural misfolding to form the early cross sheet aggregate whereas the final amyloid fibrillar structures only form in a second step. Despite the initial difference, both pathways are conceptually similar: a misfolded state, monomeric or oligomeric, is necessary to nucleate the formation of the universal amyloidogenic cross β-sheet structure[15].

2.2.1. Aβ and α-synuclein: two case studies

It is widely accepted that Alzheimer and Parkinson disease are associated to intrinsically disordered proteins: the amyloid precursor protein and α-synuclein, respectively[19].

The first indication that protein misfolding and aggregation were involved in neurodegenerative diseases came from post-mortem neuropathological studies. Almost a century ago, Alois Alzheimer described the typical neuropathological hallmarks of the disease that takes his name: neuritic amyloid plaques and neurofibrillary tangles. In the case of Alzheimer disease, amyloid plaques are deposited extracellularly in the brain parenchyma and around the cerebral vessel walls, and their main component is a 40- or 42-residue peptide: amyloid-β protein (Aβ)[20]. It has been observed, in patients with PD, that the cytoplasm of neurons from the *substantia nigra* contains aggregates called Lewy bodies[21], and the major constituents of these aggregates were fragments of α-synuclein. Support for a causal role of protein misfolding in neurodegenerative diseases has come more recently from genetic studies[22]. Mutations in the genes that encode the protein components of fibrillar aggregates are genetically associated with the inherited forms of all neurodegenerative diseases.

Mutations in the respective fibrillar proteins have been found in AD and PD. The generation of transgenic animal models bearing mutant forms of the human genes encoding the fibrillar protein have provided good evidence for the contribution of protein misfolding to disease pathogenesis.

Nevertheless, the pathologies of neurodegenerative diseases are still unclear; indeed, it should be taken into account that many pathways are possible before the mature fibril formation, due to the wide number of species that can perform a function in the biological systems. For example, it is well assessed that Aβ 1-42 and α-synuclein interacts with membranes, in particular with lipid rafts, that are characterized by a high content in gangliosides, sphingomyelin and cholesterol[23,24] however, the role of this interaction in the complex mechanism of cytotoxicity for neuronal cells is still under investigation. In this respect many the efforts are addressed to deciphering the unique mechanism for the neurodegenerative related pathologies.

2.3. The role of membranes

Soluble oligomeric intermediates, rather than fully formed fibrils, are currently recognized as the predominant toxic species, capable of initiating pathogenic events[25]. Many experimental evidences indicate that the interactions with neuronal membranes play an important role in the Aβ 1-42 toxicity[26], but until now the valence (positive or negative) of the membrane action is an open question. Considerable attention has also been focused on the membrane associated state of α-synuclein, which has been suggested to be of great significance in both physiological and pathological contexts. It is indeed evident that α-synuclein exists in vivo in an equilibrium between cytosolic and membrane-bound states, with membrane partitioning being tightly regulated[27].

A particularly intriguing issue in this context is the mechanism by which the affinity of those amyloidogenic protein to lipid membranes is modulated. On one hand, the membrane biophysical properties, such as electrostatic potential,

hydrophobicity, water content, rigidity and curvature, are supposed to affect the amyloidogenic process. Many studies have been carried out with many lipid membranes, consisting on different phospholipids and thus characterized by different lipid phases[28].

In the case of Aβ 1-42 self-aggregation the membrane surface has been proposed to catalyse the first stages of the, acting as template[29], or that lipid bilayers can solubilize preformed Aβ fibrils, leading to the formation of neurotoxic oligomers able to form unregulated ion channels among the phospholipids, which favours membrane disruption. In any case, both processes probably coexist, the prevalence of one of them being determined by the membrane composition[26].

For α-synuclein, there is strong evidence that the population of the bound state is regulated by the intrinsic structural properties of α-synuclein and by the composition and the physical properties of the membrane bilayer, but even in this case it is difficult to rationalize, the proper effect of the lipid membranes in terms of biophysical properties[30].

Although the literature on the effect of lipid bilayer on the aggregation process of amyloid peptide is wide, the question is controversial and still debated.

In the last ten years, it has been proposed that several distinct amyloid proteins could generate a common oligomer structure[31], then a common pathogenesis for various neurodegenerative diseases can occur[32]. In this respect, the discovery of amyloid pores[33] has given a robust structural background for the so-called "calcium hypothesis" of Alzheimer's disease, a concept that has been initially proposed in the early 1990's[34] and has recently gained renewed interest.

Such membrane-embedded structures have been initially described as a class of "annular protofibrils" sharing structural similarities with bacterial cytolysins16. These annular protofibrils, formed by both Aβ and α-synuclein (the protein associated with Parkinson disease), were recognized as a new type of "amyloid" assembly and logically referred to as "amyloid pores". From a functional point of view, amyloid pores behave as Ca^{2+} selective channels responsible for a

dysregulated entry of Ca^{2+} in the cytoplasm of brain cells. The structure of amyloid pores has been extensively studied by ultrastructural methods including atomic force microscopy, and by *in silico* approaches[35]. The constant in the two theories is the affinity that Aβ and α-synuclein has for lipid usually associated to lipid rafts, in particular the cholesterol molecule.

2.3.1. The role of cholesterol

Cholesterol is known to bind to the amyloid protein precursor and α-synuclein[29,36] and to regulate its membrane insertion[37, 38], once the sterol molecule is embedded in lipid rafts. Recently we have shown that cholesterol is required for the assembly of amyloid pores formed by various Aβ peptides: cholesterol promoted the insertion of Aβ in the plasma membrane, induced α-helical structuration, and forced the peptide to adopt a tilted topology that favour the oligomerization process. This finding is consistent with *in vitro* studies indicating that Aβ can form ion channels in planar lipid membranes only in presence of at least 30% cholesterol[39]. Also in the case of α-synuclein, it has been shown that, three distinct regions of this protein (the N-terminal, central and C-terminal segments) interact in very different ways with lipid bilayers as a result of their different structural and dynamical properties. The central segment of the protein (residues 26–97), which can be described as a membrane-sensor region, has intermediate dynamical properties. It is legitimate to assume, however, based on EPR measurements and transferred NOE data[40], that this membrane-sensor region adopts α-helical structure when transiently bound to a lipid membrane surface. A combined study carried out on both the Aβ and α-synuclein using a combination of molecular modelling and physicochemical approaches, shows that they contain both proteins contain a cholesterol-binding domain[35].

So far two linear consensus cholesterol-binding domains have been characterized. The first one is the CRAC domain (an acronym standing for "Cholesterol Recognition/interaction Amino acid Consensus sequence"[41]), which is a short

motif which fulfils the simple algorithm (L/V)-X1-5-(Y)- X1-5-(K,R). Although the CRAC motif has been found in various proteins that bind cholesterol, the simplicity of the consensus sequence defined by only three specific amino acids and up to ten undefined residues (thus referred to as "X" in the algorithm) has raised some scepticism about its predictive value. However, the cholesterol-binding activity of CRAC has been carefully established by mutational studies[42].

The second consensus cholesterol-binding motif is a reversed version of the CRAC algorithm, i.e. (K/R)-X1-5-(Y/F)- X1-5-(L,V) that was logically coined "CARC"[43]. This new cholesterol-binding motif has been discovered in the human nicotinic acetylcholine receptor, whose trans-membrane domains do not display the CRAC motif. Despite all these CRAC domains may have the intrinsic capability to bind cholesterol, their location outside the membrane renders such interactions highly unlikely *in vivo*.

The findings suggest the intriguing possibility of a dual lipid control of membrane permeabilization by amyloid proteins and the roles of cholesterol in the formation of Ca^{2+}permeable amyloid pores.

2.3.2. The effect of omega-3 fatty acids

The adherence to a Mediterranean diet profile, including fish, vegetables, fruits, coffee, and light-to-moderate alcohol intake, seems to reduce the incidence of these pathologies[44]. The beneficial effects of fish are at least partially ascribed to the high content of polyunsaturated fatty acids (PUFAs), and specifically of omega-3 ones[45].

However, the effectiveness of these molecules is still controversial, and their mechanism of action remains elusive. Among other hypotheses, mainly based on the PUFAs radical-scavenging and anti-inflammatory action[46,47], it has been proposed that omega-3 fatty acids, once converted to phospholipids, could alter the structure and functionality of neuronal membranes, whose involvement in AD aetiology is widely accepted[48]. DHA is found in extraordinarily high

concentration in the plasma membranes of neural tissues, reaching up to 50% of the total acyl chains and it is an omega-3 fatty acid that is essential for normal brain growth and cognitive function[49]. Furthermore, its decline has been associated with the loss of memory and learning, suggesting that the omega-3 fatty acids modulate the membranes properties and influence the molecular mechanism of AD[50]. Despite being an abundant fatty acid in brain phospholipids, DHA cannot be *de novo* synthesized in brain and must be imported across the blood–brain barrier, but mechanisms for DHA uptake in brain have remained enigmatic. Recently, it has been identified a member of the major facilitator superfamily - Mfsd2a (previously an orphan transporter) - as the major transporter for DHA uptake into brain[51]. Mfsd2a is found to be expressed exclusively in endothelium of the blood–brain barrier of micro-vessels. Lipidomic analysis indicates that Mfsd2a-deficient (Mfsd2a-knockout) mice show markedly reduced levels of DHA in brain accompanied by neuronal cell loss in hippocampus and cerebellum, as well as cognitive deficits and severe anxiety, and microcephaly. Unexpectedly, cell-based studies indicate that Mfsd2a transports DHA in the form of lyso-phosphatidylcholine (LPC), but not free fatty acid, in a sodium-dependent manner. Moreover, the phosphor-zwitterionic headgroup of LPC is critical for transport. Many studies tried to understand at a molecular level which is the role played by DHA in the amyloid fibrils formation, in the case of Aβ. Recently, the group were I conduced this Ph.D. project found that DHA containing phospholipids are able to solubilize different fragments of Aβ, suggesting that the fluidification effects of such fatty acids in able to internalize peptides in the bilayer, inducing the arrest in the aggregation process [52,53]. Katsaras also shown that the unique conformation of DHA is able to segregates cholesterol in the centre of the bilayer[54] and recent works conduced on a more complex lipid membrane models, containing brain sphingomyelin and cholesterol, demonstrate that DHA has the ability to rearrange phase separated microdomain[55].

In this context, the understanding of the effect of phospholipid containing DHA on dynamics and microstructures of lipid membranes and how those effects can regulate the interaction with amyloid oligomers is crucial. Indeed, even if the role of cholesterol and gangliosides is assessed, the effect of DHA phospholipids on those lipid organization and the consequent interaction with amyloid peptides or protein is still unclear.

2.4. Nucleophosmin-1: an unexpected amyloid protein

Nucleophosmin-1 (NPM1) is an abundant multifunctional protein and a nuclear chaperon[56] essential for embryonic development and prevalently localized in nucleoli[57,58]. It integrates with proteins containing arginine-rich linear motifs (R-motifs) and ribosomal RNA (rRNA) within the nucleolus[59]. Its N-terminal region is an oligomerization domain mainly involved in its chaperone activity, the central portion is an IDR (Intrinsically Disordered Region) that crucially assists[60] the DNA/RNA recognition by the C-terminal domain (CTD)[61,62] that is constituted by a three-helix bundle in which helices H1 and H3 are almost coaxial, whereas the connecting helix H2 is tilted, by $\sim45°$, with respect to other helices (**Figure 2.2**). The bundle is stabilized by a small hydrophobic core, formed by four aromatic residues: Phe[268], Phe[276], Trp[288] and Trp[290] [63]. NPM1 is involved in several biological processes such as ribosome biogenesis, tumor suppression and nucleolar stress response[64]. It was found over-expressed or mutated in tumors of different histological origin and in various hematological malignancies [57,58,65]. It is highly expressed in the brain and in neurons but, herein, its functions are poorly understood: emerging evidences indicate that the nucleolus, of which NPM1 is an important component, has a crucial role in neuronal development and maintenance as well as in neurodegenerative diseases[66]. It was reported that its expression is increased in the striatum of the R6/2 transgenic and 3-nitropropionic acid (3-NP) injected mouse models of Huntington's disease (HD). Its ectopic expression on cultured neurons indicated that increasing NPM1 levels are toxic

to both healthy cerebellar granule cells and cortical neurons and that this toxicity depends on its cytoplasmic localization and oligomerization status[67].
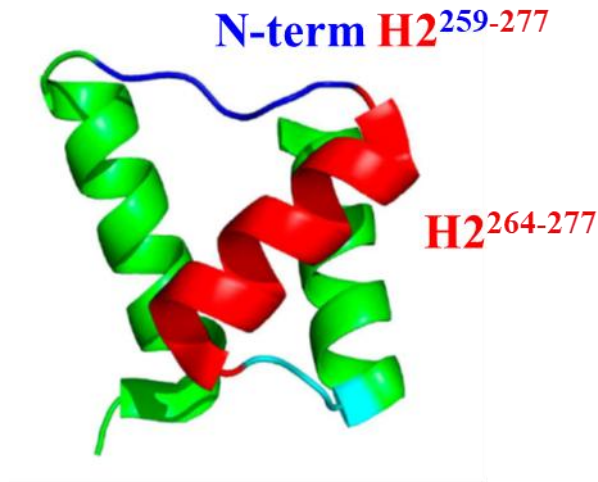
Figure 2.2: Three-helix bundle in which helices H1 and H3 are almost coaxial, whereas the connecting helix H2 is tilted, by ∼45°, with respect to other helices.

Moreover, protein localization in the nucleoplasm or in other cellular compartments was reported for cells exposed to different types of stress[68,69] and appeared driven by the expression levels of its interactors[70]. NPM1 is recognized as the most frequently mutated gene in acute myeloid leukemia (AML) patients, ∼ 30% of cases[71-76,56]. The leukemogenic potential of these mutations still needs to be elucidated: they make the protein unable to bind to G-quadruplexes[77] and cause the aberrant accumulation of this protein in the cytoplasm of leukemic cells (hence the term NPM cytoplasmic positive NPMc+)[75,56,63,78,79]. The cytoplasmatic mislocation of NPM1 causes the loss of its nuclear functions and the impairment of the activities of its interactors. Additionally, AML-NPM1 mutants acquire new properties such as the ability to interact and inhibit the cell death activity of caspase-6 and caspase-8 in the cytoplasm[80]. The induction of the most abundant AML variant, named NPM1-mutA, into Myeloid ELF1-like factor (MEF/ELF4) -overexpressing NIH3T3 cells facilitates leukemic transformation. In addition, clinical leukemia samples with NPM1 mutations presented higher Human Double

Minute 2 homolog (HDM2) mRNA expression, with respect to healthy cells, suggesting a direct link between NPM1 mutants and HDM2 expression in leukemogenesis[81]. Recently it was found that NPM1-mutA enhances the adhesive, migratory and invasive potential of THP-1 leukemia cells *in vitro*, that it directly interacts with Ki-ras2 Kirsten rat sarcoma viral oncogene homolog (K-Ras) and activated MEK/ERK signaling[82] and that its enforced expression inhibits myeloid differentiation of leukemic cells, whereas knockdown of NPM1-mutA has the opposite effect[83].

In order to gain insights into Structure-Activity Relationships (SAR) of isolated protein fragments, NPM1-CTD was previously dissected into three peptides corresponding to the three helices[60] and demonstrated that the H2[84] and several H3-AML mutated variants[85] form amyloid-like assemblies endowed with fibrillar morphology and β-sheet structures that resulted toxic in cell viability assays. In particular, we showed that the H2 sequence is the most amyloidogenic region of NPM1[86] while the extension of the H2 sequence beyond its N-terminus, in the Nterm H2 peptide, delayed aggregation and its associated cytotoxicity in SH-SY5Y cell lines through the influx of extracellular Ca^{2+} ions assay (**Figure 2.3**).

The underlying hypothesis of the investigations carried out in this project, relies in the structural destabilization of the helical bundle of CTD due to AML mutations[63] that causes the exposure of both amyloidogenic regions, H2 and mutated H3 region leading to the formation of toxic aggregates. It is widely accepted that the disruption of intracellular Ca^{2+} homeostasis is one of the earliest biochemical consequences of the interaction of prefibrillar aggregates with cell membranes[87-89]. Furthermore, the oligomer toxicity of amyloidogenic species not only depends on specific structural properties of the oligomers themselves, but also on the biochemical and biophysical properties of the membrane they interact with, in a delicate and complex interplay between the structural and physicochemical features of both[26,90]. Indeed, the influence of cholesterol on the toxicity of the amyloidogenic Aβ-peptide (1-40) and, more specifically, on the

membranotropic propensity of Aβ-peptide fragments[91] has been largely investigated with controversial results[92].
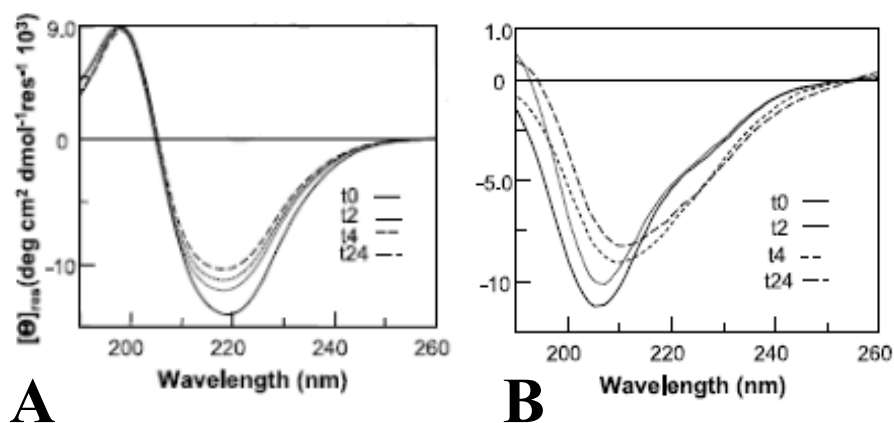
Figure 2.3: circular dichroism spectra over time of A) H2 peptide and B) Nterm H2.

Further it was demonstrated that cholesterol can promote the insertion of Aβ in the plasma membrane, induce α-helical structuration and force sequences to adopt a tilted topology that favoured the oligomerization process[93]. In this context both the modifications of the rigidity of the membrane due to the presence of cholesterol and the direct interaction with cholesterol should be considered[94]. In this last direction previous investigations delineated two consensus amino acidic sequences termed CRAC [(L/V)-$X_{1–5}$-(Y)-$X_{1–5}$-(K/R)] and CARC [(K/R)-$X_{1–5}$-(Y/F)-$X_{1–5}$-(L/V)][41] that, even if not exhaustive, are often recurrent in peptides known to bind cholesterol. In the present work, to shed light on the cytotoxicity mechanisms of amyloidogenic regions of NPM1, their interaction with model lipid membranes were investigated, focusing on both the aggregation behaviour in the presence of Large Unilamellar Vesicles (LUVs) mimicking the cell membrane and the effects that these interactions have on the structure and dynamic of the LUV itself[95]

2.5. References

1 Westermark, P. *et al.* A primer of amyloid nomenclature. *Amyloid : the international journal of experimental and clinical investigation : the official journal of the International Society of Amyloidosis* **14**, 179-183, doi:10.1080/13506120701460923 (2007).

2 Sipe, J. D. *et al.* Amyloid fibril proteins and amyloidosis: chemical identification and clinical classification International Society of Amyloidosis 2016 Nomenclature Guidelines. *Amyloid : the international journal of experimental and clinical investigation : the official journal of the International Society of Amyloidosis* **23**, 209-213, doi:10.1080/13506129.2016.1257986 (2016).

3 Knowles, T. P. J., Vendruscolo, M. & Dobson, C. M. The amyloid state and its association with protein misfolding diseases. *Nat Rev Mol Cell Bio* **15**, 384-396, doi:10.1038/nrm3810 (2014).

4 Dobson, C. M. Protein folding and misfolding. *Nature* **426**, 884-890, doi:10.1038/nature02261 (2003).

5 Lashuel, H. A., Overk, C. R., Oueslati, A. & Masliah, E. The many faces of alpha-synuclein: from structure and toxicity to therapeutic target. *Nature reviews. Neuroscience* **14**, 38-48, doi:10.1038/nrn3406 (2013).

6 Suh, Y. H. & Checler, F. Amyloid precursor protein, presenilins, and alpha-synuclein: molecular pathogenesis and pharmacological applications in Alzheimer's disease. *Pharmacological reviews* **54**, 469-525 (2002).

7 Ruggeri, F. S. *et al.* Influence of the beta-sheet content on the mechanical properties of aggregates during amyloid fibrillization. *Angewandte Chemie* **54**, 2462-2466, doi:10.1002/anie.201409050 (2015).

8 Zandomeneghi, G., Krebs, M. R., McCammon, M. G. & Fandrich, M. FTIR reveals structural differences between native beta-sheet proteins and amyloid fibrils. *Protein science : a publication of the Protein Society* **13**, 3314-3321, doi:10.1110/ps.041024904 (2004).

9 Habchi, J., Tompa, P., Longhi, S. & Uversky, V. N. Introducing protein intrinsic disorder. *Chemical reviews* **114**, 6561-6588, doi:10.1021/cr400514h (2014).

10 Turoverov, K. K., Kuznetsova, I. M. & Uversky, V. N. The protein kingdom extended: ordered and intrinsically disordered proteins, their folding, supramolecular complex formation, and aggregation. *Progress in biophysics and molecular biology* **102**, 73-84, doi:10.1016/j.pbiomolbio.2010.01.003 (2010).

11 Onuchic, J. N., Luthey-Schulten, Z. & Wolynes, P. G. Theory of protein folding: the energy landscape perspective. *Annual review of physical chemistry* **48**, 545-600, doi:10.1146/annurev.physchem.48.1.545 (1997).

12 Baldwin, A. J. *et al.* Metastability of Native Proteins and the Phenomenon of Amyloid Formation. *J Am Chem Soc* **133**, 14160-14163, doi:10.1021/ja2017703 (2011).

13 Chua, C. E. & Tang, B. L. Rabs, SNAREs and alpha-synuclein--membrane trafficking defects in synucleinopathies. *Brain research reviews* **67**, 268-281, doi:10.1016/j.brainresrev.2011.03.002 (2011).

14 Nayak, A., Sorci, M., Krueger, S. & Belfort, G. A universal pathway for amyloid nucleus and precursor formation for insulin. *Proteins* **74**, 556-565, doi:10.1002/prot.22169 (2009).

15 Ruggeri, F. S., Habchi, J., Cerreta, A. & Dietler, G. AFM-Based Single Molecule Techniques: Unraveling the Amyloid Pathogenic Species. *Current pharmaceutical design* **22**, 3950-3970 (2016).

16 LeVine, H., 3rd. Quantification of beta-sheet amyloid fibril structures with thioflavin T. *Methods in enzymology* **309**, 274-284 (1999).

17 Cohen, S. I., Vendruscolo, M., Dobson, C. M. & Knowles, T. P. From macroscopic measurements to microscopic mechanisms of protein aggregation. *Journal of molecular biology* **421**, 160-171, doi:10.1016/j.jmb.2012.02.031 (2012).

18 Kakio, A., Nishimoto, S., Yanagisawa, K., Kozutsumi, Y. & Matsuzaki, K. Interactions of amyloid beta-protein with various gangliosides in raft-like membranes: importance of GM1

ganglioside-bound form as an endogenous seed for Alzheimer amyloid. *Biochemistry* **41**, 7385-7390 (2002).

19 Soto, C. Unfolding the role of protein misfolding in neurodegenerative diseases. *Nature reviews. Neuroscience* **4**, 49-60, doi:10.1038/nrn1007 (2003).

20 Glenner, G. G. & Wong, C. W. Alzheimer's disease: initial report of the purification and characterization of a novel cerebrovascular amyloid protein. 1984. *Biochemical and biophysical research communications* **425**, 534-539, doi:10.1016/j.bbrc.2012.08.020 (2012).

21 Forno, L. S. Neuropathology of Parkinson's disease. *Journal of neuropathology and experimental neurology* **55**, 259-272 (1996).

22 Hardy, J. & Gwinn-Hardy, K. Genetic classification of primary neurodegenerative disease. *Science* **282**, 1075-1079 (1998).

23 Park, J. Y. *et al.* ON THE MECHANISM OF INTERNALIZATION OF alpha-SYNUCLEIN INTO MICROGLIA: ROLES OF GANGLIOSIDE GM1 AND LIPID-RAFT. *Glia* **57**, S131-S131 (2009).

24 Kakio, A., Nishimoto, S., Kozutsumi, Y. & Matsuzaki, K. Formation of a membrane-active form of amyloid beta-protein in raft-like model membranes. *Biochemical and biophysical research communications* **303**, 514-518 (2003).

25 Sengupta, U., Nilson, A. N. & Kayed, R. The Role of Amyloid-beta Oligomers in Toxicity, Propagation, and Immunotherapy. *Ebiomedicine* **6**, 42-49, doi:10.1016/j.ebiom.2016.03.035 (2016).

26 Cecchi, C. & Stefani, M. The amyloid-cell membrane system. The interplay between the biophysical features of oligomers/fibrils and cell membrane defines amyloid toxicity. *Biophysical chemistry* **182**, 30-43, doi:10.1016/j.bpc.2013.06.003 (2013).

27 Bodner, C. R., Dobson, C. M. & Bax, A. Multiple tight phospholipid-binding modes of alpha-synuclein revealed by solution NMR spectroscopy. *Journal of molecular biology* **390**, 775-790, doi:10.1016/j.jmb.2009.05.066 (2009).

28 Valincius, G. *et al.* Soluble amyloid beta-oligomers affect dielectric membrane properties by bilayer insertion and domain formation: implications for cell toxicity. *Biophysical journal* **95**, 4845-4861, doi:10.1529/biophysj.108.130997 (2008).

29 Matsuzaki, K. Physicochemical interactions of amyloid beta-peptide with lipid bilayers. *Biochimica et biophysica acta* **1768**, 1935-1942, doi:10.1016/j.bbamem.2007.02.009 (2007).

30 Fantini, J., Carlus, D. & Yahi, N. The fusogenic tilted peptide (67-78) of alpha-synuclein is a cholesterol binding domain. *Biochimica et biophysica acta* **1808**, 2343-2351, doi:10.1016/j.bbamem.2011.06.017 (2011).

31 Jang, H. *et al.* Structural Convergence Among Diverse, Toxic beta-Sheet Ion Channels. *J Phys Chem B* **114**, 9445-9451, doi:10.1021/jp104073k (2010).

32 Kayed, R. *et al.* Common structure of soluble amyloid oligomers implies common mechanism of pathogenesis. *Science* **300**, 486-489, doi:DOI 10.1126/science.1079469 (2003).

33 Lashuel, H. A., Hartley, D., Petre, B. M., Walz, T. & Lansbury, P. T., Jr. Neurodegenerative disease: amyloid pores from pathogenic mutations. *Nature* **418**, 291, doi:10.1038/418291a (2002).

34 Pollard, H. B., Rojas, E. & Arispe, N. A new hypothesis for the mechanism of amyloid toxicity, based on the calcium channel activity of amyloid beta protein (A beta P) in phospholipid bilayer membranes. *Annals of the New York Academy of Sciences* **695**, 165-168 (1993).

35 Di Scala, C. *et al.* Common molecular mechanism of amyloid pore formation by Alzheimer's beta-amyloid peptide and alpha-synuclein. *Sci Rep-Uk* **6**, doi:Artn 2878110.1038/Srep28781 (2016).

36 Fortin, D. L. *et al.* Lipid rafts mediate the synaptic localization of alpha-synuclein. *The Journal of neuroscience : the official journal of the Society for Neuroscience* **24**, 6715-6723, doi:10.1523/JNEUROSCI.1594-04.2004 (2004).

37 Lahdo, R. & De La Fourniere-Bessueille, L. Insertion of the amyloid precursor protein into lipid monolayers: effects of cholesterol and apolipoprotein E. *The Biochemical journal* **382**, 987-994, doi:10.1042/BJ20040777 (2004).

38 Kubo, S. *et al.* A combinatorial code for the interaction of alpha-synuclein with membranes. *The Journal of biological chemistry* **280**, 31664-31672, doi:10.1074/jbc.M504894200 (2005).

39 Di Scala, C. *et al.* Mechanism of cholesterol-assisted oligomeric channel formation by a short Alzheimer beta-amyloid peptide. *Journal of neurochemistry* **128**, 186-195, doi:10.1111/jnc.12390 (2014).

40 Vilar, M. *et al.* The fold of alpha-synuclein fibrils. *P Natl Acad Sci USA* **105**, 8637-8642, doi:10.1073/pnas.0712179105 (2008).

41 Li, H. & Papadopoulos, V. Peripheral-type benzodiazepine receptor function in cholesterol transport. Identification of a putative cholesterol recognition/interaction amino acid sequence and consensus pattern. *Endocrinology* **139**, 4991-4997, doi:10.1210/endo.139.12.6390 (1998).

42 Epand, R. M. Cholesterol and the interaction of proteins with membrane domains. *Progress in lipid research* **45**, 279-294, doi:10.1016/j.plipres.2006.02.001 (2006).

43 Fantini, J. & Barrantes, F. J. How cholesterol interacts with membrane proteins: an exploration of cholesterol-binding sites including CRAC, CARC, and tilted domains. *Frontiers in physiology* **4**, 31, doi:10.3389/fphys.2013.00031 (2013).

44 Singh, B. *et al.* Association of mediterranean diet with mild cognitive impairment and Alzheimer's disease: a systematic review and meta-analysis. *Journal of Alzheimer's disease : JAD* **39**, 271-282, doi:10.3233/JAD-130830 (2014).

45 Cunnane, S. C. *et al.* Fish, docosahexaenoic acid and Alzheimer's disease. *Progress in lipid research* **48**, 239-256, doi:10.1016/j.plipres.2009.04.001 (2009).

46 Bazinet, R. P. & Laye, S. Polyunsaturated fatty acids and their metabolites in brain function and disease. *Nature reviews. Neuroscience* **15**, 771-785, doi:10.1038/nrn3820 (2014).

47 Hjorth, E. *et al.* Omega-3 fatty acids enhance phagocytosis of Alzheimer's disease-related amyloid-beta42 by human microglia and decrease inflammatory markers. *Journal of Alzheimer's disease : JAD* **35**, 697-713, doi:10.3233/JAD-130131 (2013).

48 Williamson, R. & Sutherland, C. Neuronal Membranes are Key to the Pathogenesis of Alzheimer's Disease: the Role of Both Raft and Non-Raft Membrane Domains. *Curr Alzheimer Res* **8**, 213-221 (2011).

49 Shaikh, S. R., Kinnun, J. J., Leng, X. L., Williams, J. A. & Wassall, S. R. How polyunsaturated fatty acids modify molecular organization in membranes: Insight from NMR studies of model systems. *Bba-Biomembranes* **1848**, 211-219, doi:10.1016/j.bbamem.2014.04.020 (2015).

50 Escriba, P. V. *et al.* Membrane lipid therapy: Modulation of the cell membrane composition and structure as a molecular base for drug discovery and new disease treatment. *Progress in lipid research* **59**, 38-53, doi:10.1016/j.plipres.2015.04.003 (2015).

51 Nguyen, L. N. *et al.* Mfsd2a is a transporter for the essential omega-3 fatty acid docosahexaenoic acid. *Nature* **509**, 503-+, doi:10.1038/nature13241 (2014).

52 Vitiello, G., Di Marino, S., D'Ursi, A. M. & D'Errico, G. Omega-3 fatty acids regulate the interaction of the Alzheimer's abeta(25-35) peptide with lipid membranes. *Langmuir : the ACS journal of surfaces and colloids* **29**, 14239-14245, doi:10.1021/la403416b (2013).

53 Emendato, A. *et al.* Preferential interaction of the Alzheimer peptide Abeta-(1-42) with Omega-3-containing lipid bilayers: structure and interaction studies. *FEBS letters* **590**, 582-591, doi:10.1002/1873-3468.12082 (2016).

54 Kucerka, N. *et al.* The functional significance of lipid diversity: orientation of cholesterol in bilayers is determined by lipid species. *J Am Chem Soc* **131**, 16358-16359, doi:10.1021/ja907659u (2009).

55 Konyakhina, T. M. & Feigenson, G. W. Phase diagram of a polyunsaturated lipid mixture: Brain sphingomyelin/1-stearoyl-2-docosahexaenoyl-sn-glycero-3-phosphocholine/cholesterol. *Biochimica et biophysica acta* **1858**, 153-161, doi:10.1016/j.bbamem.2015.10.016 (2016).

56 Falini, B. *et al.* Altered nucleophosmin transport in acute myeloid leukaemia with mutated NPM1: molecular basis and clinical implications. *Leukemia* **23**, 1731-1743, doi:10.1038/leu.2009.124 (2009).

57   Maggi, L. B., Jr. *et al.* Nucleophosmin serves as a rate-limiting nuclear export chaperone for the Mammalian ribosome. *Molecular and cellular biology* **28**, 7050-7065, doi:10.1128/MCB.01548-07 (2008).

58   Colombo, E., Alcalay, M. & Pelicci, P. G. Nucleophosmin and its complex network: a possible therapeutic target in hematological diseases. *Oncogene* **30**, 2595-2609, doi:10.1038/onc.2010.646 (2011).

59   Mitrea, D. M. *et al.* Nucleophosmin integrates within the nucleolus via multi-modal interactions with proteins displaying R-rich linear motifs and rRNA. *eLife* **5**, doi:10.7554/eLife.13571 (2016).

60   Scognamiglio, P. L. *et al.* G-quadruplex DNA recognition by nucleophosmin: new insights from protein dissection. *Biochimica et biophysica acta* **1840**, 2050-2059, doi:10.1016/j.bbagen.2014.02.017 (2014).

61   Gallo, A. *et al.* Structure of nucleophosmin DNA-binding domain and analysis of its complex with a G-quadruplex sequence from the c-MYC promoter. *J Biol Chem* **287**, 26539-26548, doi:10.1074/jbc.M112.371013 (2012).

62   Arcovito, A. *et al.* Synergic role of nucleophosmin three-helix bundle and a flanking unstructured tail in the interaction with G-quadruplex DNA. *J Biol Chem* **289**, 21230-21241, doi:10.1074/jbc.M114.565010 (2014).

63   Grummitt, C. G., Townsley, F. M., Johnson, C. M., Warren, A. J. & Bycroft, M. Structural consequences of nucleophosmin mutations in acute myeloid leukemia. *The Journal of biological chemistry* **283**, 23326-23332, doi:10.1074/jbc.M801706200 (2008).

64   Okuwaki, M., Iwamatsu, A., Tsujimoto, M. & Nagata, K. Identification of nucleophosmin/B23, an acidic nucleolar protein, as a stimulatory factor for in vitro replication of adenovirus DNA complexed with viral basic core proteins. *Journal of molecular biology* **311**, 41-55, doi:10.1006/jmbi.2001.4812 (2001).

65   Grisendi, S., Mecucci, C., Falini, B. & Pandolfi, P. P. Nucleophosmin and cancer. *Nature reviews. Cancer* **6**, 493-505, doi:10.1038/nrc1885 (2006).

66   Hetman, M. & Pietrzak, M. Emerging roles of the neuronal nucleolus. *Trends in neurosciences* **35**, 305-314, doi:10.1016/j.tins.2012.01.002 (2012).

67   Pfister, J. A. & D'Mello, S. R. Regulation of Neuronal Survival by Nucleophosmin 1 (NPM1) Is Dependent on Its Expression Level, Subcellular Localization, and Oligomerization Status. *J Biol Chem* **291**, 20787-20797, doi:10.1074/jbc.M116.723015 (2016).

68   Yogev, O., Saadon, K., Anzi, S., Inoue, K. & Shaulian, E. DNA damage-dependent translocation of B23 and p19 ARF is regulated by the Jun N-terminal kinase pathway. *Cancer Res* **68**, 1398-1406, doi:10.1158/0008-5472.CAN-07-2865 (2008).

69   Dhar, S. K. & St Clair, D. K. Nucleophosmin blocks mitochondrial localization of p53 and apoptosis. *The Journal of biological chemistry* **284**, 16409-16418, doi:10.1074/jbc.M109.005736 (2009).

70   Zoughlami, Y., van Stalborgh, A. M., van Hennik, P. B. & Hordijk, P. L. Nucleophosmin1 Is a Negative Regulator of the Small GTPase Rac1. *PloS one* **8**, doi:ARTN e68477 10.1371/journal.pone.0068477 (2013).

71   Balusu, R. *et al.* Targeting levels or oligomerization of nucleophosmin 1 induces differentiation and loss of survival of human AML cells with mutant NPM1. *Blood* **118**, 3096-3106, doi:10.1182/blood-2010-09-309674 (2011).

72   Falini, B. *et al.* Immunohistochemistry predicts nucleophosmin (NPM) mutations in acute myeloid leukemia. *Blood* **108**, 1999-2005, doi:10.1182/blood-2006-03-007013 (2006).

73   Falini, B. *et al.* Cytoplasmic nucleophosmin in acute myelogenous leukemia with a normal karyotype. *The New England journal of medicine* **352**, 254-266, doi:10.1056/NEJMoa041974 (2005).

74   Falini, B. *et al.* Translocations and mutations involving the nucleophosmin (NPM1) gene in lymphomas and leukemias. *Haematologica* **92**, 519-532 (2007).

75 Falini, B., Nicoletti, I., Martelli, M. F. & Mecucci, C. Acute myeloid leukemia carrying cytoplasmic/mutated nucleophosmin (NPMc+ AML): biologic and clinical features. *Blood* **109**, 874-885, doi:10.1182/blood-2006-07-012252 (2007).

76 Okuwaki, M. *et al.* Function of homo- and hetero-oligomers of human nucleoplasmin/nucleophosmin family proteins NPM1, NPM2 and NPM3 during sperm chromatin remodeling. *Nucleic acids research* **40**, 4861-4878, doi:10.1093/nar/gks162 (2012).

77 Chiarella, S. *et al.* Nucleophosmin mutations alter its nucleolar localization by impairing G-quadruplex binding at ribosomal DNA. *Nucleic Acids Res* **41**, 3228-3239, doi:10.1093/nar/gkt001 (2013).

78 Scaloni, F., Gianni, S., Federici, L., Falini, B. & Brunori, M. Folding mechanism of the C-terminal domain of nucleophosmin: residual structure in the denatured state and its pathophysiological significance. *FASEB journal : official publication of the Federation of American Societies for Experimental Biology* **23**, 2360-2365, doi:10.1096/fj.08-128306 (2009).

79 Scaloni, F., Federici, L., Brunori, M. & Gianni, S. Deciphering the folding transition state structure and denatured state properties of nucleophosmin C-terminal domain. *Proceedings of the National Academy of Sciences of the United States of America* **107**, 5447-5452, doi:10.1073/pnas.0910516107 (2010).

80 Leong, S. M. *et al.* Mutant nucleophosmin deregulates cell death and myeloid differentiation through excessive caspase-6 and -8 inhibition. *Blood* **116**, 3286-3296, doi:10.1182/blood-2009-12-256149 (2010).

81 Ando, K. *et al.* Mutations in the nucleolar phosphoprotein, nucleophosmin, promote the expression of the oncogenic transcription factor MEF/ELF4 in leukemia cells and potentiates transformation. *J Biol Chem* **288**, 9457-9467, doi:10.1074/jbc.M112.415703 (2013).

82 Xian, J. *et al.* Nucleophosmin Mutants Promote Adhesion, Migration and Invasion of Human Leukemia THP-1 Cells through MMPs Up-regulation via Ras/ERK MAPK Signaling. *International journal of biological sciences* **12**, 144-155, doi:10.7150/ijbs.13382 (2016).

83 Zou, Q. *et al.* The human nucleophosmin 1 mutation A inhibits myeloid differentiation of leukemia cells by modulating miR-10b. *Oncotarget* **7**, 71477-71490, doi:10.18632/oncotarget.12216 (2016).

84 Di Natale, C. *et al.* Nucleophosmin contains amyloidogenic regions that are able to form toxic aggregates under physiological conditions. *FASEB journal : official publication of the Federation of American Societies for Experimental Biology*, doi:10.1096/fj.14-269522 (2015).

85 Scognamiglio, P. L. *et al.* Destabilisation, aggregation, toxicity and cytosolic mislocalisation of nucleophosmin regions associated with acute myeloid leukemia. *Oncotarget*, doi:10.18632/oncotarget.10991 (2016).

86 Russo, A. *et al.* Insights into amyloid-like aggregation of H2 region of the C-terminal domain of nucleophosmin. *Biochimica et biophysica acta* **1865**, 176-185, doi:10.1016/j.bbapap.2016.11.006 (2017).

87 Kourie, J. I. Mechanisms of prion-induced modifications in membrane transport properties: implications for signal transduction and neurotoxicity. *Chem Biol Interact* **138**, 1-26, doi:S0009279701002289 [pii] (2001).

88 Demuro, A. *et al.* Calcium dysregulation and membrane disruption as a ubiquitous neurotoxic mechanism of soluble amyloid oligomers. *J Biol Chem* **280**, 17294-17300, doi:M500997200 [pii]10.1074/jbc.M500997200 (2005).

89 Baglioni, S. *et al.* Prefibrillar amyloid aggregates could be generic toxins in higher organisms. *The Journal of neuroscience : the official journal of the Society for Neuroscience* **26**, 8160-8167, doi:10.1523/JNEUROSCI.4809-05.2006 (2006).

90 Evangelisti, E. *et al.* Membrane lipid composition and its physicochemical properties define cell vulnerability to aberrant protein oligomers. *Journal of cell science* **125**, 2416-2427, doi:10.1242/jcs.098434 (2012).

91 D'Errico, G. *et al.* Interaction between Alzheimer's Abeta(25-35) peptide and phospholipid bilayers: the role of cholesterol. *Biochimica et biophysica acta* **1778**, 2710-2716, doi:10.1016/j.bbamem.2008.07.014 (2008).

92 Wood, W. G., Li, L., Muller, W. E. & Eckert, G. P. Cholesterol as a causative factor in Alzheimer's disease: a debatable hypothesis. *J Neurochem* **129**, 559-572, doi:10.1111/jnc.12637 (2014).

93 Di Scala, C., Chahinian, H., Yahi, N., Garmy, N. & Fantini, J. Interaction of Alzheimer's beta-Amyloid Peptides with Cholesterol: Mechanistic Insights into Amyloid Pore Formation. *Biochemistry* **53**, 4489-4502, doi:10.1021/bi500373k (2014).

94 Vitiello, G. *et al.* Fusion of raft-like lipid bilayers operated by a membranotropic domain of the HSV-type I glycoprotein gH occurs through a cholesterol-dependent mechanism. *Soft Matter* **11**, 3003-3016, doi:10.1039/c4sm02769h (2015).

95 Hane, F., Drolle, E., Gaikwad, R., Faught, E. & Leonenko, Z. Amyloid-beta aggregation on model lipid membranes: an atomic force microscopy study. *Journal of Alzheimer's disease : JAD* **26**, 485-494, doi:10.3233/JAD-2011-102112 (2011).

Chapter 3:

Effect of DHA-phospholipids

# on L$_\alpha$ phases

3.1. Work outline

DocosaHexaenoic Acid (DHA) is the longest and most unsaturated fatty acid present in cell membranes, playing a pivotal role in the prevention of cardiovascular diseases and cancer and exerting a strong neuroprotective effect[1]. Among other hypotheses, mainly based on their radical-scavenging and anti-inflammatory action[2] it has been proposed that omega-3 fatty acids, to which DHA belongs, once converted to lipids could alter the structure of biological membranes, whose involvement in major biological processes, such as signaling and protein trafficking, is reported. However, how one molecule can be associated to many different beneficial effects is still unclear.

Lipid diversity regulates a wealth of biomembranes processes, because these molecules can tune the physicochemical characteristics of the lipid bilayer, such as elasticity, curvature, surface charge, hydration and the formation of domains by specific interactions involving the chemical structure, conformation and dynamics of the lipid head groups and acyl chains. For instance, it has been shown that certain lipids can promote non-lamellar phase formation, such as inverted hexagonal and cubic phases, as well as favor insertion of proteins into the membrane. These lipids, including sphingolipids and lysolipids, are defined non-bilayer lipids. Moreover, both theoretical and experimental data provide clear indications that, at least transiently, non-lamellar structural intermediates must exist *in vivo*[3].

With the aim to understand the functional role of DHA, two different phospholipids containing this fatty acid, i.e. 1-stearoyl-2-docosahexanoyl-*sn*-glycero-phpsphocholine and 1,2-didocosahexanoyl-glycero-phosphocholine, reported in **Figure 3.1**, were characterized at different scale levels, from microstructure to overall morphology. The effect on liquid crystalline phases, L_{α}, a liquid disordered (L_d) one, consisting on 1-palmitoyl-2-oleyl-*sn*-glycero-phpsphocholine (POPC), and a liquid ordered (L_o) phase, consisting on POPC/Cholesterol with a mole ratio 6/4 (POPC/Chol), was investigated by means

of different physico-chemical techniques such as Electron Spin Resonance (ESR) spectroscopy with the spin-labelling approach and Neutron Reflectivity (NR).

SDPC   **DDPC**
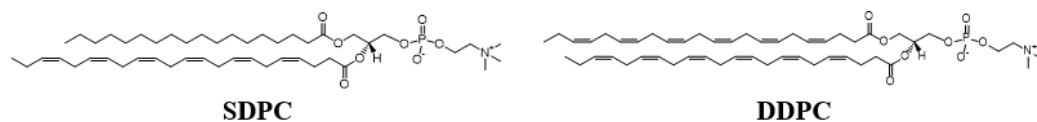
Figure 3.1: structures of the two phospholipids under investigation.

3.2. Materials and methods

Materials

Chloroform, dichloromethane and methanol, HPLC-grade solvents, were obtained from Merck (Darmstadt, Germany). 1-Palmitoyl-2-oleoyl-*sn*-glycero-3-phosphatidylcholine (POPC), 1-d31-Palmitoyl-2-oleoyl-*sn*-glycero-3-phosphatidylcholine (dPOPC), 1-stearoyl-2-docosahexaenoyl-*sn*-glycero-3-phosphocholine (SDPC), 1,2-didocosahexaenoyl-*sn*-glycero-3-phosphocholine (DDPC) were obtained from Avanti Polar Lipids (Birmingham, AL, USA). Spin-labelled phosphatidylcholines (1-palmitoyl-2-stearoyl-(n-doxyl)-*sn*-glycero-3-phosphocholine, *n*-PCSL) with the nitroxide group in the positions 5, 7, 10 and 14 of the acyl chain and 25-doxyl-cholesterol were also obtained from Avanti Polar Lipids. Cholesterol (Chol), D_2O (99% purity) and Phosphate Buffer Saline (PBS) tabs were provided from Sigma Aldrich (St. Louis, MO).

Lipid mixtures preparation

All lipid mixtures were prepared mixing appropriate amounts of lipids, dissolved in a chloroform/methanol (2:1 v/v) in a round-bottom test tube. For Electron Spin Resonance measurements spin-labeled phosphatidylcholines (*n*-PCSL) were alternatively added to the lipid mixture (1% mol% on the total lipid) by mixing appropriate amounts of a spin-label solution in ethanol (1 mg/mL) with the lipid organic mixture. A thin lipid film was produced by evaporating the solvents with dry nitrogen gas and final traces of solvents were removed by subjecting the

sample to vacuum desiccation for at least 3 h. The samples were then hydrated with the proper amount of buffer (i.e. PBS, Phosphate buffer 10mM) pH=7.4, repeatedly vortexed, avoiding any further treatment of the samples.

Supported lipid bilayer.

Neutron reflectometry measurements were performed on lipid bilayers deposited on monocrystalline silicon supports through the vesicle fusion protocol[4]. A vesicle suspension, 0.5 mM, prepared in PBS-D_2O was injected in the solid-liquid reflectometry flow cell and equilibrated with the silicon support surface for 30 min. Then pure D2O was injected into the cell, leading to the rupture of the vesicles and formation of the desired planar lipid bilayers.

Control for lipid breakdown

PUFA breakdown is readily initiated by free-radical formation and subsequent propagation of a chain-reaction that proceeds autocatalytically. In order to minimize the lipid breakdown our protocol produces consist on reducing factors such as oxygen, light and iron ions. All physical handling of lipids is performed in an inert atmosphere under low light conditions. All solvents and buffers were deoxygenated by bubbling with inert gas to carry away dissolved oxygen. The UV spectroscopic assay for lipid breakdown was used. Samples for UV spectroscopic assay were prepared by a dilution of the aqueous MLVs suspensions. Lipids without conjugated double bonds have a single strong absorption peak at ~200 nm. Breakdown-induced conjugation yields a strong peak at 235 nm. The ratio of peak heights at 235/200 was used to monitor breakdown.

Electron Spin Resonance (ESR) Spectroscopy

ESR spectra were recorded with a 9 GHz Bruker Elexys E-500 spectrometer (Bruker, Rheinstetten, Germany). The capillaries containing MLVs suspensions, were placed in a standard 4 mm quartz sample tube containing light silicone oil for thermal stability. All the measurements were performed at 25 °C. Spectra were recorded using the following instrumental settings: sweep width, 100 G; resolution, 1024 points; time constant, 20.48 ms; modulation frequency, 100 kHz;

modulation amplitude, 1.0 G; incident power, 6.37 mW. Several scans, typically 16, were accumulated to improve the signal-to-noise ratio. For the spectra simulation the g_{ii} values for the coupling between the electron spin and the magnetic field were these which gave the best fitting for all spectra: g_{ii}=2.0075, 2.006, 2.003. In some cases, due to fitting improvements, 2.0027 was used instead of 2.003 for g_{zz}. About the A_{ii} values for the coupling between the electron spin and the nitrogen nuclear spin, which give a measure of the environmental polarity, we maintained constant A_{xx}=7.1 G and A_{yy}=7.2 G values, which were also well fitting all the spectra, while it was needed to change the A_{zz} value from one to another system, where we list the $<A>=(A_{xx}+A_{yy}+A_{zz})/3$ values. In order to quantitatively analyse the spectra, we calculated the order parameter, **S**, using a spectra parameterization method defined in **Equation 3.1**.

$$S = \frac{T_{\parallel} - T_{\perp}}{T_{zz} - T_{xx}} \cdot \frac{a_N}{a\prime_N} \qquad \textbf{Eq.3.1}$$

Where:

- T_{xx} and T_{zz} are the principal elements of the real hyperfine splitting tensor in the spin Hamiltonian of the spin-label, which can be measured from the corresponding single-crystal EPR spectrum and are reported in the literature (T_{xx}=6.1 G and T_{zz}=32.4 G)[5];

- $T_{\parallel}$ and $T_{\perp}$ are two phenomenological hyperfine splitting parameters which can be determined experimentally for each spin-labeled phospholipid as shown in **Figure 3.2** (note that $T_{\perp} = \frac{2T'_{\perp}+1.16}{2}$)[6].

- a_N is the isotropic hyperfine coupling constants for the spin-label in crystal state, given by $a_N = \frac{1}{3} \cdot (T_{zz} - 2T_{xx})$;

- a'$_N$ is the spin-label isotropic hyperfine coupling constant given by $a'_N = \frac{1}{3} \cdot (T_{\parallel} - 2T_{\perp})$.
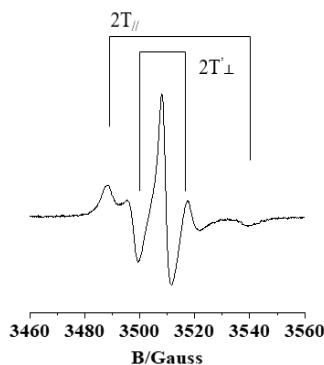
Figure 3.2: Two phenomenological hyperfine splitting parameters for 5-PCSL spectrum.

S is a measure of the local orientational ordering of the labelled acyl chain with respect to the normal to the bilayer surface, therefore is an index of the acyl chain mobility and then of their microstructural state.

Neutron Reflectivity (NR)

NR allows determining structure and composition of layers at interfaces. Measurements were performed on the D17 reflectometer[7] at the high flux reactor of the Institute Laue-Langevin (ILL, Grenoble, France) in time-of-flight mode using a spread of wavelengths between 2 and 20 Å with two incoming angles of 0.8 and 3.2° and on Maria reflectometer[8] of the Jülich Centre for Neutron Science at MLZ (Garching, Germany) varying the incidence angle of the incoming beam using two different wavelengths: 12 Å for the low-q region and 6 Å for the high-q region up to 0.20 Å^{-1}, with a wavelength spread $\Delta\lambda/\lambda = 0.1$. The specular reflection at the silicon/water interface, *R(q),* defined as the ratio between the reflected and the incoming intensities of a neutron beam, is measured as a function of the wave vector transfer, *q*, perpendicular to the reflecting surface. *R(q)* is related to the scattering length density across the interface, ρ*(z),* which depends on the composition of the adsorbed species. The neutron scattering length density, ρ*(z)*, is defined by the following relation:

$$\rho(z) = \sum_j n_j(z)b_j \quad \textbf{Eq.3.2}$$

where $n_j(z)$ is the number of nuclei per unit volume and b_j is the scattering length of nucleus j. The scattering lengths of the constituent fragments of any species adsorbed at the surface are the fundamental quantities from which the interfacial properties and microstructural information on the lipid bilayer are derived. The theoretical ρ values of the used lipids were calculated through **Eq.3.2**, are shown in **Table 3.1**. The volume chain was calculated according with Koenig et al.[9]

Table 3.1: Parameters used for the fitting of reflectivity profiles.

	d31-POPC	POPC	DDPC	SDPC	Chol
$V_{headgroup}$ (Å^3)	322.1	322.1	322.1	322.1	602
$\rho_{headgroup}$ ($\times 10^{-6}$ Å^{-2})	1.86	1.86	1.86	1.86	0.22
V_{chains} (Å^3)	933.7	933.7	1137.36	1093.52	
ρ_{chains} ($\times 10^{-6}$ Å^{-2})	3.1	-0.36	0.36	-0.018	

Measurement of a sample in different solvent contrasts greatly enhances the sensitivity of the technique[10]. Samples were measured using H_2O, SMW (silicon-matched water) and D_2O as solvent contrasts. SMW ($\rho = 2.07 \times 10^{-6}$ Å^{-2}) is a mixture of 38 vol % D_2O ($\rho = 6.35 \times 10^{-6}$ Å^{-2}) and 62 vol % H_2O ($\rho = -0.56 \times 10^{-6}$ Å^{-2}) with the same refraction index for neutrons as a bulk silicon. Neutron Reflectivity profiles were analysed by box model, **Figure 3.3**, fitting starting with simulations from the AuroreNR program[10]. The supported membrane is modelled as a series of boxes corresponding to the different bilayer regions. The program allows the simultaneous analysis of reflectivity profiles from the same sample in different water contrasts, characterizing each box by its thickness, scattering length density (ρ), solvent volume fraction, and interfacial roughness. All the parameters were varied until the optimum fit to the data was found. Although more than one model could be found for a given experimental curve, the number of possible models was greatly reduced by a prior knowledge of the system, which

allows defining upper and lower limits of the parameters to be optimized, by the elimination of the physically meaningless parameters, and most importantly by the use of different isotopic contrasts.
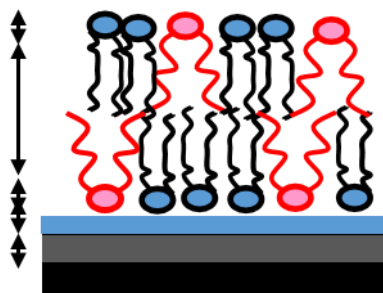
Figure 3.3: Schematic representation of the five boxes model used for the NR curves fit.

The bare silicon substrate was characterized first in terms of thickness and roughness of the native oxide layer. The set of NR profiles were calculated for a uniform single layer model (the silicon oxide layer) of thickness 10 ± 1 Å, roughness 3 ± 1 Å, and a scattering length density of 3.41×10^{-6} Å^{-2}, corresponding to 100% SiO$_2$. This step was followed by the characterization of the lipid bilayers with different composition.

Cryogenic transmission electron microscopy

Cryogenic transmission electron microscopy (cryo-TEM) images were carried out at the Heinz Maier-Leibnitz Zentrum, Garching, Germany on a JEOL 200 kV JEM-FS2200 with a field emission gun (FEG). A small drop of the sample solution was applied on a copper EM grid with a holey carbon film, and excess solution was blotted with a filter paper, leaving thus a thin sample film spanning the holes in the carbon film. The samples used for the Cryo-TEM characterization were the same used for the ESR characterization.

3.3. Effect of SDPC and DDPC on POPC lipid membranes

3.3.1. Electron spin resonance analysis

The study was realized by analyzing the ESR spectra of phosphatidylcholine spin-labeled at different positions, n, in the sn-2 chain (n-PCSL, n = 5, 7, 10 and 14) incorporated in the membranes at 1% by weight on total lipids. The analysis of the spectra gives information about the local microstructure and polarity experienced by the radical reporter groups[11]. Initially, the 5-PCSL spectrum of POPC alone (black lines in **Figure 3.4**) and in the presence of increasing amount of SDPC (**Panel A**) and DDPC (**Panel B**) in the lipid mixtures were acquired.
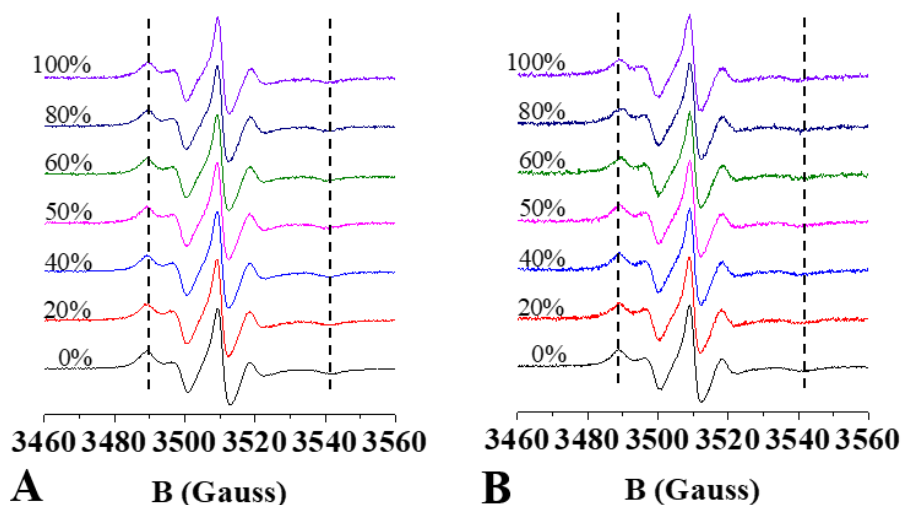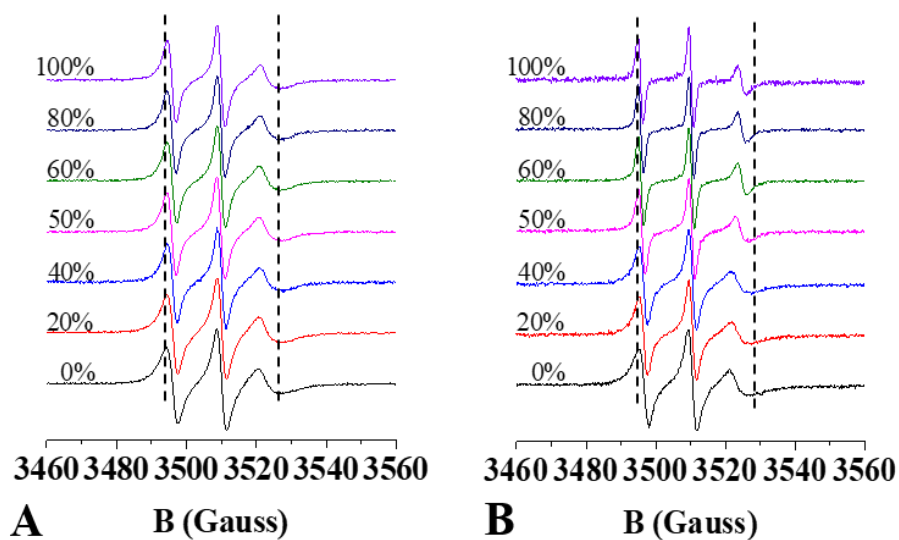

Figure 3.4: ESR spectra of 5-PCSL in POPC bilayers (black lines) containing SDPC, in Panel A, and DDPC, in Panel B, at different molar fractions.

Inspection of **Figure 3.4**, shows that the 5-PCSL spectrum, in all the investigated samples, presents a clearly defined axially anisotropic line shape, as detectable from the splitting of the high- and low-field peaks. The anisotropy is the index of the restricted motion of the label due to the packing near the hydrophilic region and it is preserved in all the investigated samples. In the case of high amount of DDPC (**Panel B**) a shift of the high field minimum is observed which reflects the reduction of the anisotropy.

In the case of the 14-PCSL, representing the motion in the hydrophobic section, the spectrum shows a three-line quasi-isotropic line shape (**Figure 3.5**), which is more sensitive to the lipid composition of the mixtures.


Figure 3.5: ESR spectra of 14-PCSL in POPC bilayers (black lines) containing SDPC, in Panel A, and DDPC, in Panel B, at different molar fractions.

Indeed, a typical slow-motion spectrum, with broad signals, is observed in the case of POPC alone. When the molar fraction of phospholipids containing DHA increase, the peaks appear narrower. Notably, when the DHA is present up to 50%, (more than 50% DDPC, **Panel** B) significant reduction of the peaks broadening occur, which is an indication of a locally unrestrained motions.

In order to quantitatively analyze the spectra, we evaluated the order parameter, S, and the isotropic hyperfine coupling constant, a'_N, using a spectra parameterization method reported in **Section 3.2.5**.

S is a measure of the local orientational ordering of the labeled acyl chain with respect to the normal to the bilayer surface, while a'_N, is an index of the micropolarity experienced by the nitroxide; in **Figure 3.6** the values of these parameters for 5-PCSL are reported for increasing amount of SDPC and DDPC, respectively.
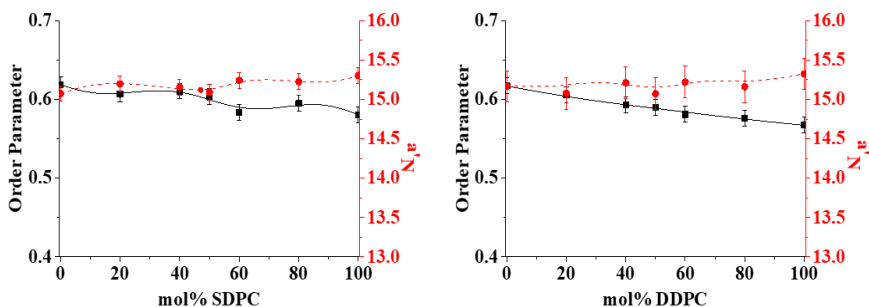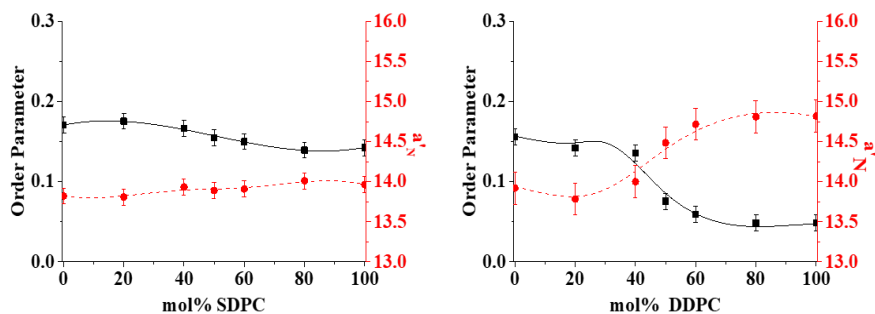
Figure 3.6: Trend of the order parameter, *S*, and a'$_N$ for 5-PCSL. Left: POPC containing SDPC at different molar fraction; right: POPC containing DDPC at different molar fraction.

For both phospholipids SDPC and DDPC, a very weak and gradual S decrease is observed moving from 0% to 100%. At the same time a'$_N$ values remain almost constant; these evidences suggest that the microstructure and local polarity experienced by the acyl chain segments close to the headgroups is not affected by the presence of omega-3 species.

Moving deep into the hydrophobic portion of the bilayer, S and a'$_N$ for the 14-PCSL are reported in **Figure 3.7.** The S trends show a different behaviour depending on the phospholipid containing DHA: a less decrease occurs between 40 and 60 % of SDPC compared to the addition of DDPC. For the di-esterified phospholipid containing DHA, this result indicates a dramatic reduction of that the ordering of the acyl chain termini. In the case of a bilayer rich in DHA (more than 50% DDPC), even the a'$_N$ significantly changes, the increase indicates that the local environment is more polar. A similar result was already observed by ^{2}H NMR study of perdeuterated phospholipids containing DHA: the order parameter obtained show a lower value compared with monounsaturated and saturated acyl chains[12]. In order to investigate the phase that characterizes the bilayers with different composition of DHA, a combined use of the different spin-labels, that permits the entire membrane profile to be monitored, from the interface to the deep interior, was used.

Reporting the S parameter against the nitrosyl label position on the acyl chain, it is possible to obtain a trend that describes the phase of the lipid bilayer[13].

Figure 3.7: Trend of the order parameter, S, and a'$_N$ for 5-PCSL. Left: POPC containing SDPC at different molar fraction; right: POPC containing DDPC at different molar fraction.

For this reason, the 7-PCSL and 10-PCSL were incorporated into the lipid aggregates and the spectra were acquired. The lipid bilayer compositions under investigation were choose considering 20% of DHA (40%SDPC and 20% DDPC), an average amount of DHA contained in cell membranes, and higher concentrations of DHA exceeding the 50% to deepen the investigation. Thus, to study the effect of a highly containing DHA model membranes and to compare the two phospholipids effect POPC lipid system in presence of 100% SDPC and at 80% DDPC were considered (**Figure 3.8)**. The flexibility gradient for the POPC alone is a characteristic hallmark of the disordered state of liquid-crystalline phospholipid bilayers, L$_d$[14]. The addition of 20% of DHA (40% SDPC or 20% DDPC) to the POPC system, show the same profile. On the contrary, when the DHA fraction is 50% (100% of SDPC), it induces a small reduction of the order parameter for all spin-labelled lipids. These results point to a weak enhancement of the POPC bilayer fluidity. The flexibility gradient for the POPC alone is a characteristic hallmark of the disordered state of liquid-crystalline phospholipid bilayers, L$_d$[14]. The addition of 20% of DHA (40% SDPC or 20% DDPC) to the POPC system, show the same profile. On the contrary, when the DHA fraction is 50% (100% of SDPC), it induces a small reduction of the order parameter for all spin-labelled lipids.
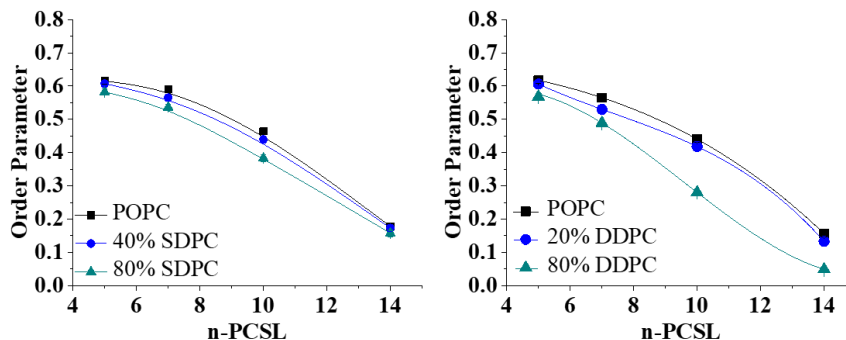
Figure 3.8: *n*-PCSL profiles for POPC bilayers containing 40% and 100% SDPC, left, and 20% and 80% of DDPC, right.

These results point to a weak enhancement of the POPC bilayer fluidity. Interestingly, when the amount the DHA reaches the 80 % (80% DDPC, **Figure 3.8B**) significant changes in the S trend are observed. Specifically, a strong reduction is observed for 10- and 14-PCSL, indicating a dramatic increase of the segmental chain mobility. According to Hardman et al. this gradient profile is associated to a different mesophase, the H_{II}. Furthermore, the a'$_N$ values for 14-PCSL (**Figure 3.7B**) confirm a more polar environment near the nitroxide group, which are consistent with the exposure of the hydrophobic tails to the water solution, suggesting one again a different organization of lipids in a phase that is not lamellar. The ability of phospholipid containing DHA to give an H_{II} phase was already reported but for a phospholipid with a different headgroup: the phosphor-ethanolamine; such headgroup occupy a smaller volume than phosphocholine, allowing a cone shape lipid with a form factor less than 1, that are recognized to be non-lamellar lipids[15,16]. The ability of phospholipid containing DHA to give an H_{II} phase was already reported but for a phospholipid with a different headgroup: the phosphor-ethanolamine; such headgroup occupy a smaller volume than phosphocholine, allowing a cone shape lipid with a form factor less than 1, that are recognized to be non-lamellar lipids[15,16]. It is also known that the DHA can assume hairpin-like or coiled conformations, that can be described by the acyl chain tilted near the headgroup than induce a higher area

per lipid of such fatty acid[17]. Therefore, the hypothesis is that the DDPC can give an inverted phase at room temperature and in physiological pH.

3.3.2. Neutron reflectivity analysis

First, supported lipid bilayer of pure POPC were realized and measured in the three different solvent contrasts D_2O, SMW and H_2O that greatly enhances the sensitivity of the technique[10];the reflectivity profiles and related best fits are shown in **Figure 3.9**.
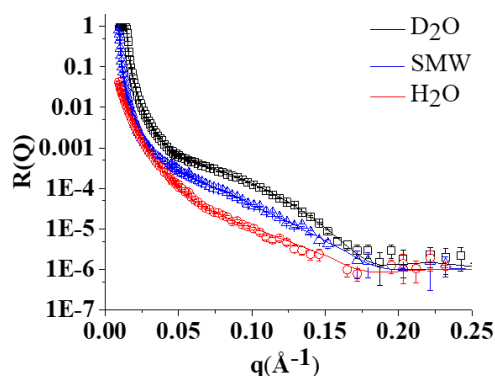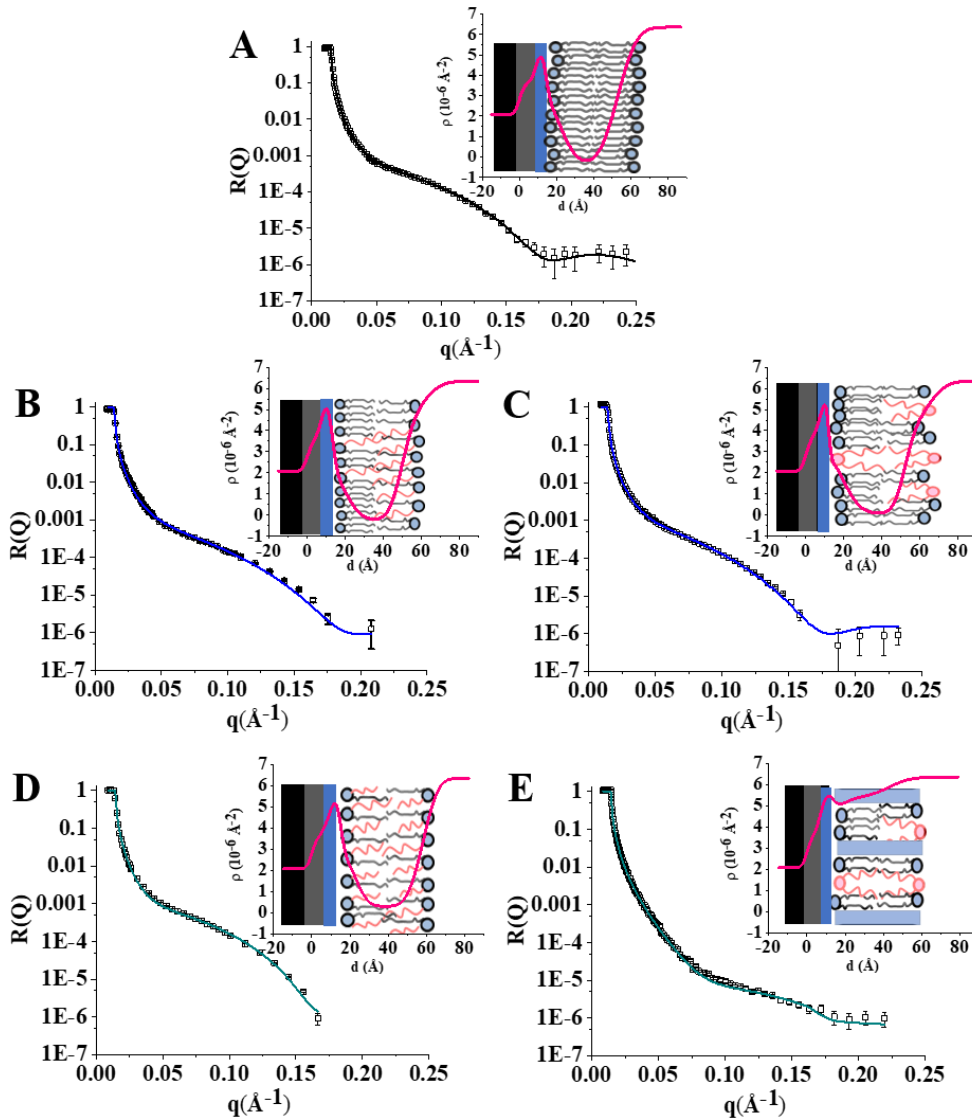

Figure 3.9: Experimental data and the best fitting curves in D_2O, black, SMW, blue and H_2O, red, for pure POPC.

The method was adopted in all the cases: lipid bilayers with different molar fraction of either SDPC or DDPC were investigated to discriminate the effects of DHA on the structural organization of the biomembranes; all the experimental data and relative fit curves are reported in the **Appendix B**. The experimental data were modelled with a five-layer model (as already described in **Figure 3.3**). In particular, the lipid molecules were considered as composed by two different regions with different scattering length density, i.e. the polar headgroup region and the apolar acyl chains region. Glycerolphosphocholine headgroups represent the polar portions of the phospholipid molecules, facing the support and the bulk aqueous solvent. The acyl chains represent the hydrophobic portion of the bilayer, which stays away from the aqueous solvent. In the case of the investigated

samples, the scattering length density (SLD) of the different bilayer regions was first calculated considering the scattering length of POPC, SDPC, DDPC and the molecular volumes of the two phospholipids (**Table 3.1**) and then adjusted during the fitting procedures. The experimental data in D_2O, with the best fitting curves, and the scattering length density, ρ, profiles are shown in **Figure 3.10**.

Figure 3.10: Experimental data and the best fitting curves in D_2O and relative SLD profiles for lipid systems: A) POPC, B) POPC/ SDPC 60/40, C) POPC/DDPC 80/20, D) SDPC and E) POPC/DDPC 20/80, respectively.

The profiles indicate that almost in all the cases a single lipid bilayer has formed on the SiO$_2$ substrate, thus it is possible to proceed with the data analysis. The parameters obtained from the best fit procedure, the thickness, the roughness plus the solvent content expressed as volume percent, are reported in **Table 3.1**.

Table 3.2: Parameters derived from model fitting of the reflectivity profiles.

|	Interfacial Layer	Thickness (Å)	solvent (%)	Roughness (Å)
POPC	inner headgroups	8±1	30±5	6±1
	chain region	28±1	-	7±1
	outer headgroup	8±1	30±5	6±1
40% SDPC	inner headgroups	7±1	27±5	7±1
	chain region	30±1	2±1	5±1
	outer headgroup	10±1	40±5	7±1
100% SDPC	inner headgroups	8±1	25±5	5±1
	chain region	31±1	5±1	5±1
	outer headgroup	10±1	45±5	5±1
20% DDPC	inner headgroups	8±1	30±5	7±1
	chain region	32±1	5±2	5±1
	outer headgroup	12±1	45±5	9±1
80% DDPC	inner headgroups	6±1	55±10	10±1
	chain region	16±1	15±10	13±1
	outer headgroup	6±1	55±10	10±1

Pure POPC bilayers present a total thickness of 44 ± 3 Å, consistent with the results reported in a previous work[18]. The presence of DHA, depending on the phospholipids in which it is contained, SDPC or DDPC, influences the POPC lipid bilayer. At 40% SDPC (**Panel B**), an increase of the thickness (~ 4 Å) and

an asymmetric solvent content in the two headgroup layers is observed. These effects are more pronounced in the system including DDPC at the same DHA content (**Panel D**). Notably, at 80% DDPC the high solvent content in the tail region and the high roughness observed are inconsistent with a supported bilayer, supporting the hypothesis that DHA-containing phospholipid induce an asymmetric reorganization of the lipid structure, eventually causing, in the presence of 80% DDPC, the formation of non-bilayer structures and the consequent detachment of the lipid system from the support (**Panel E**).

3.3.3. Cryogenic transmission electron microscopy

From ESR and NR, it is clear DHA affects in different ways the bilayer structure and dynamics depending on the phospholipid is incorporated. The DDPC can fluidify a liquid disordered phase and to rearrange the bilayer structure when this phospholipid reaches a concentration higher that 50%. To get morphological information on the lipid aggregates containing DDPC, Cryo-TEM images were acquired at MLZ by Dr. Marie-Sousai Appovau.
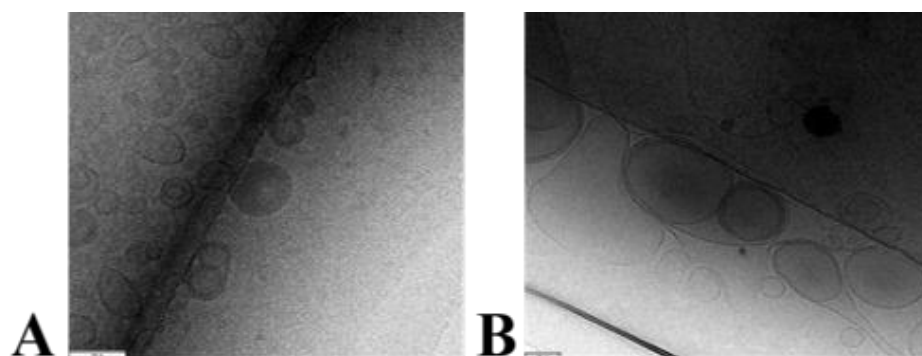

Figure 3.11: Vesicles containing A) pure POPC and B) POPC/DDPC 80/20.

In **Figure 3.11** images of pure POPC vesicles and containing 20% DDPC are reported. The sample consisting on pure POPC shows unilamellar vesicles with a mean radius of 60 nm, with some multilamellar structure. In the case of 20% of DDPC the extrusion process does not give stable unilamellar vesicles as in the case of pure POPC; indeed, in **Panel B** rearranged and elongated structures are

observed, suggesting that tis small amount of DHA is able to promote fusion processes. On the other hand, an unexpected result was obtained for the system containing 80% mol% and shown in **Figure 3.12**; the coexistence of different lipid aggregates are observed.
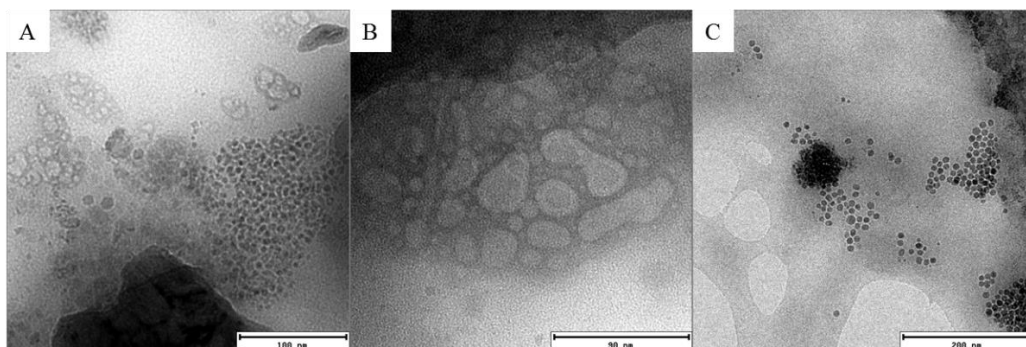
Figure 3.12: Cryo-TEM images of the lipid formulation POPC/DDPC 20/80 A) showing the coexistence of different type of aggregates; B) very polydispersed and irregular vesicles; C) very small and monodispersed aggregates resembling micellar aggregates with a mean radius 10 nm.

Small and monodispersed particles with a mean radius 10 nm, resembling micellar aggregates, are observed (**Figure 3.12 A and C**). Even big aggregates with an elongated morphology, which contain water in the inner core (light portion of the images), are observed indicating that DDPC has a different aggregation property. The presence of micellar-type was quite unexpected, because in this condition the polyunsaturated fatty acids is not able to give a long range H_{II} mesophase, as hypothesized in previous study[15].

3.4. Effect of SDPC and DDPC on POPC/Chol lipid membranes

3.4.1. Electron spin resonance analysis

Once assessed the effect of the two phospholipids containing DHA on the microstructural properties of lipid bilayers in a liquid disordered phase, the same study was carried out on a liquid ordered phase, formed by POPC/Chol 6/4. The choice was made considering that this lipid system is characterized by L_o phase[19],

which is associated to biological relevant mesophases called lipid raft. The study was realized by analyzing the ESR spectra of phosphatidylcholine spin-labeled at different positions, *n*, in the *sn*-2 chain (*n*-PCSL, *n* = 5, 7, 10 and 14) and a spin labelled cholesterol analogue, 25-doxyl-cholesterol (CNO), incorporated in the membranes at 1% by weight on total lipids. As already reported for the investigation on a L_d phase (see previous section), first, the 5-PCSL spectra for POPC/Chol alone (black lines in **Figure 3.13** and **3.14**, respectively) and in the presence of increasing amount of SDPC (**Panel A**) and DDPC (**Panels B**) in the lipid mixtures were analyzed. Inspection of **Figure 3.13** shows that the 5-PCSL spectra in all the investigated samples present a clearly defined axially anisotropic line shape, as detectable from the splitting of the high- and low-field peaks. For this spin-label, scarce effects of SDPC are observed; indeed, no variation of the line shape was observed (**Panel A**).
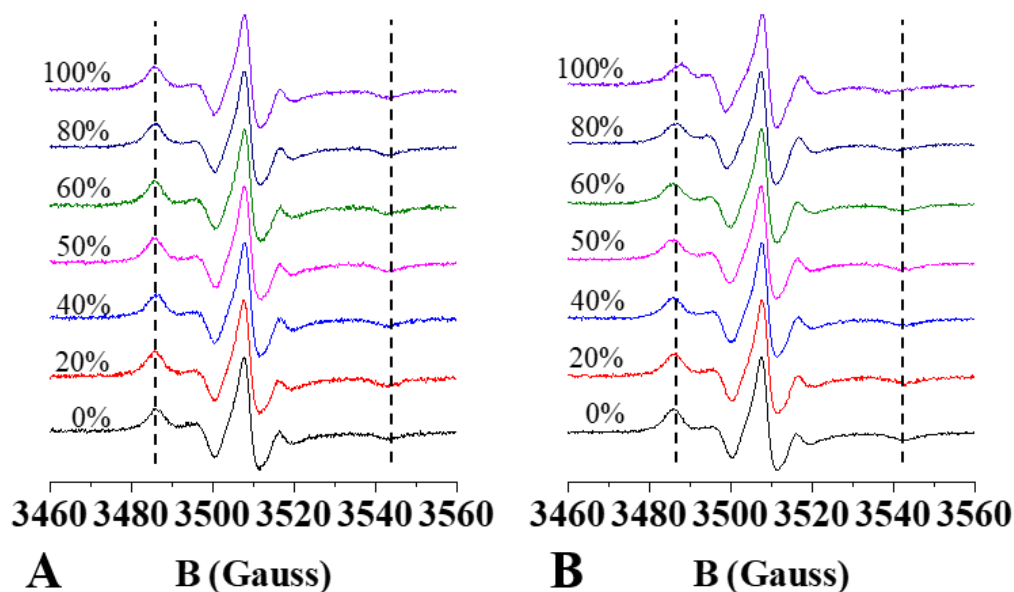
Figure 3.13: ESR spectra of 5-PCSL in POPC/Chol bilayers (black lines) containing SDPC, in Panel A, and DDPC, in Panel B, at different molar fractions.

In contrast, in the case of DDPC, when DHA is present as 80% of total acyl chains, the spectrum present decrease in the anisotropy, as can be detected by the shift of the low field maximum and high field minimum (**Figure 3.14**, **Panel B**). Once

again, to investigate what is happening in the hydrophobic portion of the bilayer, the 14-PCSL was used; the spectra for the same lipid mixtures studied by 5-PCSL are reported in **Figure 3.14**.
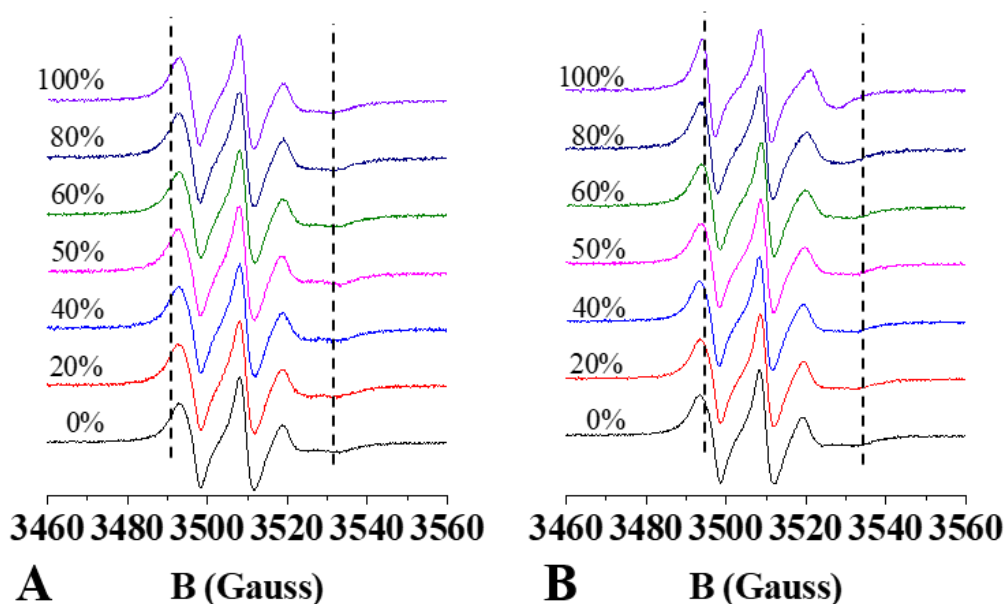

Figure 3.14: ESR spectra of 14-PCSL in POPC/Chol bilayers (black lines) containing SDPC, in Panel A, and DDPC, in Panel B, at different molar fractions.

The spectra for the POPC/Chol lipid systems has a different line shape compared with POPC alone, the spectrum shows a quasi-anisotropic one due to the presence of cholesterol. Indeed, the 14-PCSL is more sensitive than 5-PCSL and shows the restricted motion of acyl chains. Even in this case, notably, the major effects in the dynamics of the bilayer are observed in the presence of DDPC (**Panel** B); the spectra for high amount of DHA are more isotropic describing the unrestrained motions of the 14-PCSL. As described in previous section, S and a'_N, for 5-PCSL and 14-PCSL are reported in **Figure 3.15** and **Figure 3.16**, respectively. In the case of SDPC, moving from 0% to 100%, S and a'_N, remain constant, thus this phospholipid does not affect the hydrophilic part of the bilayer. On the other hand, when DDPC is added a gradual decrease of the order is observe, associated to a more polar environment, indeed a'_N increases up to 50% of DDPC (**Panel B**).
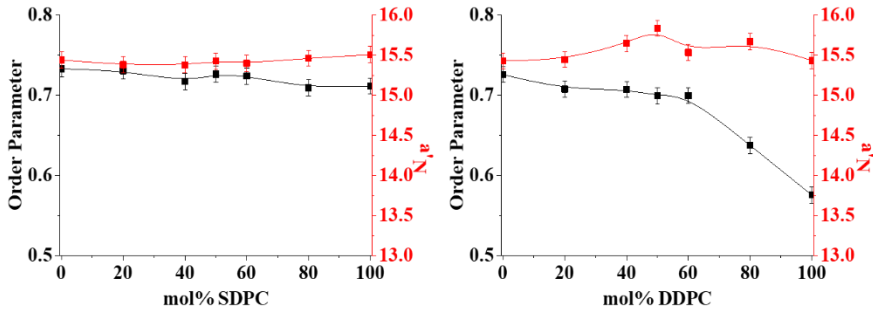
Figure 3.15: Trend of the order parameter, *S*, and a'$_N$ for 5-PCSL. Left: POPC/Chol containing SDPC at different molar fraction; right: POPC/Chol containing DDPC at different molar fraction.

A threshold concentration of DHA (60% DDPC), as also recorded for a L$_d$ phase, induces a steep decrease of the order parameter, S of both 5- and 14-PCSL. However, in this case, the associated a'$_N$ is not affected, probably due to the presence of cholesterol.
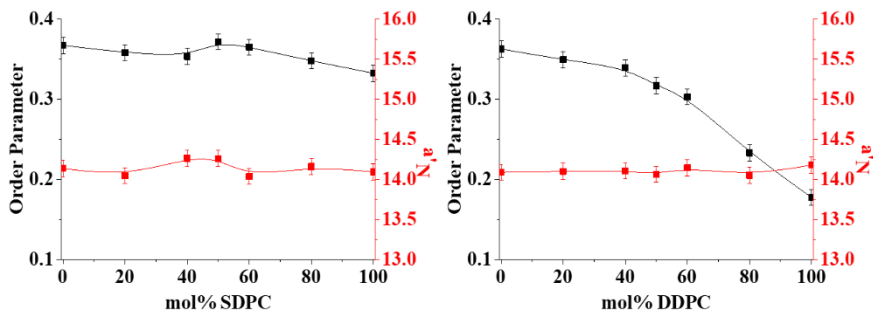
Figure 3.16: Trend of the order parameter, *S*, and a'$_N$ for 5-PCSL. Left: POPC/Chol containing SDPC at different molar fraction; right: POPC/Chol containing DDPC at different molar fraction.

In **Figure 3.17**, the order parameters *versus* the label position, for different concentration of SDPC and DDPC are reported. The lipid mixtures compositions were chosen in agreement with the samples in the L$_d$ phase already investigated. The profiles show a gradient of the order parameter values, with a reduced slope compared with L$_d$ phase, that is characteristic of a L$_o$ phase. Similarly, to the effect on the pure POPC, the high amount of DDPC causes a change in the n-PCSL

profile, from a gradient corresponding to a liquid ordered phase to a profile associated to a disordered phase.
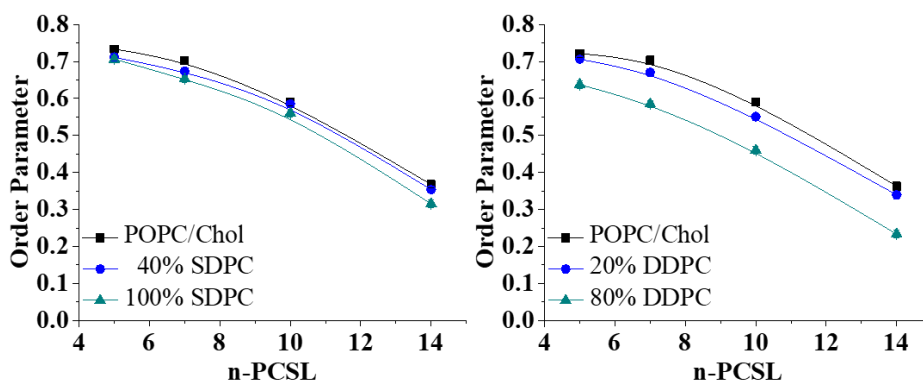
Figure 3.17: n-PCSL profiles for POPC/Chol bilayers containing 40% and 100% SDPC, left, and 20% and 80% of DDPC, right.

Brzustowich and co-workers studied the molecular organization of cholesterol into bilayer consisting on DDPC, and found that this small sterol has a low solubility in such systems, corresponding to 8% mol% compared to 55% in SDPC bilayer[20]. Katsaras et al in 2009 proposed a different location of cholesterol in highly polyunsaturated lipid bilayer: the molecule reside in the centre of the bilayer[21]. The evidences show that cholesterol is not excluded by the membranes due to the presence of SDPC, because the line-shape in the case of 5-PCSL a 14-PCSL remains almost the same. In addition, the n-PCSL profile show that a Lo phase still exists. In the case of high amounts of di-esterified DDPC a spectra line-shape variation occurs and it is associated to an overall reduction of the order parameter for the entire bilayer. Thus, these evidences confirm that highly polyunsaturated lipid mixtures assume a lamellar phase due to the presence of small amount of cholesterol. To further investigate the cholesterol dynamics, once the composition of the bilayer changes, ESR spectra of a cholesterol analogue spin-labelled at position 25 (CNO spin label) embedded in the POPC/Chol bilayers (as 1% of the total lipid acquired (**Figure 3.18**). Indeed, the analysis of

CNO ESR spectra allows to get almost straight information on the positioning of cholesterol in the investigated membranes[22].
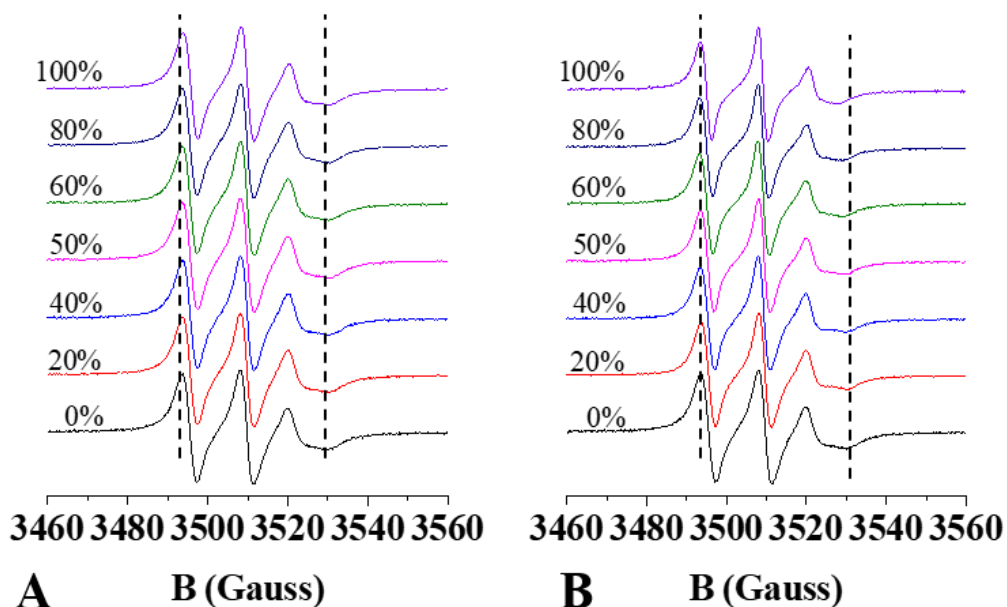
Figure 3.18: ESR spectra of CNO in POPC/Chol bilayers (black lines) containing SDPC, in Panel A, and DDPC, in Panel B, at different molar fractions.

CNO spectrum in POPC/Chol presents an almost isotropic line-shape, like the 14-PCSL spectrum, ruling out the possibility of cholesterol segregation leading to domain formation.
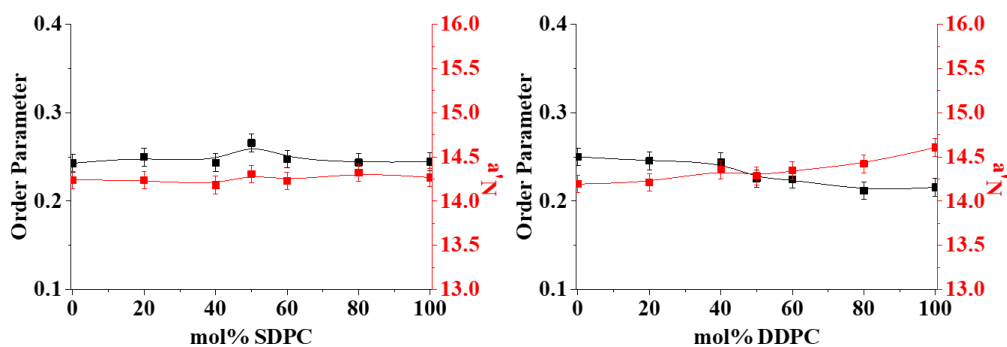
Figure 3.19: Trend of the order parameter, S, and a'_N for CNO. Left: POPC/Chol containing SDPC at different molar fraction; right: POPC/Chol containing DDPC at different molar fraction.

The effects of the polyunsaturated become clearer reporting S and a'$_N$ as function of the phospholipid amount (**Figure 3.19**). In the case of SPDC, the S value remains almost constant going from pure POPC to 100% SDPC, indicating that the change in lipid composition does not affect the cholesterol content or its position. For the DDPC, the S decreases, associated to a higher a'$_N$, for the CNO spin label, show the unrestricted dynamics of the little acyl chain present in the cholesterol, that occurs in a more polar environment, suggesting that the sterol squeezed out of the membrane.

3.4.2. Neutron reflectivity analysis

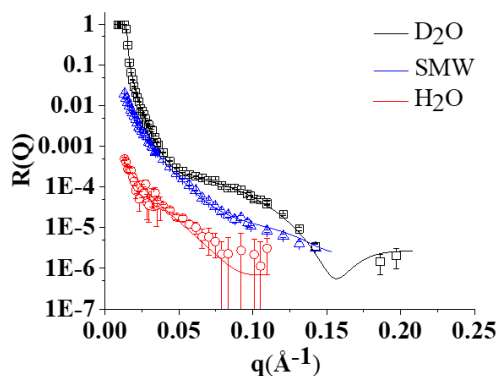Even in this case, supported lipid bilayer used as control, d31-POPC/Chol, were realized and measured in the three different solvent contrasts D$_2$O, SMW and H$_2$O; the reflectivity profiles and related best fits are shown in **Figure 3.20**.

Figure 3.20: Experimental data and the best fitting curves in D$_2$O, black, SMW, blue and H$_2$O, red, for pure d31-POPC/Chol.

Notably, the profiles are quite different from pure POPC, mainly for two reasons: i) the POPC molecule carry in 1-*sn-* position a palmitoyl perdeuterated chain; ii) the supported lipid bilayer is supposed to be more rigid, thus thicker. In this case the d31-POPC was used; indeed, it has a scattering length density completely different from the DHA acyl chains and cholesterol molecules giving an enhanced contrast that allows a best fit.
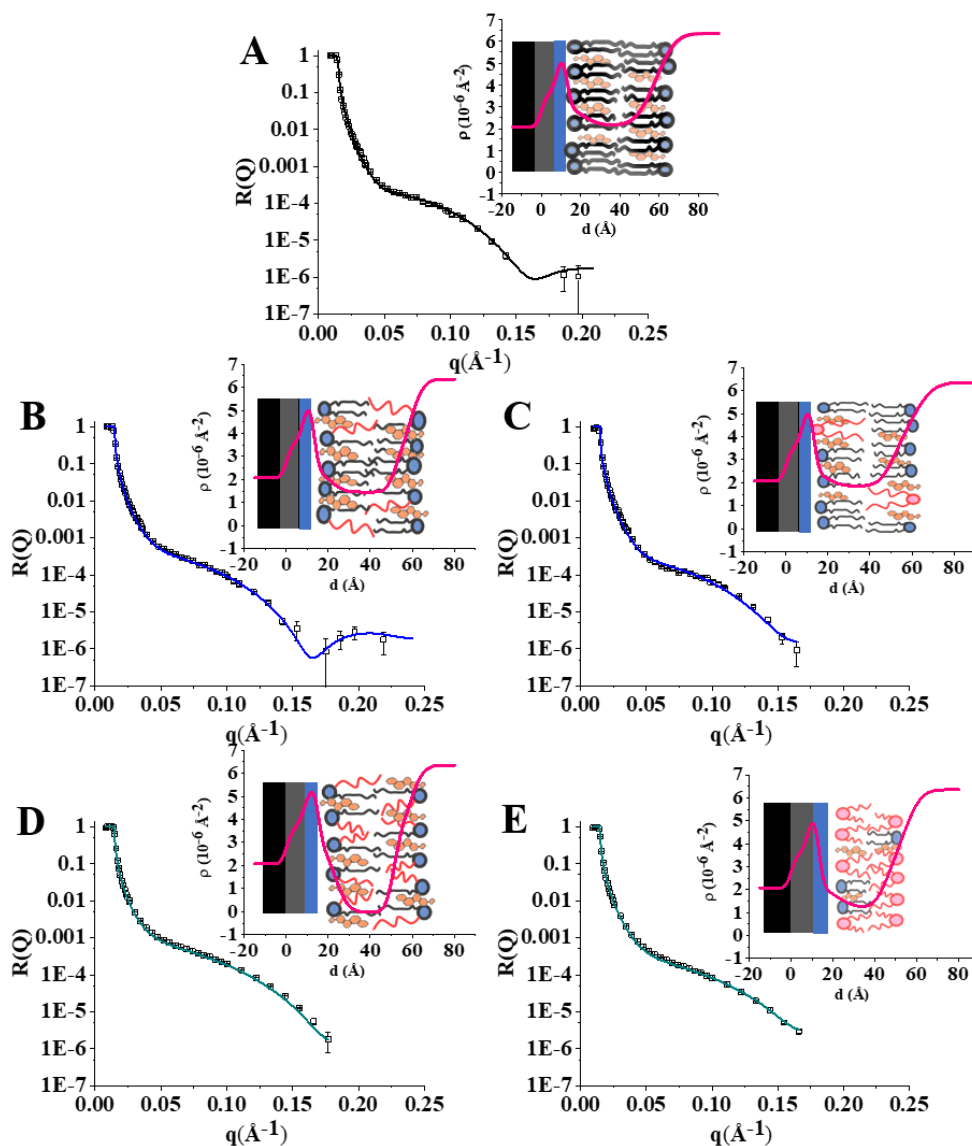
Figure 3.21: Experimental data and the best fitting curves in D_2O and relative SLD profiles for lipid systems: A) POPC/Chol, B) POPC/SDPC 60/40 40% Chol, C) POPC/DDPC 80/20 40% Chol, D) SDPC/Chol and E) POPC/DDPC 20/80 40% Chol, respectively.

In **Figure 3.21** the experimental data in D_2O, which is the most informative one, with the best fitting curves, and the scattering length density, ρ, profiles are reported, like **section 3.3.2**; all the experimental data and relative fit curves are reported in **Appendix B**. It has to be highlighted that the profiles show a lipid deposition in all the cases. The data obtained from the best fit are listed in **Table**

3.3. d31-POPC/Chol bilayer present a thickness of 48 ± 1 Å, according to the values reported in literature for same systems[18]. Indeed, the presence of cholesterol causes an increase of the thickness of the hydrophobic region, going from 28 ± 2 Å (pure POPC) to 32 ± 2 Å. At the same time, the scattering length density value corresponding to this region decreases from the assessed $3.1 \cdot 10^{-6}$ Å^{-2} of pure deuterated d31-POPC to 2.08×10^{-6} Å^{-2}. The change of the scattering length density in the hydrophobic core is associated to a decrease in the scattering length density of headgroups, suggesting that cholesterol positions is between the hydrophilic and hydrophobic region[23]. Also for this lipid system, the presence of SDPC influences the overall lipid bilayer. The replacement of 40% of d31-POPC with SDPC decreases the thickness (~2Å) and the roughness in the chain region and decrease the solvent content and the roughness in the head portion, as reported in **Table 3.3**; the trend is confirmed when the total amount of d31-POPC is replaced by SDPC. The results rule out that probably the cholesterol is disclosed in the hydrophilic region of the bilayer. In the case of DDPC, the d31-POPC /Chol undergoes to a significant change of the bilayer structural properties. Specifically, a small amount of this phospholipid - 20% - decreases (~4 Å) the thickness value for chain region and induce an asymmetry in the bilayer, as in the case of POPC. The outer headgroup region become thicker and also the roughness increases. Also, the scattering length density of acyl chains region varies from $2.08 \cdot 10^{-6}$ Å^{-2} for d31-POPC/Chol to $1.75 \cdot 10^{-6}$ Å^{-2}. A significant increase in the roughness values of both hydrophilic and hydrophobic regions was also observed, and a high solvent volume content was found in both regions (see **Table 3.3**), when the DDPC reaches the 80%, confirming that a great amount of DDPC effectively modified the structural organization and lipid packing also in the case of POPC/Chol biomembranes. The unique features of DHA to assume a hairpin like conformation can explain the realization of a bilayer thicker than d31-POPC/Chol and with scattering length density that exclude cholesterol from the composition of bilayer.

Combining these results with the once obtained by ESR, probably the low amount of cholesterol, that is soluble in the bilayer[24], is able to induce a lamellar structure that DDPC alone is not able to assume.

Table 3.3: Parameters derived from model fitting of the reflectivity profiles.

	Interfacial Layer	Thickness (Å)	solvent (%)	Roughness (Å)
d31-POPC/Chol	inner headgroups	8±1	35±5	7±1
	chain region	32±1	-	6±1
	outer headgroup	8±1	35±5	7±1
40% SDPC	inner headgroups	7±1	20±5	5±1
	chain region	30±1	5±1	3±1
	outer headgroup	8±1	25±5	5±1
100% SDPC	inner headgroups	7±1	35±5	5±1
	chain region	28±1	5±1	3±1
	outer headgroup	7±1	35±5	5±1
20% DDPC	inner headgroups	7±1	15±5	5±1
	chain region	28±1	5±2	8±1
	outer headgroup	12±1	35±5	8±1
80% DDPC	inner headgroups	8±1	15±5	10±1
	chain region	24±1	10±5	5±1
	outer headgroup	10±1	35±5	6±1

Nevertheless, further investigations are necessary to define the positioning of cholesterol in such systems, because the results are still controversial.

3.5. Conclusions

Polyunsaturated phospholipids, in particular omega-3 class, play a key role in many biological processes and non-specific functions have been proposed for this class of fatty acids. The effects of Docosahexaenoic acid (DHA), once converted to phospholipids, on the membrane reorganization and on the ability to induce lipid phases separation were extensively studied.

In this work the dynamics of the binary mixture POPC/SDPC or POPC/DDPC, where all the phospholipids have the same headgroup, to identify the role of the omega-3 polyunsaturated fatty chains were investigated. In addition, the effects of the SDPC and DDPC on the ability to realize a liquid ordered phase such as POPC/Chol 6/4 were investigated.

The results provide the evidence that the phospholipids in which DHA is esterified (SDPC or DDPC), affect differently a L_d or L_o phase. The DDPC, that bear two DHA chains, shows the most interesting behaviour: even small amounts of DDPC can induce changes in the lamellar lipid arrangement. When 20% of DDPC is added to a L_d phase consisting of POPC, the bilayer becomes rougher and characterized by a higher content of water; when it is added to a cholesterol-containing L_o phase, it induces the same changes, re-locating the cholesterol closer to the aqueous environment. Interestingly, addition of higher amounts of DDPC to either L_d or L_o bilayers causes more dramatic effects: in the former case, when 50% of POPC is substituted with DDPC, nonlamellar structures form; in the latter, lamellar structures are thinner than POPC/Chol ones and characterized by a scattering length density indicating that cholesterol is not embedded in bilayer anymore, but squeezed out of the membrane.

The DDPC unique ability of assuming different conformations resulting in different features of the membrane can explain the role it plays in neuronal membranes, whose involvement in amyloidogenic processes is widely accepted.

3.6. References

1   Laye, S. Polyunsaturated fatty acids, neuroinflammation and well being. *Prostaglandins, leukotrienes, and essential fatty acids* **82**, 295-303, doi:10.1016/j.plefa.2010.02.006 (2010).

2   Bazinet, R. P. & Laye, S. Polyunsaturated fatty acids and their metabolites in brain function and disease. *Nature reviews. Neuroscience* **15**, 771-785, doi:10.1038/nrn3820 (2014).

3   Goni, F. M. The basic structure and dynamics of cell membranes: an update of the Singer-Nicolson model. *Biochimica et biophysica acta* **1838**, 1467-1476, doi:10.1016/j.bbamem.2014.01.006 (2014).

4   Lind, T. K., Cardenas, M. & Wacklin, H. P. Formation of Supported Lipid Bilayers by Vesicle Fusion: Effect of Deposition Temperature. *Langmuir* **30**, 7259-7263, doi:10.1021/la500897x (2014).

5   Gordon, L. M. & Sauerheber, R. D. Studies on spin-labelled egg lecithin dispersions. *Biochimica et biophysica acta* **466**, 34-43 (1977).

6   Aloia, R. C. E., Curtain, C. C. E. & Gordon, L. M. E. *Methods for studying membrane fluidity*. (Alan R Liss Inc., 1988).

7   Rheinstadter, M. C., Ollinger, C., Fragneto, G., Demmel, F. & Salditt, T. Collective dynamics of lipid membranes studied by inelastic neutron scattering. *Physical review letters* **93**, 108107, doi:10.1103/PhysRevLett.93.108107 (2004).

8   Stefan Mattauch, A. K., Sabine Pütter. MARIA: Magnetic reflectometer with high incident angle. *Journal of large-scale research facilities* **1**, doi:http://dx.doi.org/10.17815/jlsrf-1-29 (2015).

9   Koenig, B. W. & Gawrisch, K. Specific volumes of unsaturated phosphatidylcholines in the liquid crystalline lamellar phase. *Biochimica et biophysica acta* **1715**, 65-70, doi:10.1016/j.bbamem.2005.07.006 (2005).

10   Fragneto, G., Thomas, R. K., Rennie, A. R. & Penfold, J. Neutron reflection from hexadecyltrimethylammonium bromide adsorbed on smooth and rough silicon surfaces. *Langmuir* **12**, 6036-6043, doi:Doi 10.1021/La9604644 (1996).

11   Sankaram, M. B., Marsh, D. & Thompson, T. E. Determination of fluid and gel domain sizes in two-component, two-phase lipid bilayers. An electron spin resonance spin label study. *Biophysical journal* **63**, 340-349, doi:10.1016/S0006-3495(92)81619-3 (1992).

12   Holte, L. L., Peter, S. A., Sinnwell, T. M. & Gawrisch, K. 2H nuclear magnetic resonance order parameter profiles suggest a change of molecular shape for phosphatidylcholines containing a polyunsaturated acyl chain. *Biophysical journal* **68**, 2396-2403, doi:10.1016/S0006-3495(95)80422-4 (1995).

13   Hubbell, W. L. & McConnell, H. M. Molecular motion in spin-labeled phospholipids and membranes. *J Am Chem Soc* **93**, 314-326 (1971).

14   Galdiero, S. *et al.* Role of membranotropic sequences from herpes simplex virus type I glycoproteins B and H in the fusion process. *Biochimica et biophysica acta* **1798**, 579-591, doi:10.1016/j.bbamem.2010.01.006 (2010).

15   Shaikh, S. R., Brzustowicz, M. R., Stillwell, W. & Wassall, S. R. Formation of inverted hexagonal phase in SDPE as observed by solid-state (31)P NMR.

Biochemical and biophysical research communications **286**, 758-763, doi:10.1006/bbrc.2001.5454 (2001).

16   Sjolund, M., Rilfors, L. & Lindblom, G. Reversed hexagonal phase formation in lecithin-alkane-water systems with different acyl chain unsaturation and alkane length. *Biochemistry* **28**, 1323-1329 (1989).

17   Gawrisch, K., Eldho, N. V. & Holte, L. L. The structure of DHA in phospholipid membranes. *Lipids* **38**, 445-452 (2003).

18   Vitiello, G. *et al.* Cholesterol modulates the fusogenic activity of a membranotropic domain of the FIV glycoprotein gp36. *Soft Matter* **9**, 6442-6456, doi:10.1039/c3sm50553g (2013).

19   Ionova, I. V., Livshits, V. A. & Marsh, D. Phase Diagram of Ternary Cholesterol/Palmitoylsphingomyelin/Palmitoyloleoyl-Phosphatidylcholine Mixtures: Spin-Label EPR Study of Lipid-Raft Formation. *Biophysical journal* **102**, 1856-1865, doi:10.1016/j.bpj.2012.03.043 (2012).

20   Shaikh, S. R., Locascio, D. S., Soni, S. P., Wassall, S. R. & Stillwell, W. Oleic- and docosahexaenoic acid-containing phosphatidylethanolamines differentially phase separate from sphingomyelin. *Biochimica et biophysica acta* **1788**, 2421-2426, doi:10.1016/j.bbamem.2009.08.019 (2009).

21   Kucerka, N. *et al.* The functional significance of lipid diversity: orientation of cholesterol in bilayers is determined by lipid species. *J Am Chem Soc* **131**, 16358-16359, doi:10.1021/ja907659u (2009).

22   Marsh, D. Molecular motion in phospholipid bilayers in the gel phase: long axis rotation. *Biochemistry* **19**, 1632-1637 (1980).

23   Luchini, A. *et al.* Neutron Reflectometry reveals the interaction between functionalized SPIONs and the surface of lipid bilayers. *Colloids and surfaces. B, Biointerfaces* **151**, 76-87, doi:10.1016/j.colsurfb.2016.12.005 (2017).

24   Lee, C. W., Brzustowicz, M. R., Zerouga, M., Stillwell, W. & Wassall, S. R. Molecular organization of cholesterol in polyunsaturated phospholipid membranes: A solid state NMR investigation. *Biophysical journal* **80**, 516a-516a (2001).

Chapter 4:

Amyloidogenic peptides

from NMP-1

and model membranes

4.1. Work outline

Nucleophosmin-1 (NPM1) is an abundant multifunctional protein, implicated in a variety of biological processes and in the pathogenesis of several human malignancies. Its C-terminal domain (CTD) is endowed with a three helix bundle and it has been demonstrated that several regions within it, including those associated with Acute Myeloid Leukemia (AML), have a strong tendency to form amyloid-like assemblies with β-sheet structures and cellular toxicity. In particular, the central helix of the bundle (H2- residues 264-277) resulted the most amyloidogenic region; it has a strong tendency to form amyloid-like assemblies endowed with fibrillar morphology and β-sheet structure toxic to neuroblastoma cells, while the addition of a short loop at the N-terminus of the helix (peptide N-term, residues 259-277) delays the aggregation process. To shed light in the cytoxic processes of two peptide sequences covering H2 and understand if the polyunsaturated fatty acid DHA which neuroprotective effect is assessed, the conformational and aggregation behaviour of H2 and Nterm H2, in the presence of model membranes, has been investigated. Different lipid membranes, composed by 1-palmitoyl-2-oleoyl-phosphatidylcholine (POPC), Cholesterol (Chol) and 1,2-didocosahexaenoyl-phosphatidylcholine (DDPC), characterized by different liquid crystalline mesostructures (e.g., ordered, L_o, vs. disordered, L_d), have been prepared. To gain insights into the microstructural changes of the lipid bilayer and the conformational rearrangement of the interacting peptides, a combined approach including Electron Spin Resonance (ESR) spectroscopy and Circular Dichroism (CD) was used. It has been found that the model membranes interact with the H2 an Nterm H2 and their presence induce a change in conformation and aggregation process of these peptides.

4.2. Materials and methods

Materials

Chloroform, dichloromethane and methanol, HPLC-grade solvents, were obtained from Merck (Darmstadt, Germany). 1-Palmitoyl-2-oleoyl-sn-glycero-3-phosphatidylcholine (POPC), 1,2-didocosahexaenoyl-sn-glycero-3-phosphocholine (DDPC) were obtained from Avanti Polar Lipids (Birmingham, AL, USA). Spin-labelled phosphatidylcholines (1-palmitoyl-2-stearoyl-(n-doxyl)-sn-glycero-3-phosphocholine, *n*-PCSL) with the nitroxide group in the positions 5, 7, 10 and 14 of the acyl chain and 25-doxyl cholesterol were also obtained from Avanti Polar Lipids. Cholesterol (Chol), Sodium Phosphate mono and di-hydrate and 1,1,1,3,3,3-hexafluoro-2-propanol (HFIP) were provided from Sigma Aldrich (St. Louis, MO).

H2 derived peptides, whose sequences are reported in **Table 4.1**, were synthesized and purified as already reported [1]. Purified peptides were pretreated with HFIP for 2 h (50 % v/v) and then lyophilized and stored at -20 °C until use. The sample was then freeze-dried and dissolved filtered phosphate buffer 10mM pH 7, and then the UV and CD spectra were recorded to assess the starting concentration.

Table 4.1: Peptides sequences

H2	^{264}VEAKFINYVKNCFR^{277}
Nterm H2	^{259}GSLPKVEAKFINYVKNCFR^{277}

Large unilamellar vesicles

Large unilamellar vesicles (LUVs), used for ESR spectroscopy and CD spectroscopy, were prepared as described in **Section 3.2.2** and then extruded through a 0.1 μm polycarbonate membranes 21 times. Briefly, the lipid mixtures were prepared mixing appropriate amounts of lipids, dissolved in a chloroform/methanol (2:1 v/v) in a round-bottom test tube. Spin-labeled

phosphatidylcholines (*n*-PCSL) and CNO were added to the lipid mixture (5% mol% on the total lipid) by mixing appropriate amounts of a spin-label solution in ethanol (1 mg/mL) with the lipid organic mixture.

A thin lipid film was produced by evaporating the solvents with dry nitrogen gas and final traces of solvents were removed by subjecting the sample to vacuum desiccation for at least 3 h. The samples were then hydrated with the proper amount of Phosphate buffer 10mM pH=7.4, in order to obtain the final concentration of 500 µM of lipids. The luvs solutions used for the ESR and CD characterization were the same.

Electron Spin Resonance (ESR) Spectroscopy

ESR spectra were recorded with a 9 GHz Bruker Elexys E-500 spectrometer (Bruker, Rheinstetten, Germany). The capillaries containing LUVs suspensions, in absence and presence of the investigated peptides, were placed in a standard 4 mm quartz sample tube containing light silicone oil for thermal stability. All the measurements were performed at 25 °C. Spectra were recorded using the following instrumental settings: sweep width, 100 G; resolution, 1024 points; time constant, 20.48 ms; modulation frequency, 100 kHz; modulation amplitude, 1.0 G; incident power, 6.37 mW. Several scans, typically 32, were accumulated to improve the signal-to-noise ratio. The spectra were quantitatively analysed by the parametrization method already described in **section 3.2**.

Circular Dichroism (CD)

CD spectra of H2, Nterm H2, were acquired with a Jasco J-810 spectropolarimeter (Jasco international Co. Ltd, Tokyo, Japan) in the range of 200–260 nm using a 0.1 cm path length quartz cuvette at 20 °C in continuous scanning mode (20 nm/min, with a 4.0 s response and a 1.0 nm band width). Spectra corresponding only to the solvent or lipid bilayers in the absence of the peptide have been recorded thoroughly during the measurements and subtracted from the corresponding peptide/lipid bilayer spectrum. The data were accumulated over 3 runs, the presented data being the average. The results are not converted to molar

ellipticity because in the resence of an aggregation process is not possible to determine the peptide concentration.

4.3. Effects of lipid membranes L_d and L_o on conformation of NPM1 peptides
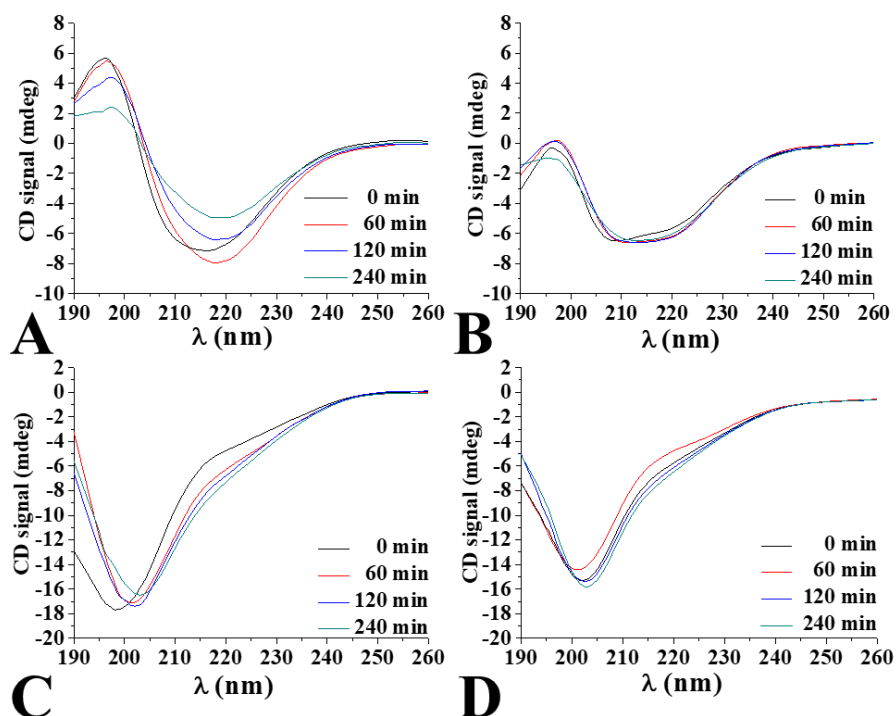
4.3.1. Circular dichroism

The CD characterization of H2 derived peptides in phosphate buffer was already reported[1] H2 exhibited a characteristic β-sheet profile with a slight decrease in the overall signal, within 24 h, due to aggregation, while Nterm H2 presented features suggesting of a mixture of different secondary structure conformations (α-helix, β-sheet and random coil) with an evolution toward an enrichment of the β-structure content.

In the present study the influence of membrane models on the conformation of H2 peptides was investigated.

Freshly dissolved solutions of the H2 or Nterm H2 peptides were added to LUV solutions of either POPC or POPC/Chol, to get a lipid/peptide molar ratio of 10. Upon the addition of peptides, CD spectra were recorded (**Figure 4.1**, black lines) and the samples were monitored for 4 h.

At t=0 the two peptides present different spectra also depending on the lipid bilayer: H2 presents CD spectra with a single minimum at ~ 215 nm in the presence of pure POPC (**Figure 4.1A**) and with two minima at around 208 and 220 nm, in the presence of POPC/Chol (**Figure 4.1B**). Those results show differences in the peptide conformations, probably due to the interaction of the peptide H2 with POPC and POPC/Chol bilayers; while POPC do not affect the conformation and aggregation properties of the peptide, which preserves a β-sheet structure and aggregates with time, the presence of cholesterol induces a slight conformational transition, from a β-structure to a more α-helical conformation. Since the decrease of Cotton effect is due to a variation of nominal concentration

of the peptide upon aggregation, the presence of cholesterol seems to have also a delaying aggregation effect on both derived H2 sequences.

Figure 4.1: Circular dichroism spectra over time of H2 (A and B) and Nterm H2 (C and D) in the presence of POPC and POPC/Chol lipid systems (A and C and B and D, respectively).

These results clearly show that the helical conformation of the native H2 region could have a protective role with respect to amyloid-like aggregation as previously suggested: indeed wt NPM1-CTD unfolds through compact states retaining residual α-helical structure just in the H2 region[2-4].

On the other hand, Nterm H2 is characterized by a spectrum with a minimum at ~ 200 nm for POPC system (**Figure 4.1C**) while, for POPC/Chol, also a shoulder at 222 nm is observed suggesting a mixed state random coil+ α-helix (**Figure 4.1D**). In the presence of POPC, Nterm H2 shows the onset of the shoulder at 222 nm, starting from 60 min, and a slight shift of the minimum toward higher wavelength that makes CD profiles more similar to those shown in POPC/Chol

over time. For Nterm H2, the effects of lipid model membranes seem to be less significant: no

conformational change is detected but only a suppression or delay of the aggregation process, both in the presence of POPC and POPC/Chol LUVs.


4.3.2. Electron spin resonance

To deepen the influence of protein regions on lipid membrane ordering and dynamics ESR investigations, using purposely selected spin-labelled lipids were carried out. The ESR spin labels approach, described in **Chapter 3** was adopted: spin-labeled at the position 5 and 14 along the acyl chain (5-PCSL and 14-PCSL, respectively), embedded in the two LUV systems (as 5% of the total lipid molar content) were acquired. From the spectra analysis, it is possible to estimate the order parameter S, an index of the mobility of the acyl chains, with higher values associated to more rigid systems. Comparison between the S values allows the local ordering of the two lipid systems in the absence and in the presence of the peptides to be investigated. Time course samples prepared for CD experiments were also analysed by means of ESR, by monitoring the S changes immediately after addition of the peptides and for the following 4 h.

For the POPC lipid system, in the presence of H2, S remains constant over time for both 5- and 14-PCSL (**Figure 4.2A**). This result indicates that the acyl chain mobility is not significantly affected by the peptide, neither in the hydrophilic region nor in the hydrophobic one. Upon the addition of Nterm H2 (**Figure 4.2C**), S suddenly increases with respect to the values registered in the peptide absence; then for 5-PCSL it decreases with time, going back to a value similar to that of the lipid alone; on the contrary, for 14-PCSL it remains constant, i.e. slightly higher with respect to the starting one. In the case of POPC/Chol system, immediately upon the H2 addition, the order parameter of spin labels decreases, passing through a minimum before reaching a constant value after 2 h (**Figure 4.2B**). This trend is the same for both spin labels, but it is more evident for 14-

PCSL than for 5-PCSL. In the presence of Nterm H2, we observe an increased S value, more marked with respect to POPC alone (**Figure 4.2D**).

After 1 h, the strong increase observed for the hydrophilic label 5-PCSL remains constant and S for the inner hydrophobic 14-PCSL decreases, reaching a lower value with respect to that of the bilayer in the absence of the peptide.
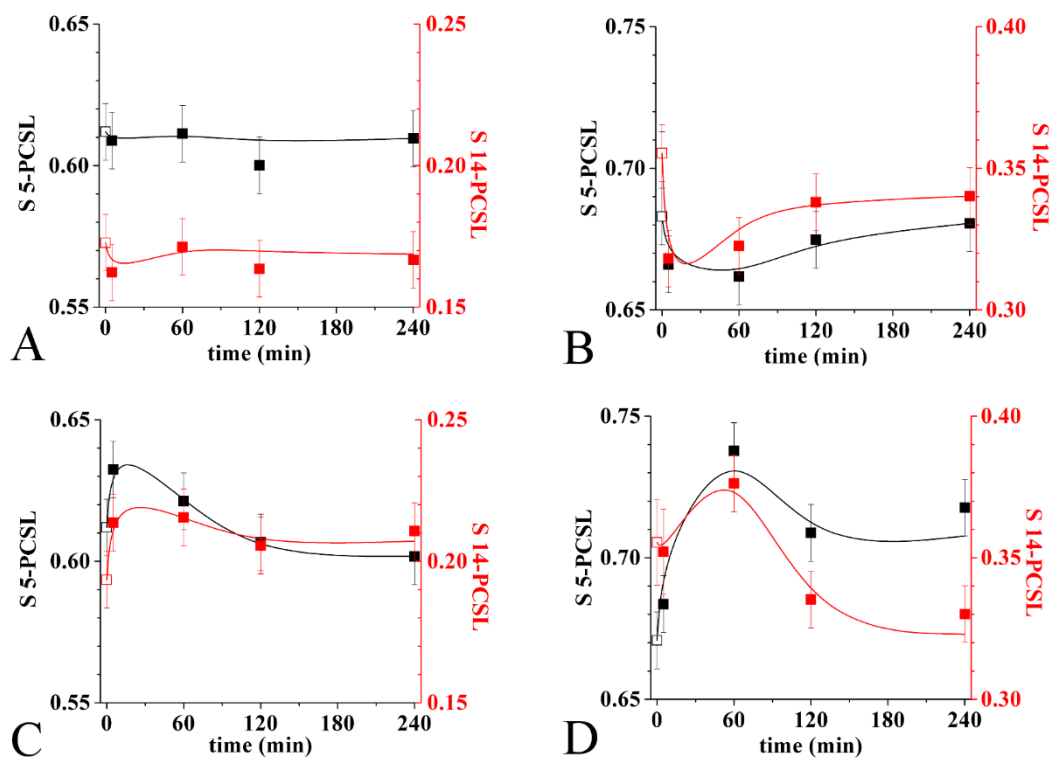

Figure 4.2: Order Parameter, S, of 5-PCSL (black scale) and 14-PCSL (red scale) in POPC (A and C) and POPC/Chol (B and D) lipid systems in the presence of H2 (A and B) and Nterm H2 (C and D), respectively. The order parameter in POPC and POPC/Chol before addition of the peptides is reported in the figures as an open symbol for comparison.

These data clearly indicate that both H2 and Nterm H2 exert stronger effects on POPC/Chol with respect to POPC bilayers: these differences can arise *i*) from the presence of cholesterol-rich crystalline domains within POPC/Chol system, that mediate the interaction of amyloidogenic peptides with membranes, *ii*) from changes in the physical properties of cholesterol-rich membranes (e.g., increased

lipid ordering, reduced lipid mobility), *iii*) or also from specific interaction with the peptide sequences[5]. Thus, to unveil the mechanisms of the cholesterol effects, ESR spectra of a cholesterol analogue spin-labelled at position 25 (CNO spin label) embedded in the POPC/Chol bilayers (as 3% of the total lipid molar content), in the absence and in the presence of H2 peptides were acquired. Indeed, the analysis of CNO ESR spectra allows to get almost straight information on the positioning of cholesterol in the investigated membranes[6]. CNO spectrum in POPC/Chol presents an almost isotropic line shape, similar to the 14-PCSL spectrum, ruling out the possibility of cholesterol segregation leading to domain formation; time course measurements do not show any significant line shape variation, suggesting that no cholesterol re-arrangement occurs[6].

On the contrary, immediately upon the addition of either H2 or Nterm H2 a change of the order parameter is observed (**Figure 4.3**). Indeed, the addition of H2 causes a decrease of *S* and this value remains constant over time (**Figure 4.3A**), following the same trend already observed for 5- and 14-PCSL in the same system. Nterm H2 addition determines an increase of S that reaches a constant value upon 2 h, following the same trend of the hydrophilic label 5-PCSL.
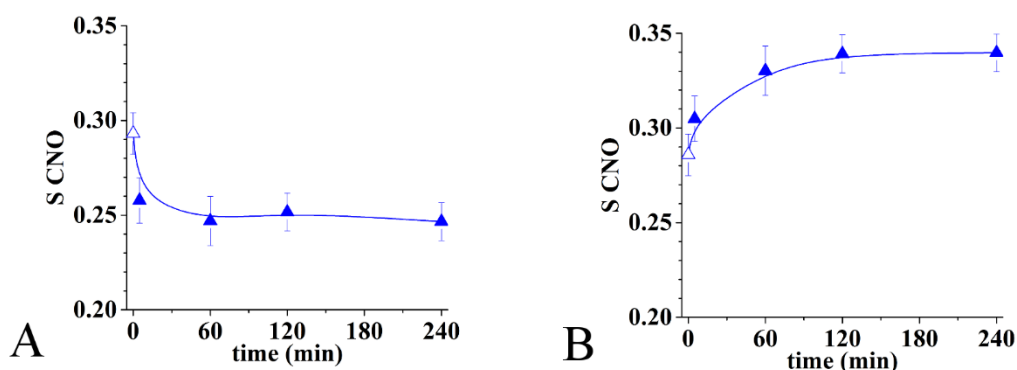
Figure 4.3: Order Parameter, S, of CNO in POPC/Chol lipid systems in the presence of H2 (A) and Nterm H2 (B), respectively. The order parameter in POPC/Chol before addition of the peptides is reported in the figures as an open symbol for comparison.

To obtain further information from the EPR spectra we calculated the hyperfine coupling constant a'_N, an index of the environment polarity experienced by the labels[7], the values obtained for the three spin labels in POPC/Chol system, in the presence of either H2 or Nterm H2, are reported in **Figure 4.4A** and **B**, respectively.
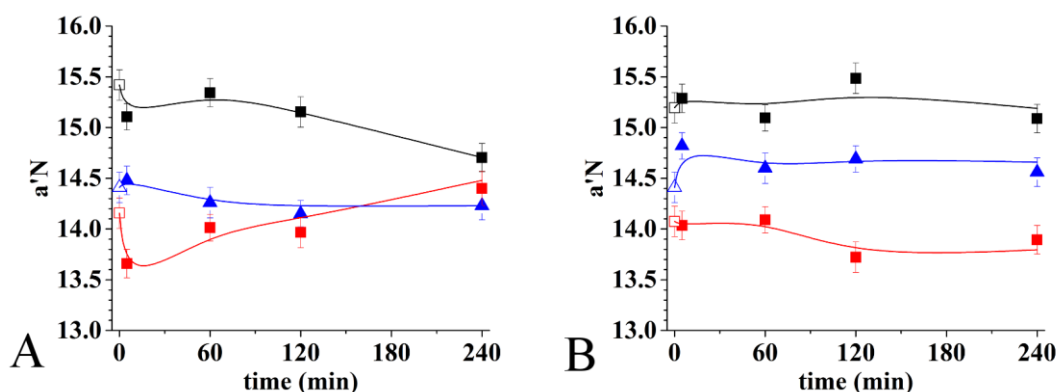
Figure 4.4: Hyperfine coupling constant, a'_N, for 5-PCSL (black), 14-PCSL (red) and CNO (blue) in POPC/Chol in the presence of H2 (A) and Nterm H2 (B), respectively. The Hyperfine coupling constant in POPC/Chol before addition of the peptides is reported in the figures as an open symbol for comparison

In the absence of peptides the a'_N values of the three spin labels are different, following the order 5-PCSL > CNO > 14-PCSL, indicating that the expected polarity gradient exists moving from the hydrophilic headgroups to the inner of the bilayer[7].

The addition of H2 peptide causes a marked change in the a'_N calculated from 5-PCSL and 14-PCSL spectra: in the former case it decreases while in the latter increases. On the contrary a'_N for CNO remains constant. Notably the variation of a'_N over time, for the three spin labels, indicates that, after 240 min, it reaches very similar values for the three systems, suggesting that in the presence of the peptide the typical bilayer polarity gradient is suppressed.

For what concern Nterm H2, the only significant change of a'_N is observed for CNO: it increases just after the addition of the peptide and remains constant with time.

Summarizing, the presence of H2 peptide causes a fluidification of the lipid bilayer, in particular of the inner core, as clearly indicated by the decrease of the order parameter for the three spin labels. On the contrary, an almost opposite effect is caused by the interaction with Nterm H2 peptide where the increase of the order parameter for 5-PCSL and CNO points towards a stiffening of the outer regions of the bilayer. It is worth to stress that this stiffening effect appears as a transient event in the POPC system (in particular when the outer region of the membrane is under observation) while it is permanent in the POPC/Chol system. ESR well highlights a deeper interaction of the cholesterol containing model membrane with respect to the pure POPC one.

4.4. Effects of lipid membranes L_d and L_o containing DPC on NPM1 peptides

4.4.1. Circular dichroism

Freshly dissolved solutions of the H2 or Nterm H2 peptides were added to LUV solutions of either POPC/DDPC or POPC/Chol, where the 20% of POPC is replaced by DDPC, to get a lipid/peptide molar ratio of 10. Upon the addition of peptides, CD spectra were recorded (**Figure 4.5**, black lines) and the samples were monitored for 4 h.

At t=0 H2 presents CD spectra with a single minimum at ~ 215 nm in the presence of pure POPC/DDPC as in the case of POPC alone (**Figure 4.5A**). Interestingly after 60 min the intensity of the signal remains unchanged indicating that an interaction with the membranes is occurring; indeed, H2 undergoes to a rapid aggregation process in POPC LUVs or in phosphate buffer. However, this interaction seems to be transient because a reduced signal is registered over time.

On the contrary, in the case of POPC/DDPC/Chol, H2 shows a spectrum at t=0 minute characterized by a minimum at ~218 nm (**Figure 4.5B**) and that there is an inhibition of the decrease of Cotton effect.

For Nterm H2, the effects of lipid model membranes seem to induce a conformational change: at t= 0 min the Nterm H2 is characterized by a spectrum with a minimum at ~ 200 nm in the presence of POPC/DDPC system (**Figure 4.5C**), with a less pronounced shoulder at 222 nm compared with the Nterm H2 in phosphate buffer.
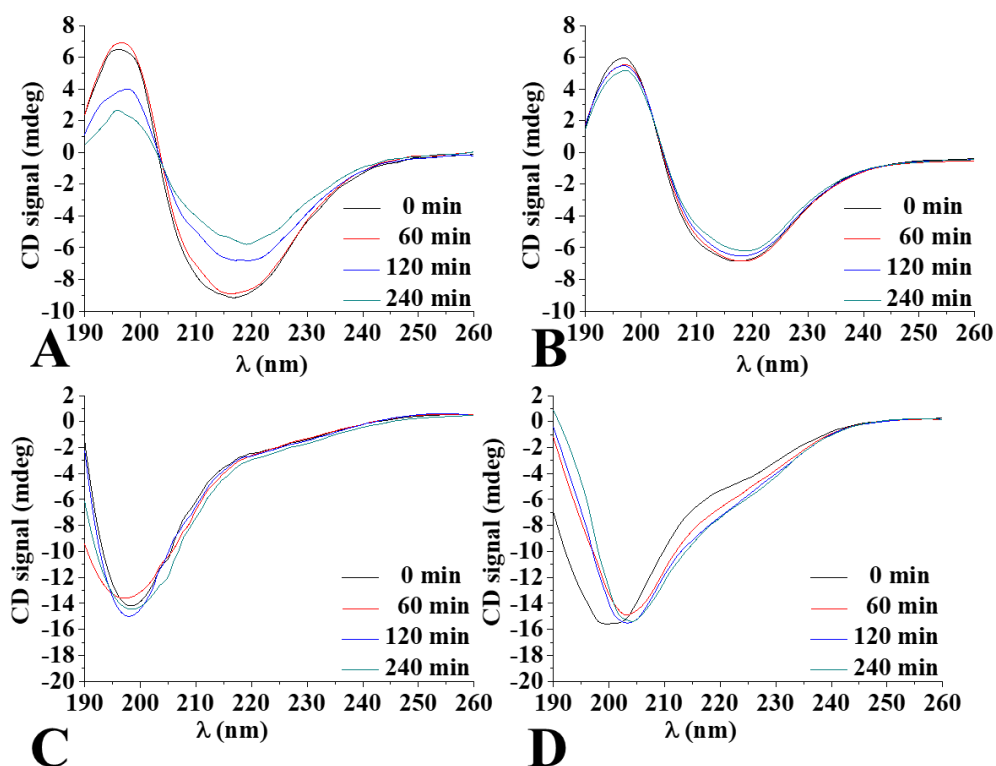
Figure 4.5: Circular dichroism spectra over time of H2 (A and B) and Nterm H2 (C and D) in the presence of POPC/DDPC and POPC/DDPC/Chol lipid systems (A and C and B and D, respectively).

After 60 min a decrease of the signal intensity is observed, but is suppressed over time. At 0 min the signal undergoes to a slight shift to higher wavelengths and it associated to a reduce intensity, which suggests the starting point of an aggregation process. In the presence of POPC/DDPC/Chol, Nterm H2 shows a spectrum similar to the one observed in the presence of POPC/Chol, that is characterized by a shoulder at 222 nm that becomes more pronounced over time.

Even in this case after 60 min the intensity at 200 nm decreases, but is also shifted to higher wavelength; the shift remains over time and, also, the intensity remains constant. Summarizing the two peptides H2 and Nterm H2 show different conformational changes in the presence of lipid mixtures containing DDPC with respect to phosphate buffer. The behavior also differs from what happens in the presence of POPC or POPC/Chol; indeed, when DDPC replace the 20% of POPC, it delays the aggregation process, and the effect is even more marked when cholesterol is present in the lipid mixtures, but with no changes in conformations associated.For Nterm H2 the effect of DDPC is even more clear: POPC/DDPC induces a more random coil conformation and inhibits over 4 h the β-sheet conformation and such inhibition is also observed in the presence of POPC/DDPC/Chol.

4.4.1. Electron spin resonance

To deepen the influence of protein regions on lipid membrane ordering and dynamics ESR investigations, using purposely selected spin-labelled lipids were carried out. The ESR spin labels approach, described in previous section was adopted and the order parameter S and hyperfine coupling constant a'_N were calculated and reported in **Figure 4.6**. Comparison between the S values allows the local ordering of the two lipid systems in the absence and in the presence of the peptides to be investigated. Time course samples prepared for CD experiments were also analysed by means of ESR, by monitoring the S changes immediately after addition of the peptides and for the following 4 h. For the POPC/DDPC lipid system, in the presence of H2, S increases after 60 min for both 5- and 14-PCSL (**Figure 4.6A**), but such change is transient, because S returns to the starting value. This result indicates that, during the first h, the acyl chain mobility is affected by the peptide, both in the hydrophilic region and in the hydrophobic one, but the perturbation is labile, because it occurs just in the first h. Upon the addition of Nterm H2 (**Figure 4.6C**), S for 5-PCSL decreases with respect to the values

registered in the peptide absence; then it increases with time, going back to a value similar to that of the lipid alone; on the contrary, for 14-PCSL it remains constant, i.e. slightly higher with respect to the starting one. In the case of POPC/DDPC/Chol system, immediately upon the H2 addition, the order parameter of spin labels increases, instead of decreases as in the case of POPC/Chol (**Figure 4.6B**).
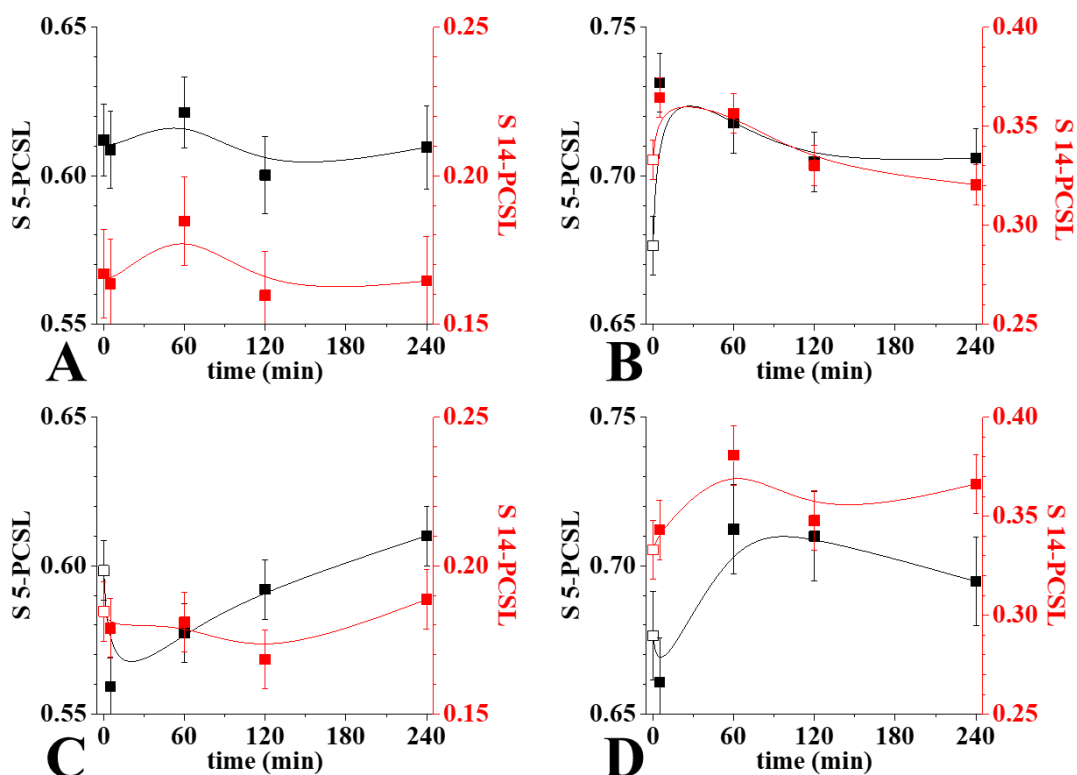
Figure 4.6: Order Parameter, S, of 5-PCSL (black scale) and 14-PCSL (red scale) in POPC/DDPC (A and C) and POPC/DDPC/Chol (B and D) lipid systems in the presence of H2 (A and B) and Nterm H2 (C and D), respectively. The order parameter in POPC/DDPC and POPC/DDPC/Chol before addition of the peptides is reported in the figures as an open symbol for comparison.

For 5-PCSL once H2 is added an increase of the S value is observed; it reaches a maximum and after 2 h tend to a constant value higher than lipid mixtures in the absence of the peptide. The 14-PCSL, that bear the label in the hydrophobic portion of the membrane, the S value follow the same trend of 5-PCSL during the

first h. Interestingly, over the 4 h, S is lower than the starting value. These observed data suggest an internalization of the peptide in the hydrophilic portion of the membrane and that, upon the interaction of the peptide with bilayer, the hydrophobic portion is fluidified, probably because the cholesterol molecule is subtracted from the center of the bilayer. On the contrary, when Nterm H2 is added to the lipid system POPC/DDPC/Chol, S does not increase as soon as the peptide is added, like H2 peptide, but after 60 min (**Figure 4.6D**), when a strong increase is observed for both for the hydrophilic 5-PCSL and the inner hydrophobic 14-PCSL; however, as in the case of POPC/Chol, the perturbation is more marked in the outer hydrophilic portion of the bilayer. These results clearly indicate that both H2 and Nterm H2 exert stronger effects on the bilayer containing Chol, as already shown in the case of the lipid mixtures POPC and POPC/Chol. Thus, even in this case, to unveil the mechanisms of the cholesterol effects, ESR spectra of a cholesterol analogue spin-labelled at position 25 (CNO spin label) embedded in the POPC/Chol bilayers (as 5% of the total lipid molar content), in the absence and in the presence of H2 peptides were acquired. Indeed, the analysis of CNO ESR spectra allows to get almost straight information on the positioning of cholesterol in the investigated membranes. CNO spectrum in POPC/Chol presents an almost isotropic line shape, similar to the 14-PCSL spectrum, ruling out the possibility of cholesterol segregation leading to domain formation; time course measurements do not show any significant line shape variation, suggesting that no cholesterol re-arrangement occurs[6]. On the contrary, immediately upon the addition of either H2 or Nterm H2 a change of the order parameter is observed (**Figure 4.7**). Indeed, the addition of either H2 or Nterm H2 causes an increase of S and this value remains constant over time, following the same trend already observed for 5- and 14-PCSL in the same system. However, Nterm H2 addition determines a stronger effect on the S that reaches a maximum value after 1 h and upon 2 h follows the same trend of the hydrophilic label 5-PCSL, where S seems to decrease.
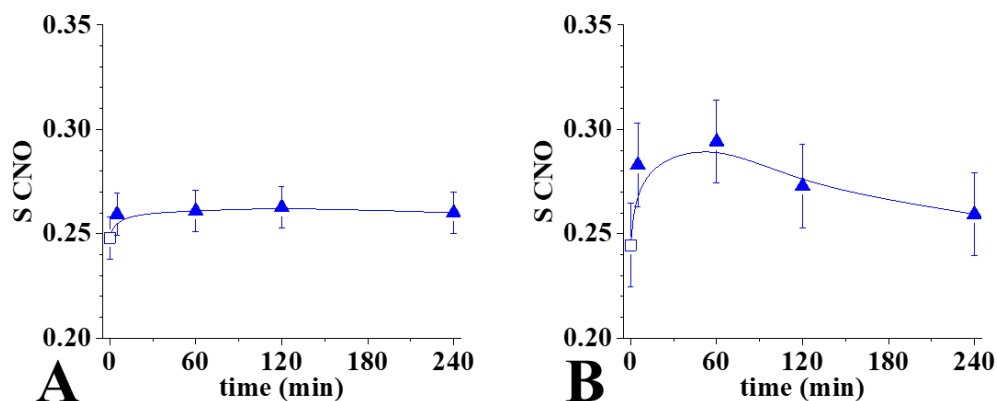
Figure 4.7: Order Parameter, S, of CNO in POPC/Chol lipid systems in the presence of H2 (A) and Nterm H2 (B), respectively. The order parameter in POPC/Chol before addition of the peptides is reported in the figures as an open symbol for comparison.

To obtain further information from the EPR spectra we calculated the hyperfine coupling constant a'_N, an index of the environment polarity experienced by the labels[7], the values obtained for the three spin labels in POPC/DDPC/Chol system, in the presence of either H2 or Nterm H2, are reported in **Figure 4.8A** and **B**, respectively. As already discussed in the previous section, in the absence of peptides the a'_N values of the three spin labels indicate the expected polarity gradient exists moving from the hydrophilic headgroups to the inner of the bilayer[7]. The addition of the two peptides causes the same changes in the polarity profiles: the a'_N for 5-PCSL remains almost unchanged; for CNO increases as in the case of the 14-PCSL. Nevertheless, the polarity gradient existing in lipid bilayer in absence of peptides remains unchanged, meaning that the interaction occurring between the peptide and the membranes does not rearrange the bilayer.
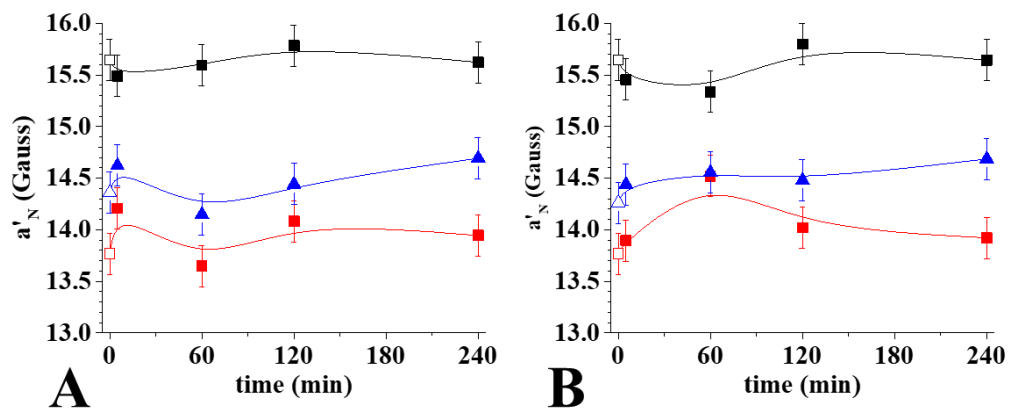
Figure 4.8: Hyperfine coupling constant, a'$_N$, for 5-PCSL (black), 14-PCSL (red) and CNO (blue) in POPC/DDPC/Chol in the presence of H2 (A) and Nterm H2 (B), respectively. The hyperfine coupling constant in POPC/DDPC/Chol before addition of the peptides is reported in the figures as an open symbol for comparison.

4.5. Conclusion

Peptides and proteins often show a conversion from their soluble forms into fibrillar aggregates, giving rise to pathological conditions ranging from neurodegenerative disorders to systemic amyloidosis and, in the fibrillar process, early oligomers are the most toxic species. Recently, it was demonstrated that several regions of the C-terminal domain of NPM1 form amyloid toxic aggregates. The sequence covering the H2 region of the CTD resulted already toxic at 0 and 1 h of aggregation, whereas the Nterm H2 peptide containing the linker loop connecting H2 with H1, appeared weakly toxic at these time points, causing the main effects after 15 h of aggregation time. Herein the biophysical features of the aggregation of several NPM1 regions were investigated in the presence of model membranes containing or not cholesterol. This study has the aim to elucidate the different toxic behaviours exhibited by the two sequences covering the H2 region of NPM1. The interaction between NPM1 regions and LUVs mimicking membranes was firstly characterized in terms of conformational effect of LUVs, by means of circular dichroism: while POPC bilayers do not affect the conformation and aggregation properties of the peptides, which preserves a β-sheet structure and aggregates with time, the presence of cholesterol induces a slight conformational transition. For Nterm H2, the effects of lipid model membranes seem to be less significant: no conformational change is detected but only a suppression or delay of the aggregation process, both in the presence of POPC and POPC/Chol LUVs. In this context it is worth to note that Nterm H2 peptide presents a cholesterol binding consensus sequence (the CARC sequence (K/R)-X $_{1-5}$-(Y/F)-X $_{1-5}$-(L/V)), but it seems able to discriminate worse between the two lipid model membranes than H2. This is likely due to the presence of two strong helical breaking residues (Gly and Pro) at the beginning of the Nterm H2 that hampers such a fold of the peptide, while CRAC and CARC sequences are known to effectively bind cholesterol when located within a α-helical stretch. On the contrary, H2 is able to fold as a distorted helix in the

presence of cholesterol, suggesting that it can bind cholesterol despite the irregular CRAC sequence (since it presents one more residue between Val and Tyr with respect to the consensus sequence). These differences may also justify peptide different effects on POPC/Chol systems: H2 that likely binds cholesterol through the CRAC sequence determines a sensitive fluidification of the whole bilayer, as already observed for similar sequences, causing the loss of a polarity gradient moving from the outer to the inner of the membrane. On the contrary Nterm H2 causes a stiffening of central and outer regions of the bilayer, and a partial fluidification of the inner hydrophobic region. The addition of the DHA containing phospholipid DDPC to both POPC and POPC/Chol shows to have an effect on both peptides.

When the mega-3 phospholipid is substituted in the liquid disordered phase, it role out a solubilization effect on the H2 and Nterm H2, that is more marked for the less amyloidogenic Nterm H2, due to the conformation changes that can be observed: indeed, it shows a more random coiled conformation. Nevertheless, for both peptides the interaction is labile, and mainly localized on the vesicles surface; indeed, it is observed that the order parameter associated to the 5-PCSL- the label positioned near the hydrophylic portion of the bilayer- is the most affected during the first h of observation. Over time, the perturbation caused by the peptides to the bilayer is suppressed.

Notably, when DDPC is added to this lipid system, no aggregation occurs but no helical conformation of H2, which is supposed to be a transient step associated to pore formation in the membranes, is promoted. The ability of DHA to solubilize H2 and at the same time inhibit a possible step for pore formation can be an explanation of the beneficial effects associated to DHA. Indeed, recently the pore formation was considered as a plausible mechanism of pathogenesis of neurodegenerative processes. In this respect, although a deeper investigation should be performed to determine the selective binding that occurs between amyloidogenic peptides and omega-3 phospholipids, the presented results could

help in the comprehension of such affinity, contributing to build a robust scientific platform for the biomedical and pharmaceutical exploitation of these molecules.

4.6. References

1 Di Natale, C. *et al.* Nucleophosmin contains amyloidogenic regions that are able to form toxic aggregates under physiological conditions. *FASEB journal : official publication of the Federation of American Societies for Experimental Biology*, doi:10.1096/fj.14-269522 (2015).

2 Scaloni, F., Gianni, S., Federici, L., Falini, B. & Brunori, M. Folding mechanism of the C-terminal domain of nucleophosmin: residual structure in the denatured state and its pathophysiological significance. *Faseb J* **23**, 2360-2365, doi:10.1096/fj.08-128306 (2009).

3 Scaloni, F., Federici, L., Brunori, M. & Gianni, S. Deciphering the folding transition state structure and denatured state properties of nucleophosmin C-terminal domain. *Proc Natl Acad Sci U S A* **107**, 5447-5452, doi:10.1073/pnas.0910516107 (2010).

4 Chiarella, S., Federici, L., Di Matteo, A., Brunori, M. & Gianni, S. The folding pathway of a functionally competent C-terminal domain of nucleophosmin: protein stability and denatured state residual structure. *Biochem Biophys Res Commun* **435**, 64-68, doi:10.1016/j.bbrc.2013.04.038 (2013).

5 Cecchi, C. & Stefani, M. The amyloid-cell membrane system. The interplay between the biophysical features of oligomers/fibrils and cell membrane defines amyloid toxicity. *Biophysical chemistry* **182**, 30-43, doi:10.1016/j.bpc.2013.06.003 (2013).

6 Marsh, D. Molecular motion in phospholipid bilayers in the gel phase: long axis rotation. *Biochemistry* **19**, 1632-1637 (1980).

7 Vitiello, G. *et al.* Fusion of raft-like lipid bilayers operated by a membranotropic domain of the HSV-type I glycoprotein gH occurs through a cholesterol-dependent mechanism. *Soft Matter* **11**, 3003-3016, doi:10.1039/c4sm02769h (2015).

Chapter 5:

Aβ 1-42 and model membranes

5.1. Work outline

Many experimental evidences indicate that the interactions with neuronal membranes play an important role in the Aβ 1-42 toxicity[1,2] and the study of the interactions between Aβ peptides and membrane model systems is a very important topic in the recent literature.

AD is also elicited by the interplay of genetic, environmental and dietary factors[3,4]. The adherence to a Mediterranean diet profile, including fish, vegetables, fruits, coffee, and light-to-moderate alcohol intake, seems to reduce the incidence of this and other neurodegenerative pathologies[5]. The beneficial effects of fish are at least partially ascribed to the high content of polyunsaturated fatty acids (PUFA), and specifically of omega-3 ones[6]. However, the effectiveness of these molecules is still controversial, and their mechanism of action remains elusive. Among other hypotheses, mainly based on the radical-scavenging and anti-inflammatory action of PUFA[7,8] it has been proposed that omega-3 fatty acids, once converted to lipids, could alter the structure and functionality of neuronal membranes, whose involvement in AD aetiology is widely accepted[2].

Docosahexaenoic acid (DHA) is found in extraordinarily high concentration in the plasma membranes of neural tissues, reaching up to 50% of the total acyl chains[9,10] and its decline has been associated with the loss of memory and learning, suggesting that the omega-3 fatty acids modulate the membranes properties and influence the molecular mechanism of AD[11,12]. Recently, it has been proposed that omega-3 lipids disturb the lipid packing in the membrane, favoring a deeper internalization of Aβ fragments among the lipid acyl chains[13] offering a possible explanation for the inhibition of Aβ self-aggregation operated by omega-3 fatty acids.

To get light in this complex scenario, the interaction of Aβ 1-42 with bilayers whose lipid composition reproduces the main components of neuronal membranes[14,15], including both zwitterionic and anionic phospholipids,

cholesterol, sphingomyelin and gangliosides has been investigated. Moreover, the effect of the inclusion of the omega-3 lipid 1,2-didocosahexaenoyl-sn-glycero-3-phosphocholine DDPC in the bilayer composition is analysed in detail.

An integrated experimental approach was applied for this study. The effect of complex lipid bilayers on Aβ 1-42 conformation/self-aggregation was monitored by Circular Dichroism (CD); the influence of Aβ 1-42 interaction on the membrane microstructure and fluidity was studied by Electron Spin Resonance (ESR) measurements; the disrupting effect of this interaction on membrane integrity was studied by a previously established FRET-based membrane leakage assay.

5.2. Materials and methods

Materials

Chloroform, dichloromethane and methanol, HPLC-grade solvents, were obtained from Merck (Darmstadt, Germany). 1-Palmitoyl-2-oleoyl-sn-glycero-3-phosphatidylcholine (POPC), 1-Palmitoyl-2-oleoyl-sn-glycero-3-phospho-L-serine (POPS), N-octadecanoyl-D-erythro-sphingosylphosphorylcholine (SM), ganglioside (GM1) ovine brain sodium salt, 1,2-didocosahexaenoyl-sn-glycero-3-phosphocholine (DDPC) were obtained from Avanti Polar Lipids (Birmingham, AL, USA). Spin-labeled phosphatidylcholines (1-palmitoyl-2-stearoyl-(n-doxyl)-sn-glycero-3-phosphocholine, *n*-PCSL) with the nitroxide group in the positions 5, 7, 10 and 14 of the acyl chain were also obtained from Avanti Polar Lipids.

Aβ 1-42 peptide was synthesized as previously reported and retreated with TFA, in order to dissolve any fibrillar aggregates, as previously described [14]. The sample was then freeze-dried and redissolved in pure HFIP, and then the UV and CD spectra were recorded to assess the acid treatment success.

Table1: Peptides sequences.

Aβ 1-42	[1]DAEFRHDSGYEVHHQKLVFFAEDVGSNKGAIIGLMVGGVVIA[42]

Lipid mixtures preparation

All lipid mixtures were prepared mixing appropriate amounts of lipids, dissolved in a chloroform/methanol (2:1 v/v) in a round-bottom test tube. For Electron Spin Resonance measurements spin-labeled phosphatidylcholines (*n*-PCSL) were alternatively added to the lipid mixture (1% mol% on the total lipid) by mixing appropriate amounts of a spin-label solution in ethanol (1 mg/mL) with the lipid organic mixture. A thin lipid film was produced by evaporating the solvents with dry nitrogen gas and final traces of solvents were removed by subjecting the sample to vacuum desiccation for at least 3 h. The samples were then hydrated with the proper amount of buffer (i.e. Phosphate buffer 10mM) pH=7.4, repeatedly vortexed, avoiding any further treatment of the samples.

Large unilamellar vesicles

Large unilamellar vesicles (LUVs) used for the supported bilayer, ESR spectroscopy and CD spectroscopy in the case of peptides interaction study with lipid membranes, were prepared as described in **Section 5.2.1** and then extruded through a 0.1 μm polycarbonate membranes 21 times.

For Aβ 1-42 investigation, LUVs consisting on POPC/POPS/Chol/SM/GM1 (8/2/9/1/1 mol/mol), henceforth indicated as neuronal membrane-like lipid bilayers, NML-LB, POPC/POPS/Chol/SM/GM1/DDPC (4/2/9/1/1/5mol/mol), henceforth indicated as O3-LB and POPC/POPS/Chol/SM/GM1/DDPC (6/2/9/1/1/2mol/mol), henceforth indicated as O3L-LB, were prepared in 20mM phosphate buffer pH 7.4, freshly degassed by nitrogen purging, at total concentration of 0.4 mg/ml.

Electron spin resonance

ESR spectra were recorded with a 9 GHz Bruker Elexys E-500 spectrometer (Bruker, Rheinstetten, Germany). The capillaries containing MLVs suspensions, were placed in a standard 4 mm quartz sample tube containing light silicone oil for thermal stability. All the measurements were performed at 25 °C. Spectra were recorded using the following instrumental settings: sweep width, 100 G;

resolution, 1024 points; time constant, 20.48 ms; modulation frequency, 100 kHz; modulation amplitude, 1.0 G; incident power, 6.37 mW. Several scans, typically 16, were accumulated to improve the signal-to-noise ratio. For the spectra simulation the gii values for the coupling between the electron spin and the magnetic field were those which gave the best fitting for all spectra: gii=2.0075, 2.006, 2.003. In some cases, due to fitting improvements, 2.0027 was used instead of 2.003 for g_{zz}. About the A_{ii} values for the coupling between the electron spin and the nitrogen nuclear spin, which give a measure of the environmental polarity, we maintained constant Axx=7.1 G and Ayy=7.2 G values, which were also well fitting all the spectra, while it was needed to change the Azz value from one to another system, where we list the <A>=(Axx+Ayy+Azz)/3 values. In order to quantitatively analyse the spectra, we calculated the order parameter, **S**, using a spectra parameterization method defined in **Equation 3.1**.

$$S = \frac{T_{\parallel} - T_{\perp}}{T_{zz} - T_{xx}} \cdot \frac{aN}{a\prime N} \quad \textbf{Eq.3.1}$$

as already discussed in **section 3.2**.

Circular Dichroism

CD spectra of H2, Nterm H2, Aβ 1-42 (0.1 mg/ml final concentration) were acquired with aJasco J-810 spectropolarimeter (Jasco international Co. Ltd, Tokyo, Japan) in the range of 200–260 nm using a 0.1 cm path length quartz cuvette at 20 °C in continuous scanning mode (20 nm/min, with a 4.0 s response and a 1.0 nm band width). Spectra corresponding only to the solvent or lipid bilayers in the absence of the peptide have been recorded thoroughly during the measurements and subtracted from the corresponding peptide/lipid bilayer spectrum. The data were accumulated over 3 runs, the presented data being the average. The results are not converted to molar ellipticity because in the presence of an aggregation process is not possible to determine the peptide concentration.

5.3. Sample condition design

Six different conditions were explored in this work; Aβ 1-42 concentration was the same for all conditions, 20 □M. Two control conditions were used: HFIP/ 0.020 M phosphate buffer, pH 7.4, 80/20 (V/V), in order to check peptide behaviour in a polar environment; 0.020 M phosphate buffer, pH 7.4 to check a polar environment. Four different liposomes composition were studied: 0.4 mg/ml of lipid bilayers formed only by palmytoil-oleil-phosphocholine (POPC-LB); 0.4 mg/ml of neuronal membrane mimicking lipid bilayer (NML-LB)[15,16]; 0.4 mg/ml of NML-LB containing also 25% w/w of the unsaturated fatty acid DDPC (O3-LB); 0.4 mg/ml of NML-LB containing 10% w/w of DDPC (O3L-LB). The two last mixtures were prepared with two different amounts of DDPC to evaluate its specific potential effect on Aβ 1-42 solubility and structure. The detailed liposome compositions are reported in the experimental section. The chemical structure of all lipids used for this study are reported in **Figure 5.1**.
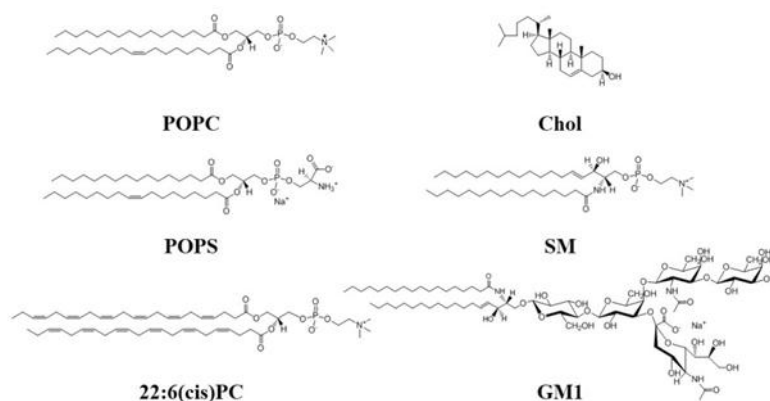

Figure 5.1: Chemical structures of all lipids used in liposomes formulation.

5.4. Circular Dichroism

In consequence of the generally low solubility of Aβ 1-42 and fast aggregation in aqueous solutions, we have checked the peptide conformation in experimental conditions already known to induce canonical secondary structures in Aβ, i.e.

HFIP/water mixture and phosphate buffer. Both the controls spectra gave the expected results, showing the typical shape of α-helix and β-sheet respectively, thus confirming the absence of pre-existing aggregates in the dry peptide film. Interestingly, in the presence of POPC-LB the spectrum of the peptide showed the shape of a β-structure, though the minimum was shifted at a slightly higher wavelength, according to the presence of aggregated forms[17]. In contrast, in the presence of more complex lipid bilayers (NML-LB, O3-LB and O3L-LB), only a low intensity CD signal was detected and no regular secondary structure could be associated to the spectrum. The CD spectra of peptide upon dissolution in every condition are reported in F**igure 5.2**. Since the kinetics of aggregation/dissolution processes and conformational transitions of Aβ 1-42 are quite slow, the CD spectra of the peptide in the different conditions was monitored over several days.
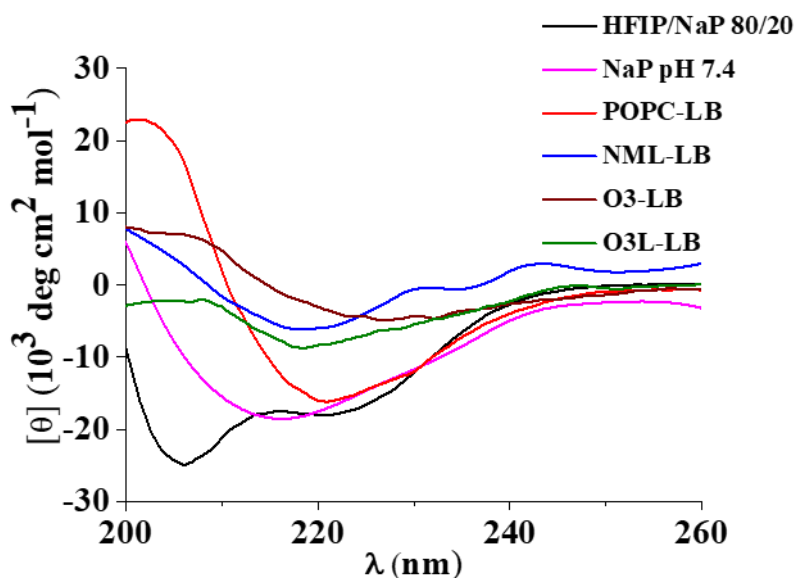
Figure 5.2 CD spectra of A Aβ 1-42 just after dissolution in the conditions studied.

The results obtained are reported in **Figure 5.3** for each liposome conditions. The control experiments gave the expected results: the spectrum in HFIP/water mixture was unaffected over the whole incubation time; on the other hand, when

the peptide was dissolved in phosphate buffer, the signal intensity decreases over time, becoming almost undetectable after 14 days, in agreement with the expected formation of insoluble aggregates in aqueous environments.
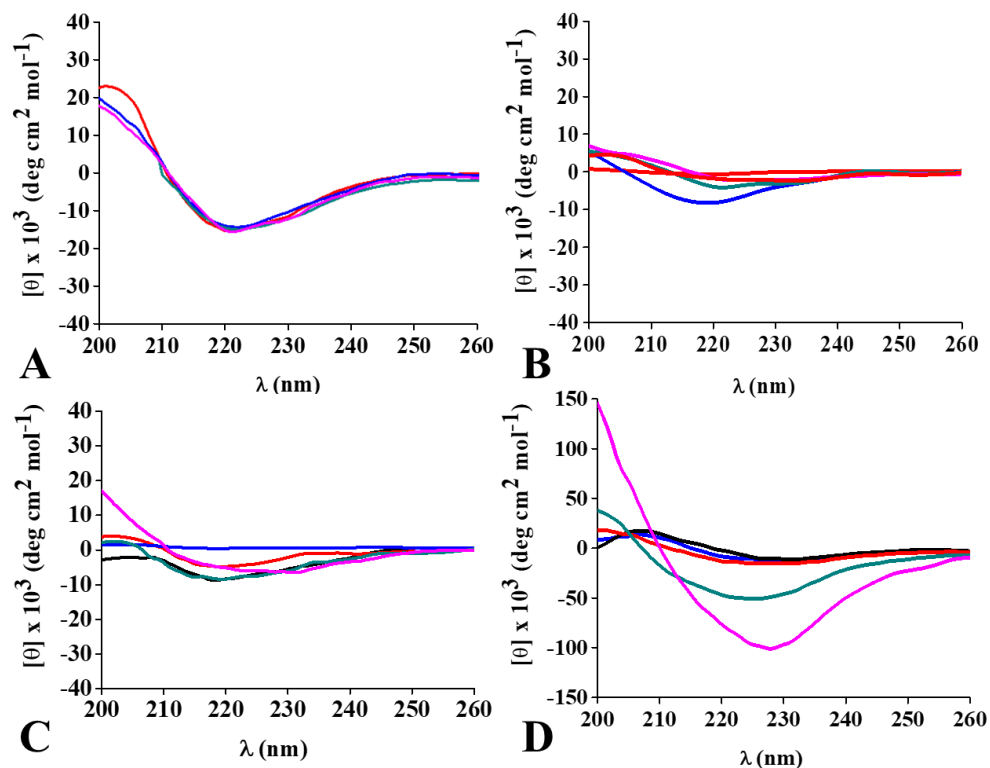
Figure 5.3: CD spectra time evolution of Aβ 1-42 interacting with different lipid bilayer: Panel A POPC-LB; Panel B NML-LB; Panel C O3L-LB**;** Panel D O3-LB.

Figure 5.3 A shows that the shape and intensity of the spectra acquired in POPC-LB over time were constant, suggesting that the soluble aggregate concentration does not change. However, the presence of insoluble, CD silent forms cannot be excluded. In the presence of NML-LB bilayers, the low intensity of the CD signal indicates that only a small fraction of the peptide was dissolved (**Panel B**), and no significant increase is appreciated over time. Yet, the spectrum shape changes during the incubation time, confirming that the lipid bilayer is able to interact with the peptide[2]. Unlike the previous cases, in the lipid bilayer O3-LB, the peptide slowly but extensively dissolves after several days, as highlighted by a consistent

increase in the CD spectrum intensity. The spectrum assumes a shape similar to that observed in the presence of POPC, except for a further red-shift of the minimum, suggesting the presence of higher size soluble aggregates. Interestingly, the time necessary to appreciate changes in the CD spectrum decreases when the amount of omega-3 lipid present in the lipid mixture increases. Indeed, while the presence of higher concentration of DDPC (**Panel D**) induces the peptide film dissolution after 21 days incubation, at lower DDPC concentration (**Panel C**) the spectrum shape changes slightly over 28 days incubation, but no clear trend can be appreciated, as in the case of NML-LB. These evidences suggest the presence of membrane interacting peptide aggregates slowly evolving over time when omega-3 lipids present in the lipid bilayer formulation. However, the kinetics of this process critically depends on the amount of omega-3 present in the lipid phase.

5.5. Electron spin resonance

The changes in lipid ordering and dynamics was studied using the spin label approach. Two spin-labeled phosphocholines were used as reporter: 5-PCSL and 14-PCSL. The former bears the radical in proximity of the polar head, just underneath the hydrophilic surface, while in the latter the label is close to the acyl chain terminus, thus spectra are representative of the inner apolar region behaviour.

The spectra of 5- and 14-PCSL in POPC bilayers are reported in **Figure 5.4**, respectively **Panel A** and **Panel B** (black lines). 14-PCSL generates an almost isotropic three-line spectrum. In contrast, a clearly defined anisotropy is observed for 5-PCSL, as highlighted by the splitting of the low- and high-field signals. Thus, the rotational motion of the label is hindered in the relatively ordered external region of the bilayer, while it is almost free in the bilayer interior. A quantitative analysis of the spectra was accomplished by determining the lipid segmental order parameter (S), as reported in the literature[18]. The S value is 0.64

for 5-PCSL and 0.14 for 14-PCSL. These evidences indicate that POPC-LB presents a marked rigidity and ordering decrease in going from the lipid polar head to the acyl tails termini, as expected for membranes in the liquid crystalline disordered state (Ld)[19]. In the case of the NML-LB, both spin-labelled lipids show anisotropic spectra (**Figure 5.4**). The S value is 0.74 for 5-PCSL and 0.41 for 14-PCSL, showing that these bilayers are more rigid than the previous ones, and the lipid ordering gradient in going from the polar head to the acyl tails termini is lower. This indicates that NML-LB are in the liquid crystalline ordered state (Lo). Also in the presence of DDPC both spin-labelled lipids have anisotropic spectra; the two omega3 containing lipid bilayers show the same lineshape, spectra for the O3-LB mixture are shown in **Figure 5.4**. No additional spectral component, evocative of domain formation[20], was detected. The rigidity of the membrane is only slightly reduced with respect to NML-LB even in the presence of the higher amount of omega-3 lipids, as the S value is 0.68 for 5-PCSL and 0.38 for 14-PCSL. This indicates that inclusion of DDPC in the lipid mixture does not change the liquid crystalline organization of the bilayer, which remains in the Lo state. In a previous work was found that DDPC is able to drive the Lo/Ld transition in the case of a POPC/SM/Chol bilayer[13]. Moreover, omega-3 lipid bearing two polyunsaturated acyl chains, like DDPC, are reported to drive the segregation of cholesterol, with formation of lipid domains[21,22]. The resistance of NML-LB to undergo any transition is probably ascribable to the presence of GM1, which is recognized as a major player in the modulation of later ordering within biological membranes[23], limiting domain growth. The presence of Aβ 1-42 in the system affects the POPC-LB organization[13,19], as revealed by the spectra of 5- and 14-PCSL registered soon after samples preparation (**Figure 5.4**, red lines). In the case of 5-PCSL a slight reduction of the spectrum anisotropy is observed, as confirmed by the decrease of the S value by ~0.02. An opposite behaviour is observed for 14-PCSL: the spectrum anisotropy increases and S raises by ~0.04. However, no evidence of a second component in the spectrum is observed, as expected for

membrane-penetrating peptides. Thus, the experimental evidences point to a positioning of the peptide close to the membrane interface, causing perturbation in the lipid dynamic and ordering that propagates to the bilayer inner core.
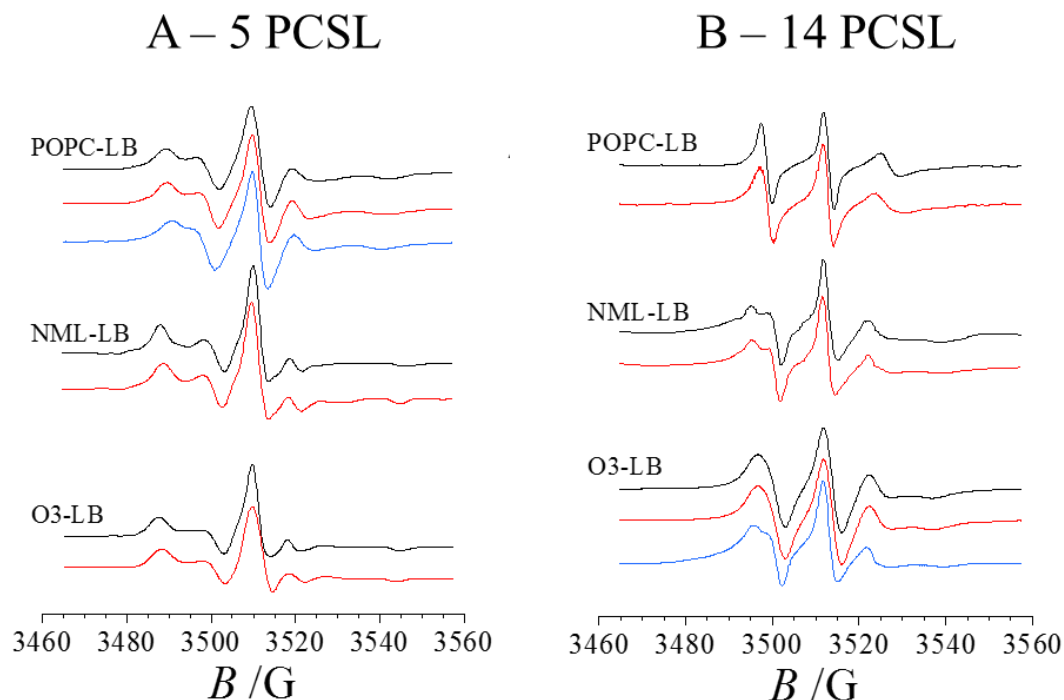
Figure 5.4: EPR spectra of the two spin reporter used in this study, 5-PCSL (Panel A) and 14-PCSL (Panel B) of the investigated liposome compositions. Black lines: EPR spectra of liposomes without Aβ 1-42. Red lines: EPR spectra just after peptide addition. Cyan lines: EPR spectra after 21 days of incubation.

Even for NML-LB the presence of Aβ 1-42 in the system causes a small reduction of the 5-PCSL spectrum anisotropy and a consequent slight S decrease of ~0.02. However, almost no variation is found in the 14-PCSL spectrum. These results indicate a weak interaction of the peptide with the membrane interface, which does not affect the inner bilayer structure. In the case of the omega-3 lipid containing lipid bilayers, similarly to what observed for NML-LB, the presence of Aβ 1-42 causes a reduction of the 5-PCSL spectrum anisotropy, as confirmed by the reduction of 0.02 in the S value, while no effect is registered for 14-PCSL.

Thus, inclusion of DDPC does not affect peptide-membrane interaction in just-prepared samples.
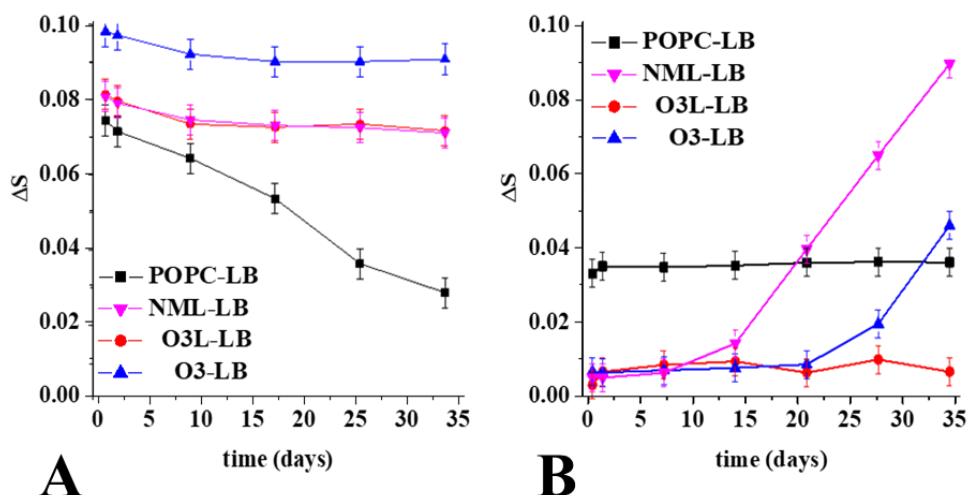
Figure 5.5: Time course evolution of □S for the spin label 5PCSL (Panel A) and for 14PCSL (Panel B) for each lipid bilayers studied when interacting with Aβ 1-42.

The evolution over time of the 5- and 14-PCSL spectra in all the considered bilayers was followed both in the absence and in the presence of Abet42. No spectra change was observed in the peptide absence. In the case of O3L-LB and O3-LB, this indicates no DDPC oxidation to occur, in line with the long-term stability of omega-3 lipids in liposomes reported in the literature[24]. For samples containing the peptide significant changes of the spectra with time were observed, depending on the bilayer lipid composition. In the case of POPC a progressive reduction of the 5-PCSL spectrum anisotropy is observed, as shown by the trend of ΔS reported in **Figure 5.5**. As an example, the spectra of the two spin labels in POPC-LB in the presence of the peptide after 21 days are shown in **Figure 5.4** (cyan lines). In contrast, the 14-PCSL S value remains almost constant (**Figure 5.5**). The 5-PCSL and 14-PCSL spectra in NML-LB exposed to Aβ 1-42 remain almost unaltered, indicating that the weak interaction of the peptide with the membrane does not strengthen with time. In the presence of omega-3 containing

lipid bilayers, for both the formulations considered (O3L-LB and O3-LB), the 5-PCSL spectrum exposed to Aβ 1-42 remains almost constant whilst, interestingly, in the case of 14-PCSL the spectrum anisotropy becomes markedly more evident after three weeks and, consequently, the S value significantly increases (**Figure 5.5**). These results indicate an increasing membrane perturbation of the bilayer inner core due to the interaction with the peptide, modulated by the amount of omega-3 lipids in the membrane, as it is elicited after a smaller time-lag for O3-LB than for O3L-LB systems (**Figure 5.5D**). Internalization of Aβ fragments has been observed in the case of POPC/SM/Chol bilayers enriched in DDPC, which, differently from the ones used in this study, are in the Ld state[13]. This could indicate that the peptide selectively interacts with omega-3 lipids, almost independently of the lipid bilayer state.

5.6. Conclutions

In conclusion, by using CD spectroscopy, we have preliminarily verified that, in phosphate buffer and in the absence of lipids, the peptide adopts the expected β conformation and undergo the subsequent self-aggregation in insoluble aggregates. The effect of single-component lipid bilayer has been also investigated by using POPC, a zwitterionic phospholipid abundant in eukaryotic cells, often chosen for membrane-peptide interaction studies. Our results show that POPC-LB stabilize for several weeks a soluble, aggregated form of Aβ 1-42, having a small but constant concentration. The CD spectrum is indeed very reproducible over time, but has a low intensity and shows a shift of the β-sheet minimum toward higher lambda values, which can be the effect of a β aggregated but soluble structure, with a scattering[25] due to the presence of high molecular weight aggregates. ESR results show that these aggregates interact with the membrane interface, increasingly disturbing its organization, while the bilayer interior is only indirectly affected. Interestingly, biomimetic lipid bilayers (NML-LB) do not present the ability to solubilize the peptide, although CD spectra suggest the presence of a small amount of peptide deprived of regular secondary structure also associated with the lipid phase. Our results indicate that, in the presence of GM1, large and likely heterogeneous aggregates interacting with the membrane interface quickly form. Furthermore, the experimental evidences clearly show that these insoluble aggregates are not able to penetrate in the lipid bilayer[2]. This could be connected with the rigidity of the lipid phase (in the Lo state), which in this case is much higher than that of POPC-LB (in the Ld state).

Inclusion of DDPC in the lipid composition does not affect the initial behavior of the membrane in the presence of Aβ 1.42: only a limited perturbation of O3-LB interface is observed, probably due to a weak interaction with large, insoluble aggregates. However, CD data clearly show that, over time, an increasing fraction of the peptide convert to soluble, lipid associated, aggregates, able to interact with the bilayer.
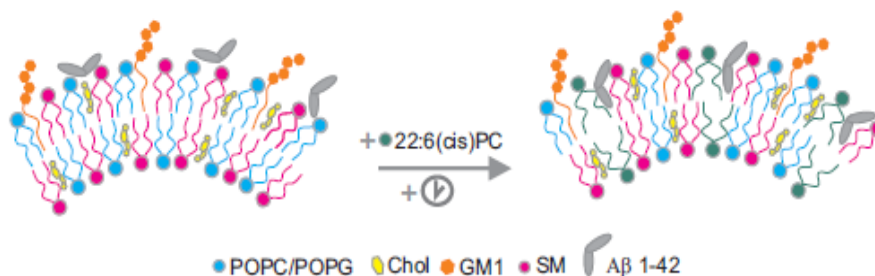
Figure 3.7 Scheme of the different interaction model proposed for Aβ 1-42 and neuronal membrane biomimetic lipid bilayers (left side), and omega-3 containing biomimetic bilayers (right side).

The β-sheet minimum indeed undergoes a further shift toward high wavelength with respect to POPC-LB, suggesting an increasing of the scattering contribution in the spectra. Furthermore, ESR spectra indicate that these aggregates are significantly embedded in the bilayer, differently from the superficial interaction in case of NML-LB, as schematised in **Figure 3.7**.

The comparison of the data obtained by introducing two different DDPC amounts in the lipid bilayer formulation indicates that qualitatively the effect of omega-3 lipid presence is independent by the amount of this component, however the extent of the perturbation and the kinetics of the process are enhanced when the omega-3 lipid concentration increases. It is to be highlighted that the dramatic enhancement of the Aβ 1-42 affinity for the membrane due to DDPC cannot be straightforwardly related to changes of the bilayer properties, considering that this lipid causes only a slight reduction of the bilayer ordering. This result could induce to speculate about a peptide molecular preference for the omega-3 lipid, which, however, should be better investigated.

Moreover, the interaction between Aβ 1-42 and the investigated lipid bilayers causes a strong permeabilization of the latter. Considering the three molecular models proposed for the Aβ 1-42 membrane disrupting activity, detailed discussed in section 1.7, the results obtained suggest that the ion channel mechanism is the most likely for the conditions studied, even if for the NML-LB

only subtle changes in the bilayer microstructure was detected by ESR. In the carpeting mechanism, a critical peptide concentration should be reached before the membrane permeabilization occurs; but, as shown in figure 3.6, the initial trend of the titration is almost linear, without any concentration lag phase at the beginning. On the other hand, in the detergent mechanism, the peptide disassembles the lipid vesicles almost completely, forming smaller species such as micelles, but such a dramatic effect on the bilayer microstructure was not detected by ESR analysis.

5.7. References

1   Matsuzaki, K. Physicochemical interactions of amyloid beta-peptide with lipid bilayers. *Biochimica et biophysica acta* **1768**, 1935-1942, doi:10.1016/j.bbamem.2007.02.009 (2007).

2   Williamson, R. & Sutherland, C. Neuronal Membranes are Key to the Pathogenesis of Alzheimer's Disease: the Role of Both Raft and Non-Raft Membrane Domains. *Curr Alzheimer Res* **8**, 213-221 (2011).

3   Hu, N. *et al.* Nutrition and the risk of Alzheimer's disease. *BioMed research international* **2013**, 524820, doi:10.1155/2013/524820 (2013).

4   Reitz, C. & Mayeux, R. Alzheimer disease: epidemiology, diagnostic criteria, risk factors and biomarkers. *Biochemical pharmacology* **88**, 640-651, doi:10.1016/j.bcp.2013.12.024 (2014).

5   Singh, B. *et al.* Association of mediterranean diet with mild cognitive impairment and Alzheimer's disease: a systematic review and meta-analysis. *Journal of Alzheimer's disease : JAD* **39**, 271-282, doi:10.3233/JAD-130830 (2014).

6   Cunnane, S. C. *et al.* Fish, docosahexaenoic acid and Alzheimer's disease. *Progress in lipid research* **48**, 239-256, doi:10.1016/j.plipres.2009.04.001 (2009).

7   Bazinet, R. P. & Laye, S. Polyunsaturated fatty acids and their metabolites in brain function and disease. *Nature reviews. Neuroscience* **15**, 771-785, doi:10.1038/nrn3820 (2014).

8   Hjorth, E. *et al.* omega-3 fatty acids enhance phagocytosis of Alzheimer's disease-related amyloid-beta42 by human microglia and decrease inflammatory markers. *Journal of Alzheimer's disease : JAD* **35**, 697-713, doi:10.3233/JAD-130131 (2013).

9   Stillwell, W., Shaikh, S. R., Zerouga, M., Siddiqui, R. & Wassall, S. R. Docosahexaenoic acid affects cell signaling by altering lipid rafts. *Reproduction, nutrition, development* **45**, 559-579, doi:10.1051/rnd:2005046 (2005).

10 Wassall, S. R. & Stillwell, W. Polyunsaturated fatty acid-cholesterol interactions: domain formation in membranes. *Biochimica et biophysica acta* **1788**, 24-32, doi:10.1016/j.bbamem.2008.10.011 (2009).

11 Escriba, P. V. *et al.* Membrane lipid therapy: Modulation of the cell membrane composition and structure as a molecular base for drug discovery and new disease treatment. *Progress in lipid research* **59**, 38-53, doi:10.1016/j.plipres.2015.04.003 (2015).

12 Prasad, M. R., Lovell, M. A., Yatin, M., Dhillon, H. & Markesbery, W. R. Regional membrane phospholipid alterations in Alzheimer's disease. *Neurochemical research* **23**, 81-88 (1998).

13 Vitiello, G., Di Marino, S., D'Ursi, A. M. & D'Errico, G. Omega-3 fatty acids regulate the interaction of the Alzheimer's abeta(25-35) peptide with lipid membranes. *Langmuir : the ACS journal of surfaces and colloids* **29**, 14239-14245, doi:10.1021/la403416b (2013).

14 Calderon, R. O., Attema, B. & Devries, G. H. Lipid-Composition of Neuronal Cell-Bodies and Neurites from Cultured Dorsal-Root Ganglia. *Journal of neurochemistry* **64**, 424-429 (1995).

15 Soderberg, M., Edlund, C., Kristensson, K. & Dallner, G. Fatty acid composition of brain phospholipids in aging and in Alzheimer's disease. *Lipids* **26**, 421-425 (1991).

16 Hennebelle, M. *et al.* Ageing and apoE change DHA homeostasis: relevance to age-related cognitive decline. *The Proceedings of the Nutrition Society* **73**, 80-86, doi:10.1017/S0029665113003625 (2014).

17 Martins, I. C. *et al.* Lipids revert inert Abeta amyloid fibrils to neurotoxic protofibrils that affect learning in mice. *The EMBO journal* **27**, 224-233, doi:10.1038/sj.emboj.7601953 (2008).

18 Vitiello, G., Grimaldi, M., D'Ursi, A. M. & D'Errico, G. The iAbeta5p beta-breaker peptide regulates the Abeta(25-35) interaction with lipid bilayers through a cholesterol-mediated mechanism. *Biochemical and biophysical research communications* **417**, 88-92, doi:10.1016/j.bbrc.2011.11.061 (2012).

19 Vitiello, G. *et al.* Cholesterol modulates the fusogenic activity of a membranotropic domain of the FIV glycoprotein gp36. *Soft Matter* **9**, 6442-6456, doi:10.1039/c3sm50553g (2013).

20 Georgieva, R. *et al.* Docosahexaenoic acid promotes micron scale liquid-ordered domains. A comparison study of docosahexaenoic versus oleic acid containing phosphatidylcholine in raft-like mixtures. *Biochimica et biophysica acta* **1848**, 1424-1435, doi:10.1016/j.bbamem.2015.02.027 (2015).

21 Brzustowicz, M. R. *et al.* Controlling membrane cholesterol content. A role for polyunsaturated (docosahexaenoate) phospholipids. *Biochemistry* **41**, 12509-12519 (2002).

22 Shaikh, S. R., Kinnun, J. J., Leng, X., Williams, J. A. & Wassall, S. R. How polyunsaturated fatty acids modify molecular organization in membranes: insight from NMR studies of model systems. *Biochimica et biophysica acta* **1848**, 211-219, doi:10.1016/j.bbamem.2014.04.020 (2015).

23 Puff, N., Watanabe, C., Seigneuret, M., Angelova, M. I. & Staneva, G. Lo/Ld phase coexistence modulation induced by GM1. *Biochimica et biophysica acta* **1838**, 2105-2114, doi:10.1016/j.bbamem.2014.05.002 (2014).

24 Rasti, B., Jinap, S., Mozafari, M. R. & Yazid, A. M. Comparative study of the oxidative and physical stability of liposomal and nanoliposomal polyunsaturated fatty acids prepared with conventional and Mozafari methods. *Food Chem* **135**, 2761-2770, doi:10.1016/j.foodchem.2012.07.016 (2012).

25 Bustamante, C., Tinoco, I., Jr. & Maestre, M. F. Circular differential scattering can be an important part of the circular dichroism of macromolecules. *Proc Natl Acad Sci U S A* **80**, 3568-3572 (1983).

Appendix A:

Effect of polyunsaturated free fatty acids on L$_\beta$ phases

A.1. Work outline

The dietary intake of Omega3 fatty acids such as DHA and EPA is linked to the prevention of cancer, hearth diseases and is associated to brain development[1,2]. Among other hypotheses, mainly based on their radical-scavenging and anti-inflammatory action[3], it has been proposed that omega-3 fatty acids, once converted to lipids[4], could alter the structure and functionality of biological membranes, whose involvement in major biological processes, such as signaling and protein trafficking, is widely reported. Thus, the effects of different lipids containing DHA on both the L_d and L_o phases have been investigated and the results are presented in chapter 3. Nevertheless also the role of free fatty acids should be taken into account; indeed the it has been found vesicle cycling, which is an important biological event, involves the interplay between membrane lipids and proteins, among which the enzyme phospholipase A2 (PLA2) plays a critical role[5]. Phospholipase A2 family consists on a group of enzymes that hydrolyze the ester bond at the sn-2 position in glycerophospholipids, inducing the release of a free fatty acid (FA) and lysophospholipid. In nervous cells, PLA2 was also shown to control the metabolic transformation of phospholipid (PL) molecules that contain PUFAs[6]. In addition, Georgieva *et al.*[7], using raft-like lipid mixtures, demonstrated that line tension and elastic properties govern budding formation after the addition of phospholipase A2 (PLA2), which explains why DHA-containing phosphatidylcholine (PC), but not oleic acid (OA)- containing PC, are able to exhibit liquid-ordered (Lo) domain budding. Very little is known about the interaction of free fatty acids with model membranes, thus the effect of polyunsaturated fatty acids, i.e. DHA and EPA, and also OA as control on DPPC membranes were investigated. The study was carried out by means of differential microCalorimetry; in addition, generalized polarization for Laurdan label imbedded in DPPC and eggPC was investigated in 0rder to obtain information on the fluidity of membranes and cconfocal microscopy of GUVs containing DHA were acquired to verify the existence of microdomains.

A.2. Materials and methods

Materials

Chloroform, dichloromethane and methanol, HPLC-grade solvents, were obtained from Merck (Darmstadt, Germany). EggPC, 1,2-dipalmitoyl-sn-glycero-3-phosphatidylcholine (DPPC) and 1-palmytoyl-2-docosahexaenoyl-sn-glycero-3-phosphocholine (PDPC) were obtained from Avanti Polar Lipids (Birmingham, AL, USA). Docosahexaenoic acid, Eicosapentaenoic acid and oleic acid were provided from Sigma Aldrich (St. Louis, MO).

### *Differential Scanning microcalorimetry (DSC)*

All measurements were performed in a VP-DSC high-sensitivity scanning microcalorimeter (MicroCal, Northampton, MA). Both lipid and buffer solutions were fully degassed before loading into the appropriate cell. Buffer was 20 mM PIPES, 150 mM NaCl, 1 mM EDTA, pH 7.4. Lipid suspensions were loaded into the microcalorimeter in the form of multilamellar vesicles. A final amount of 0.5ml at 0.5mM total lipid concentration was loaded into the calorimeter, and up to six heating scans were performed at 45 °C/h between 10 and 60 °C for all samples. Lipid concentration was determined as lipid phosphorus, and used together with data from the last scan, to obtain normalized thermograms. The software Origin 7.0 (MicroCal), provided with the calorimeter, was used to determine the different parameters for the scans. The software PeakFit v4.12 was used for curve-fitting.

Fluorescence spectroscopy

The emission maxima of LAURDAN in phospholipid bilayers depend upon the phase state of the phospholipids, being blue in the gel (maximum emission =440 nm) and green in the liquid crystalline phase (maximum emission =490 nm) (**Figure A.1**). This shift of the emission spectrum has been attributed to dipolar relaxation processes occurring in the phospholipid liquid–crystalline phase but not in the gel phase[8]. The generalized polarization (GP) of Laurdan was measured

in an Aminco Bowman Series 2 spectrofluorometer (ThermoFisher Scientific, Waltham, MA) equipped with thermoregulated cell holders.
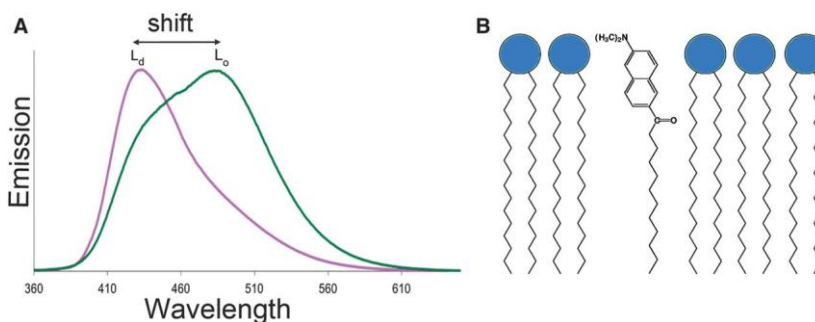
Figure A.1: A) Laurdan emission spectra in both L_β and L_α phases; B) schematic representation of Laurdan label inserted in a lipid layer[9].

The GP was calculated by the **equation A.1**:

$$GP = \frac{I_{440} - I_{490}}{I_{440} + I_{490}} \qquad \textbf{Eq. A.1}$$

where I_{440} and I_{490} are the emission intensities at 440 and 490 nm, respectively, when exciting at 360 nm. The final probe/lipid molar ratio was 1/1000.

Confocal microscopy of GUVs

Giant Unilamellar Vesicles (GUVs) were prepared using the electroformation method. For vesicle observation, a home-made chamber was used that allows direct GUV visualization under the microscope[10]. Stock lipid solutions (0.2 mg/mL total lipid containing 0.2 mol % lissamine rhodamine PE (Rho-PE)) were prepared in a chloroform/methanol (2:1, v/v) solution. Then, 3 μL of the appropriate lipid stocks were added onto the surface of Pt electrodes and solvent traces were removed by placing the chamber under high vacuum for at least 2 h. The Pt electrodes were covered with 400 mL Millipore filtered Milli-Q water previously equilibrated at 75°C. The Pt wires were connected to an electric-wave generator (TG330 function generator, Thurlby Thandar Instruments, Huntington, United Kingdom) under AC field conditions (10 Hz, 0.9 V) for 2 h at 75°C. The generator and the water bath were switched off, and vesicles were left to

equilibrate at room temperature for 1 h. After GUV formation, the chamber was placed onto an inverted confocal fluorescence microscope (Nikon D-ECLIPSE C1, Nikon, Melville, NY). The excitation wavelength for Rho-PE was 561 nm, and the images were collected using a band-pass filter of 593 5 20 nm. Image treatment and quantitation were performed using the software EZ-C1 3.20 (Nikon).

A.3. Differential scanning calorimetry

To explore the interaction between DPPC and the three free fatty acids OA, EPA and DHA, a first approach using a calorimetric assay was performed to study the effect on DPPC gel-fluid lamellar phase transition. Thermograms for the mixtures containing 0%, 5%, 10%, 20% and 30% of each fatty acid are shown in **Figure A.2**. Pure DPPC displays a cooperative rippled-fluid phase transition centred at 41.4 ºC, preceded by the so called pre-transition peak at 35.6°C, associated to the gel phase L_β to P_β'. Treatment with unsaturated fatty acids shift the phase transition temperatures of DPPC in a dose dependent manner. A small concentration of 5 mol % of both mono-unsaturated and polyunsaturated fatty acid induces different changes in the DPPC thermogram.
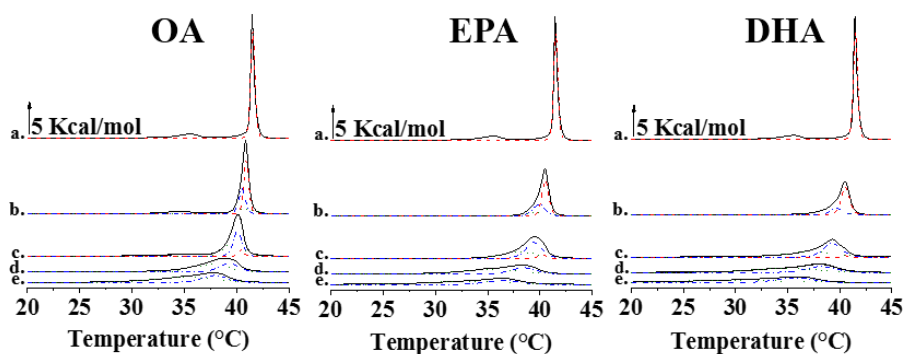
Figure A.2: Thermograms and relative fittings for DPPC alone (top Panels A,B,C) and in the presence of different concentrations of OA, EPA and DHA.

The OA causes the shift of the main transition peak and it is still the pre-transition one. On the contrary, EPA and DHA cause an asymmetry in the main peak with a shoulder at lower temperatures, more marked for DHA, on the DPPC phase transition. In the case of poly-unsaturated the disappearance of the pre-transition peak is also detected. Increasing the amount of each fatty acid, the sharp peak, associated with DPPC main transition, became more broad and asymmetric until the completely disappearance in the case of 30% DHA. Thermogram transition temperatures, enthalpies, and widths at half-height (reported in **Figure A.2**) were determined using the software ORIGIN (Microcal) provided with the calorimeter.
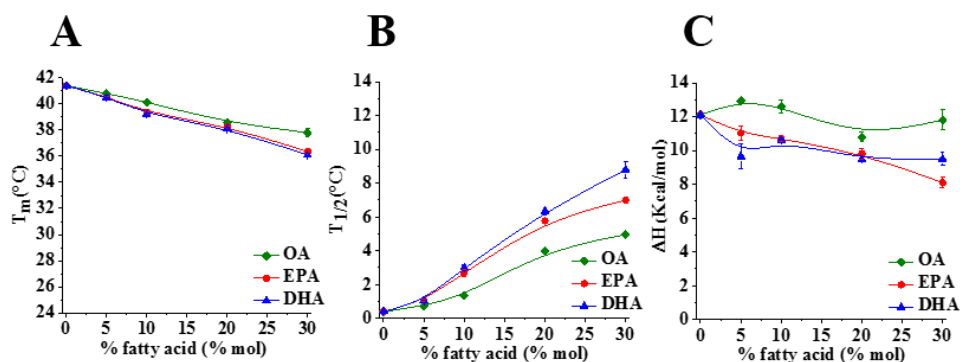

Figure A.3: Panel A**:** Transition temperatures; Panel B: The peak width, at half of its height; Panel C: ΔH; for DPPC in the presence of OA (green), EPA (red) and DHA (blue).

Concerning the transition temperatures, **Figure A.3 A** shows that T_m decreases in a dose dependent way for all the three fatty acids, suggesting that these molecules can fluidify the DPPC membrane. The $T_{1/2}$ (**Panel B**) describes the cooperativity of the transition: the higher is the $T_{1/2}$ value the less cooperative is the process; thus, increasing the amount of the fatty acids the process become less cooperative but with a different behaviour for mono-unsaturated OA and poly-unsaturated EPA and DHA suggesting a heterogeneity affect the lipid systems. The ΔH variations also indicate that the more fluid phase occurs in the presence of poly-unsaturated fatty acids, indeed a less heat in necessary to obtain the transition. In order to rationalise those results, the thermograms investigation was deepened;

indeed, due to the peak shape curves, fittings were performed by the software GRAMS_32 Spectra Notebase. Thermograms were fitted to the smallest number of Gaussian curves compatible with a statistically convergent solution with an R^2 correlation coefficient >0.99; the best fittings are reported as dotted lines in **Figure A.2.** It comes out that three different components (excluding the pre-transition) characterize the lipid mixtures as soon as the fatty acids are added (thermograms b. in **Figure A.2**). To quantitatively analyse the behaviour of those components and thus to understand their origin, the transition temperature, the half high temperature and ΔH were reported for each component in **Figure A.4**.
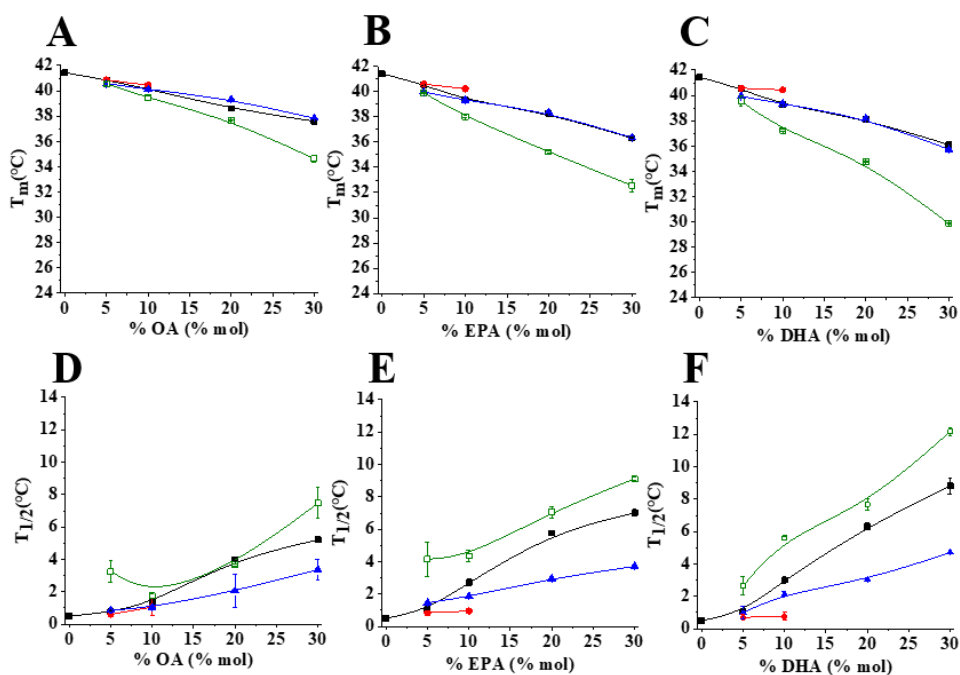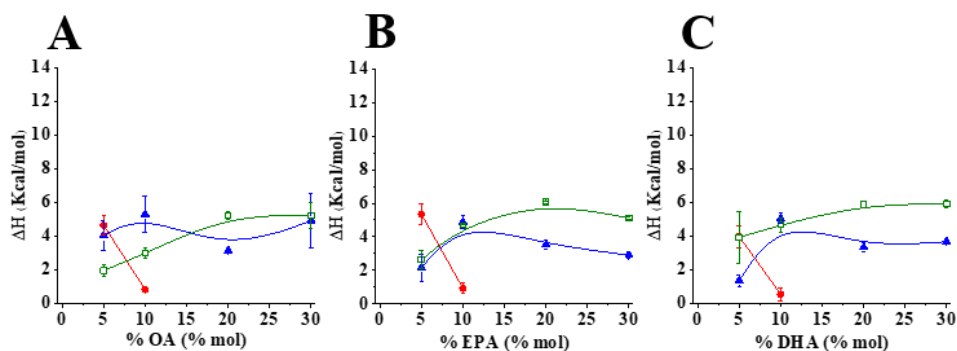

Figure A.4: T_m and $T_{1/2}$ for the three components arising in the presence of OA (A, D), EPA (B, E) and DHA (C, F)

For all the parameters the averaged values are reported in black and the three components, detected by the fitting procedures, in different colours: red, blue and green. In all the investigated samples, the component indicated in red disappears upon the addition of 10% OA or EPA or DHA; such component shows to have the same T_m and $T_{1/2}$ of DPPC transition and those values remain constant until

they disappear; thus, it is ascribed to the P_{β}' phase of DPPC alone. On the other hand, the components reported in blue and green, appear when the fatty acids are added and evolve with the increase of fatty acids molar fraction; in both cases, the transition temperatures decrease, indicating a fluidification of lipid system, but the effect is higher for the green one. Even the cooperativity of the process changes differently: it is much less in the case of the green component. Looking at the enthalpies variation of those two components (**Figure A.5**) it is possible to see that the associated ΔH increase when the ΔH for the DPPC alone decrease, and then they reach a constant value, which is higher for the green component, increasing the % of fatty acids. Those results suggest that upon the addition of a treashold concentration of each fatty acid, the DPPC phase is more fluid and it is possible to discriminate between an enriched unsaturated fatty acid phase and enriched saturated phase. Notably, DHA is the fatty acid that most affect the DPPC bilayer, probably due to the high number of unsaturation.

**Figure A.5:** ΔH for the three components arising in the presence of OA (A, D), EPA (B, E) and DHA (C, F)

A.4. Laurdan General Polarization method

In order to estimate the packing effect of single lipid species, we analysed simple one component lipid mixtures consisting on DPPC with known phase behavior[11]. Having confirmed that Laurdan emission spectrum has the λ_{max} at 440 nm, the GP value were calculated and are reported in black in **Figure A.6.**

Appendix A: Effect of polyunsaturated free fatty acids on Lβ phases

To understand the effect of OA, EPA and DHA, the GP values for different concentration of each fatty acid were calculated and reported in **Figure A.6**.

The addition of monounsaturated OA with exception of the 30% OA, causes a little increase of GP of Laurdan at all investigated temperatures; indeed, the 30% of OA reduces the GP at 37°C of the lipid mixtures compared to DPPC alone. On the contrary, lower amount of polyunsaturated fatty acids, 20%, can reduce the GP with higher effect, clear at 37°C. Reporting the GP for a wide range of the three fatty acids at a physiological temperature, the effects of polyusaturated fatty acids become clearest (**Figure A.7**). The GP value for DPPC at 37°C and the relative statistical error are reported as black dotted lines. The results show that the 20% of polyunsaturated EPA and DHA affect the hydration near the label instead of OA that does not alter the properties of DPPC alone. For the 20% of each fatty acid the temperature scan was performed for DPPC, and EggPC, reported in **Figure A.8 A** and **B**, respectively.
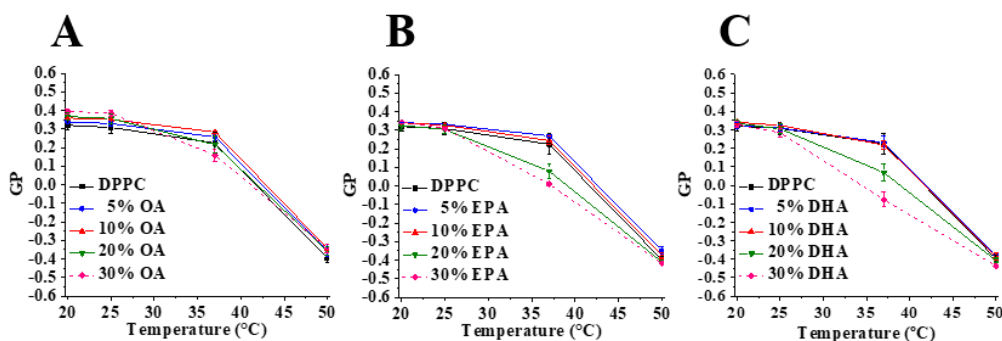
Figure A.6: Laurdan GP value at different temperature of DPPC alone (black squares) and in the presence of different concentrations of OA (A), EPA (B), DHA (C).

From the inspection of **Figure A.8A**, the two transitions for DPPC alone, reported in black, are clear, and show that reporting the GP values versus temperature is an efficient technique to investigate the phase transitions in lipid mixtures. The presence of OA, EPA or DHA induce different effects on the transition:

- at temperature below 37°C, OA induces an increase of DPPC GP, while EPA and DHA reduce it;

122

- at 37°C, GP in the presence of OA is the same observed for DPPC, but the polyunsaturated fatty acids shift the GP at lower value;

- at temperature higher than 37°C GP tend to a constant value for all the systems. Thus, from fluorescence investigation it is possible to assesses that 20% of OA, EPA or DHA at low temperature fluidify the DPPC gel phase to a P$'_\beta$, indeed the pretransition is supressed; further comparing the GP values at 37°C, the Laurdan label resides in a more polar environment when PUFAs are added to the lipid mixtures suggesting that the lipids headgroups are less packed.
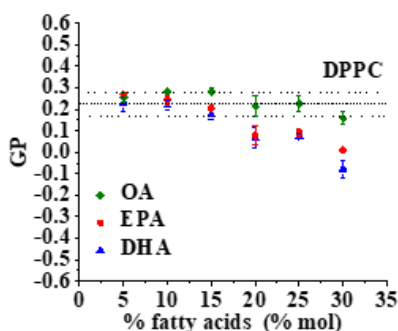
Figure A.7: Laurdan GP value of different percentage of the FFAs in a DPPC bilayer at 37°C. The Laurdan GP value and the relative standard deviation for DPPC alone are the dotted lines.

The overall effect for the three fatty acids is to shift the transition temperature, as already shown by DSC thermograms. In contrast, in the case of these low amounts of free fatty acids, no effects are shown on a liquid disordered phase, as in the case of eggPC.
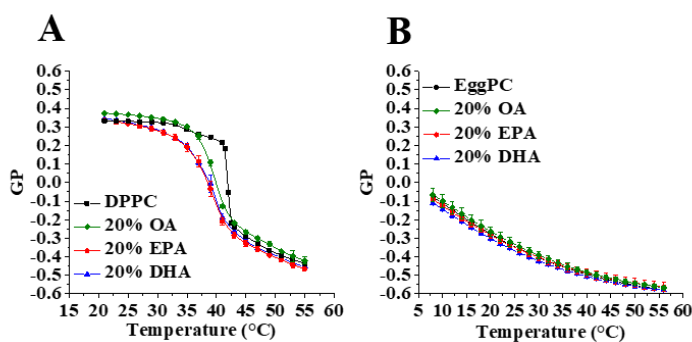
Figure A.8: Temperature scan of Laurdan GP value in absence and in presence of 20 % (mol%) of the FFAs in a DPPC bilayer (A) and in an EggPC bilayer (B).

A.5. Confocal microscopy of GUVs

Giant Unilamellar Vesicles (GUVs) of DPPC alone and DPPC/DHA with molar fractions were prepared by electroformation protocol and observed by confocal microscopy at room temperatures. In **Figure A.8** the images related to DPPC GUVs are reported.
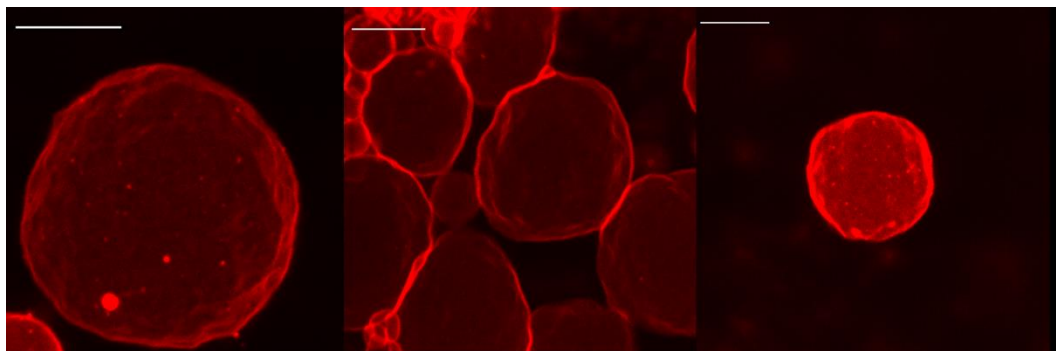
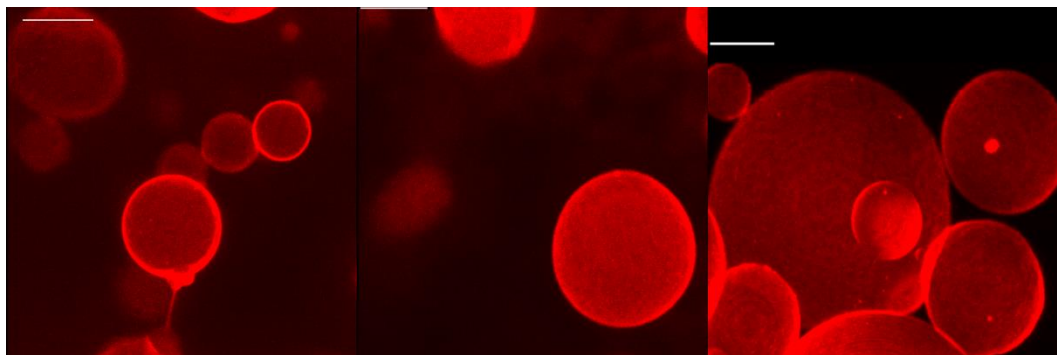
Figure A.9: Confocal microscopy images of DPPC GUVs acquired at 25°C. The scale is 500 nm.

The vesicles show a rough surface mainly due to gel phase that characterizes DPPC alone. Interestingly when 30% of DHA is present in the lipid mixtures the vesicles are smoother. The fluidification effects of DHA, already observed by DSC measurements and by fluorescence spectroscopy, were confirmed.

Appendix A: Effect of polyunsaturated free fatty acids on Lβ phases

Notably no domains are observed indicating that free fatty acid have a different ability in the lipid reorganization with respect to the phospholipid containing DHA.

Figure A.10: Confocal microscopy images of DPPC/DHA 70/30 GUVs acquired at 25°C. The scale is 500 nm

A.6. Conclusions

The effects of Docosahexaenoic acid (DHA), once converted to phospholipids, on the membrane reorganization and on the ability to induce lipid phases separation were extensively studied. However, a little is known about the effects that free fatty acids have on the lipid organization. The properties that omega3 fatty acids, EPA and DHA, can exert on a gel phase have been investigated and a comparison with the monounsaturated OA has been carried out.

The results, obtained from a calorimetry study combined with the evaluation of GP values, show that both the polyunsatutared fatty acids and monounsaturated OA affect the gel phase of DPPC in a dose dependent manner and that DHA and EPA have a stronger fluidification effect on a gel phase compared to oleic acid. Interestingly, even if the omega3 free fatty acids are able to fluidify the gel phase, are not able to induce a lipid segregation as shown by the confocal images. Combining the results obtained with those reported in literature for phospholipids containing DHA or EPA[12,13], it is possible to assess that the different geometries of phospholipids and the free fatty acids differently affect the lipid packing of DPPC.

# Appendix A: Effect of polyunsaturated free fatty acids on Lβ phases

A.7. References

1   Connor, W. E. Importance of n-3 fatty acids in health and disease. *Am J Clin Nutr* **71**, 171s-175s (2000).
2   Laye, S. Polyunsaturated fatty acids, neuroinflammation and well being. *Prostaglandins, leukotrienes, and essential fatty acids* **82**, 295-303, doi:10.1016/j.plefa.2010.02.006 (2010).
3   Bazinet, R. P. & Laye, S. Polyunsaturated fatty acids and their metabolites in brain function and disease. *Nature reviews. Neuroscience* **15**, 771-785, doi:10.1038/nrn3820 (2014).
4   Hulbert, A. J., Kelly, M. A. & Abbott, S. K. Polyunsaturated fats, membrane lipids and animal longevity. *J Comp Physiol B* **184**, 149-166, doi:10.1007/s00360-013-0786-8 (2014).
5   Gama, M. A. S. *et al.* Conjugated linoleic acid-enriched butter improved memory and up-regulated phospholipase A(2) encoding-genes in rat brain tissue. *J Neural Transm* **122**, 1371-1380, doi:10.1007/s00702-015-1401-9 (2015).
6   Lee, J. C., Simonyi, A., Sun, A. Y. & Sun, G. Y. Phospholipases A2 and neural membrane dynamics: implications for Alzheimer's disease. *Journal of neurochemistry* **116**, 813-819, doi:10.1111/j.1471-4159.2010.07033.x (2011).
7   Georgieva, R. *et al.* Phospholipase A2-Induced Remodeling Processes on Liquid-Ordered/Liquid-Disordered Membranes Containing Docosahexaenoic or Oleic Acid: A Comparison Study. *Langmuir : the ACS journal of surfaces and colloids* **32**, 1756-1770, doi:10.1021/acs.langmuir.5b03317 (2016).
8   Krasnowska, E. K., Gratton, E. & Parasassi, T. Prodan as a membrane surface fluorescence probe: Partitioning between water and phospholipid phases. *Biophysical journal* **74**, 1984-1993 (1998).
9   Ashrafzadeh, P. & Parmryd, I. Methods applicable to membrane nanodomain studies? *Essays Biochem* **57**, 57-68, doi:10.1042/Bse0570057 (2015).
10 Jimenez-Rojo, N., Garcia-Arribas, A. B., Sot, J., Alonso, A. & Goni, F. M. Lipid Bilayers Containing Sphingomyelins and Ceramides of Varying N-Acyl Lengths: a Glimpse into Sphingolipid Complexity. *Biophysical journal* **106**, 288a-288a (2014).
11 de Almeida, R. F., Fedorov, A. & Prieto, M. Sphingomyelin/phosphatidylcholine/cholesterol phase diagram: boundaries and composition of lipid rafts. *Biophysical journal* **85**, 2406-2416, doi:10.1016/S0006-3495(03)74664-5 (2003).
12 Dumaual, A. C., Jenski, L. J. & Stillwell, W. Liquid crystalline/gel state phase separation in docosahexaenoic acid-containing bilayers and monolayers. *Bba-Biomembranes* **1463**, 395-406, doi:Doi 10.1016/S0005-2736(99)00235-7 (2000).
13 Williams, J. A. *et al.* Docosahexaenoic and Eicosapentaenoic Acids Segregate Differently between Raft and Nonraft Domains. *Biophysical journal* **103**, 228-237, doi:10.1016/j.bpj.2012.06.016 (2012).

Appendix B:

Neutron reflectivity Profiles

B.1. Neutron reflectivity profiles for SDPC and DDPC in POPC lipid membranes

Supported lipid bilayers consisting on a binary mixture either SDPC/POPC or DDPC/POPC were realized as described in **section 3.2** and measured in the three different solvent contrasts D_2O, SMW and H_2O that greatly enhances the sensitivity of the technique[10];the reflectivity profiles and related best fits are shown in **Figure B.1.**
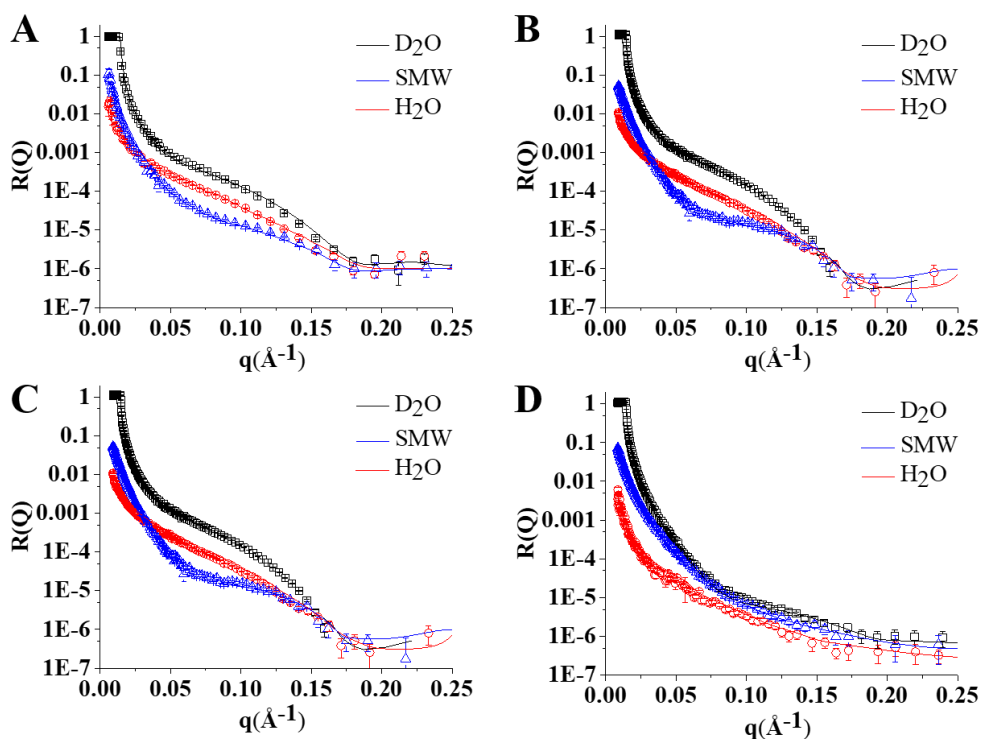
Figure 3.10: Experimental data and the best fitting curves in D_2O (black), SMW (blue) and H2O (red)for lipid systems: A) POPC/SDPC 60/40, B) POPC/DDPC 80/20, C) SDPC and D) POPC/DDPC 20/80, respectively.

B.2. Neutron reflectivity profiles for SDPC and DDPC in POPC/Chol lipid membranes

Supported lipid bilayers consisting on a ternary mixture characterized by a constant amount of cholesterol (40%) and either SDPC or DDPC combined with POPC were realized as described in **section 3.2** and measured in the three different solvent contrasts D_2O, SMW and H_2O that greatly enhances the sensitivity of the technique;the reflectivity profiles and related best fits are shown in **Figure B.1.**
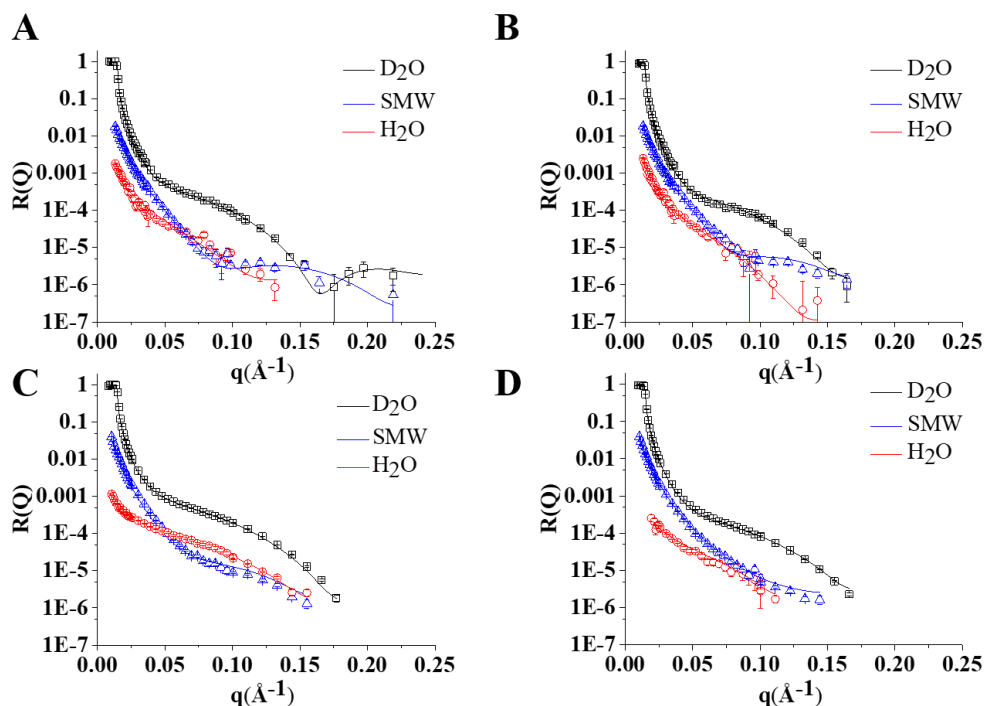
Figure 3.10: Experimental data and the best fitting curves in D_2O (black), SMW (blue) and H2O (red)for lipid systems: A) POPC/SDPC 60/40 40% Chol, B) POPC/DDPC 80/2040% Chol, C) SDPC 40% Chol and D) POPC/DDPC 20/80 40% Chol, respectively.

Publications

- **De Santis, A**.; Russo Krauss, I.; Vitiello, G., Ottaviani, M.F.; Paduano, L.; D'Errico, G.,
  Omega-3 fatty lipids modulate the microstructural properties of biomembranes
  In preparation

- **De Santis, A**.; La Manna, S.; Russo Krauss, I.; Malfitano, A.M.; Novellino, E.; Federici, L.; Di Matteo, A.; D'Errico, G.; Marasco, D. Nucleophosmin-1 aggregating regions associated with Acute Myeloid Leukemia interact differently with lipid membranes. *Biochimica et biophysica acta* **2017** *accepted with major revisions*.

Abstract

Nucleophosmin-1 (NPM1) is an abundant multifunctional protein, implicated in a variety of biological processes and in the pathogenesis of several human malignancies. Its C-terminal domain (CTD) is endowed with a three helix bundle and we demonstrated that several regions within it, including those associated with Acute Myeloid Leukemia (AML), have a strong tendency to form amyloid-like assemblies with β-sheet structures and cellular toxicity.

In particular the central helix of the bundle (H2) resulted the most amyloidgenic region: here with the dual aim to better model the processes of cytoxicity of two peptide sequences covering H2 and to get clues of a potential involvement of the interaction between CTD (in the wild type and AML-mutA variants) and cellular membrane, we investigated the interaction of CTD-NPM1 regions with models lipid membranes through ANS binding assay, as well as by Surface Plasmon Resonance, Circular Dichroism and Electron Spin Resonance spectroscopies.

These investigations demonstrated a fine interplay between self-aggregation process of peptides and their interaction with the membranes. Particularly, cholesterol plays a key role in driving the membrane interaction with amyloidogenic sequences: H2 peptide showed a specific interaction with cholesterol, determining a sensitive fluidification of the bilayer, while its N-term elongated variant non-specifically interacts with membrane causing a stiffening of the bilayer. Noticeably CTD variants also presents different mechanisms of interaction with lipid membranes.

Presented results corroborate that the aggregation of several regions of NPM1-CTD could be implicated in diseases where NPM1 is mutated (i.e. AML) and/or where its overexpression is cytotoxic.

- Russo Krauss, I.; Imperatore, R.; **De Santis, A**.; Luchini, A.; Paduano, L.; D'Errico, G., Structure and dynamics of cetyltrimethylammonium chloride-sodium dodecylsulfate (CTAC-SDS) catanionic vesicles: High-value nano-vehicles from low-cost surfactants. *Journal of colloid and interface science* **2017,** *501*, 112-122.

Abstract
Hypothesis: Catanionic vesicles based on large-scale produced surfactants represent a promising platform for the design of innovative, effective and relatively inexpensive nano-vehicles for a variety of actives. Structural, dynamic and functional behavior of these aggregates is finely tuned by the molecular features of their components and can be opportunely tailored for their applications as drug carriers.
Experiments: Here we investigate the aggregates formed by CTAC and SDS, two of the most diffused surfactants, by means of Dynamic Light Scattering, Small Angle Neutron Scattering and Electron Paramagnetic Resonance spectroscopy (EPR). The exploitation of these aggregates as nano-vehicles is explored using the poorly water-soluble antioxidant trans-resveratrol (t-RESV), testing t-RESV solubility and antioxidant activity by means of UV, fluorescence spectroscopy and EPR.
Findings: The presence of a large stability region of catanionic vesicles on the CTAC-rich side of the phase diagram is highlighted and interpreted in terms of the mismatch between the lengths of the surfactant tails and of first reported effects of the chloride counterions. CTAC-SDS vesicles massively solubilize t-RESV, which in catanionic vesicles exerts a potent antioxidant and radical-scavenging activity. This behavior arises from the positioning of the active at the surface of the vesicular aggregates thus being sufficiently exposed to the external medium.

- Lombardi, L.; Stellato, M. I.; Oliva, R.; Falanga, A.; Galdiero, M.; Petraccone, L.; D'Errico, G.; **De Santis, A**.; Galdiero, S.; Del Vecchio, P., Antimicrobial peptides at work: interaction of myxinidin and its mutant WMR with lipid bilayers mimicking the P. aeruginosa and E-coli membranes. *Scitific Report* **2017,** *7* doi:10.1038/srep44425.

Abstract
Antimicrobial peptides are promising candidates as future therapeutics in order to face the problem of antibiotic resistance caused by pathogenic bacteria. Myxinidin is a peptide derived from the hagfish mucus displaying activity against a broad range of bacteria. We have focused our studies on the physico-chemical characterization of the interaction of myxinidin and its mutant WMR, which contains a tryptophan residue at the N-terminus and four additional positive charges, with two model biological membranes

(DOPE/DOPG 80/20 and DOPE/DOPG/CL 65/23/12), mimicking respectively Escherichia coli and Pseudomonas aeruginosa membrane bilayers. All our results have coherently shown that, although both myxinidin and WMR interact with the two membranes, their effect on membrane microstructure and stability are different. We further have shown that the presence of cardiolipin plays a key role in the WMR-membrane interaction. Particularly, WMR drastically perturbs the DOPE/DOPG/CL membrane stability inducing a segregation of anionic lipids. On the contrary, myxinidin is not able to significantly perturb the DOPE/DOPG/CL bilayer whereas interacts better with the DOPE/DOPG bilayer causing a significant perturbing effect of the lipid acyl chains. These findings are fully consistent with the reported greater antimicrobial activity of WMR against P. aeruginosa compared with myxinidin.

- Randino, R.; Grimaldi, M.; Persico, M.; **De Santis, A**.; Cini, E.; Cabri, W.; Riva, A.; D'Errico, G.; Fattorusso, C.; D'Ursi, A. M.; Rodriquez, M., Investigating the Neuroprotective Effects of Turmeric Extract: Structural Interactions of beta-Amyloid Peptide with Single Curcuminoids. *Scientific Report* **2016,** *6*, doi:10.1038/srep38846.

Abstract
A broad biophysical analysis was performed to investigate the molecular basis of the neuroprotective action of Curcuma longa extracts in Alzheimer's disease. By combining circular dichroism and electron paramagnetic resonance experiments with molecular modeling calculations, the minor components of Curcuma longa extracts, such as demethoxycurcumin (2, DMC), bisdemethoxycurcumin (3, BDMC) and cyclocurcumin (4, CYC), were analyzed in a membrane environment mimicking the phospholipid bilayer. Our study provides the first evidence on the relative role of single curcuminoids interacting with Aβ-peptide. When the CYC and curcumin metabolite tetrahydrocurcumin (5, THC) were inserted into an anionic lipid solution, a significant modification of the Aβ CD curves was detected. These data were implemented by EPR experiments, demonstrating that CYC reaches the inner part of the bilayer, while the other curcuminoids are localized close to the membrane interface. Computational studies provided a model for the curcuminoid-Aβ interaction, highlighting the importance of a constrained "semi-folded" conformation to interact with Aβ analogously to the pattern observed in α-helical coiled-coil peptide structures. This combined approach led to a better understanding of the intriguing in vitro and in vivo activity of curcuminoids as anti-Alzheimer agents, paving a new path for the rational design of optimized druggable analogues.

- Oliva, R.; Emendato, A.; Vitiello, G.; **De Santis, A**.; Grimaldi, M.; D'Ursi, A. M.; Busi, E.; Del Vecchio, P.; Petraccone, L.; D'Errico, G., On the microscopic and mesoscopic perturbations of lipid bilayers upon interaction with the MPER domain of the HIV glycoprotein gp41. *Biochimica et biophysica acta* **2016,** *1858* (8), 1904-13.

Abstract

The effect of the 665-683 fragment of the HIV fusion glycoprotein 41, corresponding to the MPER domain of the protein and named gp41MPER, on the microscopic structure and mesoscopic arrangement of palmitoyl oleoyl phosphatidylcholine (POPC) and POPC/sphingomyelin (SM)/cholesterol (CHOL) lipid bilayers is analyzed. The microscopic structuring of the bilayers has been studied by Electron Spin Resonance (ESR) spectroscopy, using glycerophosphocholines spin-labelled in different positions along the acyl chain. Transitions of the bilayer liquid crystalline state have been also monitored by Differential Scanning Calorimetry (DSC). Changes of the bilayers morphology have been studied by determining the dimension of the liposomes through Dynamic Light Scattering (DLS) measurements. The results converge in showing that the sample preparation procedure, the bilayer composition and the peptide/lipid ratio critically tune the lipid response to the peptide/membrane interaction. When gp41MPER is added to preformed liposomes, it positions at the bilayer interface and the lipid perturbation is limited to the more external segments. In contrast, if the peptide is mixed with the lipids during the liposome preparation, it assumes a trans-membrane topology. This happens at all peptide/lipid ratios for fluid POPC bilayers, while in the case of rigid POPC/SM/CHOL membranes a minimum ratio has to be reached, thus suggesting peptide self-aggregation to occur. Peptide insertion results in a dramatic increase of the lipid ordering and bilayer stiffening, which reflect in significant changes in liposome average dimension and distribution. The biological implications of these findings are discussed.

- Emendato, A.; Spadaccini, R.; **De Santis, A**.; Guerrini, R.; D'Errico, G.; Picone, D., Preferential interaction of the Alzheimer peptide Abeta-(1-42) with Omega-3-containing lipid bilayers: structure and interaction studies. *FEBS letters* **2016,** *590* (4), 582-91.

Abstract

Many age-related neurodegenerative diseases, including Alzheimer Disease (AD), are elicited by an interplay of genetic, environmental, and dietary factors. Food rich in Omega-3 phospholipids seems to reduce the AD incidence. To investigate the molecular basis of this beneficial effect, we

have investigated by CD and ESR studies the interaction between the Alzheimer peptide Aβ-(1-42) and biomimetic lipid bilayers. The inclusion of 1,2-didocosahexaenoyl-sn-glycero-3-phosphocholine does not change significantly the bilayers organization, but favors its Aβ-(1-42) interaction. The Omega-3 lipid amount modulates the effect intensity, suggesting a peptide selectivity for membranes containing polyunsatured fatty acids (PUFA) and providing hints for the mechanism and therapy of AD.